



universität
wien

DIPLOMARBEIT

Titel der Diplomarbeit

NMDA-receptor functionality at the
blood-brain barrier *in vitro*

angestrebter akademischer Grad

Magister der Pharmazie (Mag.pharm.)

Verfasserin / Verfasser: Michael FREIDL
Matrikel-Nummer: 0309276
Studienrichtung /Studienzweig Pharmazie
(lt. Studienblatt):
Betreuerin / Betreuer: o.Univ.-Prof. Dipl.-Ing. Mag. Pharm. Dr. Christian R. Noe

Wien, im September 2010

Acknowledgments

Initially I would like to thank o.Univ. Prof. Mag. Dipl.-Ing. Dr. Christian R. Noe from the Department of Medicinal Chemistry for giving me the chance to accomplish my diploma thesis in the blood-brain barrier working group.

Furthermore I want to express my gratitude to all current and former members of the blood-brain barrier working group. Especially I want to thank Dipl.-Ing. Dr. Winfried Neuhaus for being my supervisor during this whole time, teaching and supporting me in a very professional but still relaxed way.

I also want to thank Dr. Michael Berger for his support during my thesis regarding to information and advices on the NMDA-receptor and furthermore for performing binding assays on our used cell lines.

Further thanks go to the working group of Ao. Univ.-Prof. Mag. Dr. Franz Gabor and Ao. Univ.-Prof.Mag. Dr. Michael Wirth from the Department of Pharmaceutical Technology and Biopharmaceutics and to the working group of Univ.-Prof. Mag. Dr. Verena Dirsch from the Department of Pharmacognosy. Without their support and permission for using some of their analytical equipments, this diploma thesis probably could not be finished the way it was planned.

I also want to thank my friends, which accompanied and supported me the whole time during my study period.

Finally I deeply thank my parents and my brother for their patience, their encourage and most of all for their support during my study period, my diploma thesis and previous stages stages of my life.

Abstract

A diversity of disease processes and conditions such as Alzheimer's disease, schizophrenia, epilepsy and stroke are major pathological conditions at present time. Although such sufferings are caused by different mechanisms they share the NMDA-receptor as one common target. The number of reports suggesting the presence of this glutamate-gated ion-channel at the blood-brain barrier and its participation in major regulatory mechanisms increased in the last years.

The first goal of this thesis was to confirm and investigate the presence of NMDAR-subunits NR-1, -2A, -2B, and -2C in human blood-brain barrier cell line ECV304 by western blot analysis and immunofluorescence microscopy in order to obtain an overview of possible compositions of a functional NMDA-receptor. Subsequently, it was aimed at establishing a 96-well plate fluorescence-assay for measuring the intracellular Ca^{2+} -level as a functional parameter of the activation of the NMDA-receptor. Furthermore, methods as the measurement of the transendothelial electrical resistance (TEER) and western blotting were to be performed in order to investigate the influence of overstimulation or inhibition of the NMDA-receptors on specific blood-brain barrier properties. The presence of all four investigated NMDA-receptor subunits in the used blood-brain barrier *in vitro* model was shown, but their localisation within the cell membrane was not proven which is suggested to be prerequisite for NMDAR-functionality as a Ca^{2+} -channel. In concordance to this, Ca^{2+} -level measurements revealed controversial results with NMDAR-agonists. For further validation of the test system, other intracellular Ca^{2+} -level modulators were additionally tested which confirmed the suitability of the test set-up. Despite of this, adverse effects of glutamate onto blood-brain barrier integrity (TEER) were confirmed which were inhibited by NMDAR-blocker MK801. Moreover, changes in the expression levels of several specific proteins of samples obtained from the TEER experiments were shown by western blotting.

Taken together, obtained data confirmed data from the literature on the one hand, but also suggested possible involvement of additional targets for NMDA-modulators NMDA and MK801 than the NMDAR on the other hand. With regard to the methods, a 96-well plate fluorescence assay was established which may be used as a first screening method to find possible substrates targeting the blood-brain barrier and regulating the intracellular Ca^{2+} -

level. In the next step, methods as western blotting and TEER measurement could be applied in order to prove the functional relevance of these intracellular calcium modulating drug.

Zusammenfassung

Eine Vielfalt an Krankheitsprozessen und Zustände wie Alzheimer-Krankheit, Schizophrenie, Epilepsie und Schlaganfall sind bedeutende pathologische Gegebenheiten in der heutigen Zeit. Obgleich diese Leiden durch verschiedene Mechanismen ausgelöst werden, teilen diese dennoch den NMDA-Rezeptor als gemeinsames Target. Von einer Anwesenheit und Beteiligung dieses Glutamat-gesteuerten Ionenkanals wird immer häufiger bei wichtigen regulatorischen Mechanismen an der Blut-Hirn-Schranke berichtet. Das erste Ziel dieser Diplomarbeit war die Anwesenheit von NMDA-Rezeptor-Untereinheiten NR-1, -2A, -2B und -2C in der humanen Blut-Hirn-Schranken Zelllinie ECV304 durch Western-Blot-Analysen und Immunofluoreszenz-Mikroskopie zu bestätigen und zu untersuchen, um einen Überblick von möglichen Zusammensetzungen eines funktionellen NMDA-Rezeptors zu bekommen. Anschließend war die Etablierung eines 96-Well Plattenfluoreszenz-Assay zum messen des intrazellulären Ca^{2+} -Spiegel, welcher als funktioneller Parameter einer NMDA-Rezeptoraktivierung gesehen werden kann, unser Ziel. Darüber hinaus wurden Methoden wie die Messung des transendothelialen elektrischen Widerstandes (TEER) und Western-Blots durchgeführt, um den Einfluss einer Überstimulation oder Inhibition des NMDA-Rezeptors auf spezifische Blut-Hirn-Schranken Eigenschaften zu überprüfen. Die Anwesenheit aller vier untersuchten NMDA-Rezeptor Untereinheiten konnte in dem verwendeten *in vitro* Blut-Hirn-Schranken Model gezeigt, jedoch ihre Lokalisation innerhalb der Zellmembran, was als Voraussetzung für NMDA-Rezeptorfunktionalität als Ca^{2+} -Kanal vermutet wird, nicht bewiesen werden. In Übereinstimmung zu diesem zeigten Messungen des Ca^{2+} -Spiegel widersprüchliche Ergebnisse mit NMDA-Rezeptor-Agonisten. Für eine weitere Validierung des Testsystems wurden zusätzlich noch weitere intrazelluläre Ca^{2+} -Spiegel-Modulatoren getestet, welche die Brauchbarkeit des Testset-ups bestätigten. Trotz allem konnten ungünstige Effekte von Glutamate auf die Blut-Hirn-Schranken-Integrität (TEER) gezeigt werden, welche durch den NMDA-Rezeptorblocker MK801 unterbunden wurden. Darüber hinaus wurden Änderungen im Expressionslevel von einigen bestimmten Proteinen, welche von Proben aus den TEER-Versuchen gewonnen wurden, mit Hilfe von Western Blots gezeigt.

Zusammenfassend bestätigten die gewonnenen Resultate einerseits jenen Daten der Literatur, jedoch auch eine mögliche Beteiligung zusätzlicher Targets für NMDA-Modulatoren wie NMDA und MK801 als den NMDA-Rezeptor wäre andererseits möglich. In Bezug zu den Methoden konnte ein 96-Well Plattenfluoreszenz-Assay etabliert werden, welcher eventuell als erste Vorscreening-Methode zur Findung mögliche Substrate, welche gegen die Blut-Hirn-Schranke gerichtet sind und den intrazellulären Ca^{2+} -Spiegel regulieren, verwendet werden kann. Anschließend können Methoden wie Western Blots und TEER-Messungen angewendet werden, um die funktionelle Bedeutung dieser intrazellulären kalziummodulierenden Substanzen zu überprüfen.

Contents

1	Introduction	1
1.1	History of the BBB	1
1.2	Components of the BBB	2
1.2.1	Endothelial cells	2
1.2.2	Astrocytes	2
1.2.3	Pericytes	2
1.2.4	Basal lamina	4
1.3	Physiology of the BBB junctional complex	4
1.3.1	Adherens junctions	4
1.3.2	Tight junctions	4
1.3.2.1	Occludin	5
1.3.2.2	Claudins	6
1.3.2.3	Junctional adhesion molecules (JAM)	7
1.3.2.4	Cytoplasmatic TJ anchoring proteins	7
1.4	Calcium signalling and calcium metabolism	7
1.4.1	Ca ²⁺ - „On“ mechanism	8
1.4.1.1	Plasma membrane channels	8
1.4.1.2	Intracellular Ca ²⁺ -channels	9
1.4.2	Ca ²⁺ - „Off“ mechanism	9
1.5	The NMDA receptor	10
1.5.1	Organization and functionality of the NMDA receptor	10
1.5.2	Role of the NMDA receptor on the BBB	12
2	Aims of this thesis	19
3	Materials & Methods	21

3.1 Chemicals	21
3.1.1 Antibodies	21
3.1.2 Chemicals	21
3.2 Materials and software	24
3.2.1 Materials	24
3.2.2 Devices and software	24
3.3 Cell lines	25
3.3.1 Rat glioma cell line C6	25
3.3.2 ECV304	26
3.4 Cell culture media and solutions	26
3.4.1 Trypsin/EDTA solutions (200 mL)	26
3.4.2 C6 medium (1000 mL)	26
3.4.3 Astrocyte conditioned medium (ACM) of C6 medium	27
3.4.4 PBMEC medium (500 mL)	27
3.4.5 Gelatine solution 1%	27
3.4.6 C6 medium (250 mL) without serum and heparin	27
3.5 Cell culture work/protocol	28
3.5.1 Coating of cell culture flasks or 96-well plates	28
3.5.2 Subculturing of ECV304 or C6 cells	28
3.5.3 ECV304 culture in a Transwell™ model and measurement of the transendothelial/electrical resistance (TEER)	29
3.5.4 Influence of glutamate on the TEER	31
3.5.5 Protein analysis	32
3.5.5.1 Bradford protein determination	32
3.5.5.2 SDS-polyacrylamid gel electrophoresis (SDS-PAGE)	33
3.5.5.3 Western blotting	37
3.5.6 Immunofluorescence microscopy	39
3.5.6.1 Protocol using methanol (MeOH)	39
3.5.6.2 Protocol using paraformaldehyde and 0.1 % Triton X-100	40
3.5.7 Intracellular Ca ²⁺ -level assay	42
3.5.7.1 Culturing ECV304 cells in a 96-well plate	42

3.5.7.2	Steady-state protocol	43
3.5.7.3	Kinetic-like protocol	45
3.5.7.4	Variable parameters in the intracellular calcium level protocol	47
4	Results	49
4.1	Presence of the NMDA receptor in cell line ECV304	49
4.1.1	Western blot analysis of the NMDA receptor subunits	49
4.1.2	Immunofluorescence microscopic analysis of the NMDA receptor subunits	52
4.2	Measurement of the intracellular calcium level	58
4.2.1	Development of a 96-well plate assay	58
4.2.1.1	Comparison of different plate reader devices	58
4.2.1.2	Influence of different cell culture durations (4, 7, 14 days)	61
4.2.1.3	Kinetic-like- vs. steady-state-studies	64
4.2.1.4	Influence of different tested parameters on the intracellular calcium level	67
4.2.2	Influence of Ca ²⁺ -level modulators	69
4.2.2.1	NMDA receptor modulators	69
4.2.2.2	Acetylcholine as calcium modulator	78
4.2.2.3	Bay-K 8664 and Verapamil as calcium modulators	82
4.2.2.4	Influence of a plasma membrane Ca ²⁺ -ATPase modulator and inhibition of the Ca ²⁺ -release from the sarcoplasmic reticulum	85
4.3	Recheck for the presence of the NMDA receptor by immunofluorescence microscopy in cell line ECV304	87
4.3.1	Immunofluorescence images of non-permeabilized ECV304 cells	87

4.3.2 Attempt to induce NMDA receptor expression on the surface of ECV304 cells by a pre-stimulation with 1 mM glutamate	98
4.4 Influence of 1 mM glutamate with/without 10 μ M MK801 on the transendothelial electrical resistance (TEER)	101
4.5 Influence of 1 mM glutamate with/without 10 μ M MK on specific protein-expressions	103
5 Discussion	109
6 Conclusion	117
7 References	119
8 Abbreviations	125
9 Curriculum Vitae	129

1 Introduction

The blood-brain barrier (BBB) is an essential protection system to maintain the function of the central nervous system. Interactions between endothelial cells, astrocytic end-feet, pericytes and basal membrane primarily induce those special properties which lead to a functional BBB. With the emerging features and characteristics this barrier is able to control the supplies of nutrients for the brain and ion gradients as it also prevents uncontrolled flux of ions, amino acids, peptides and xenobiotics capable of disturbing neuronal functions [1].

The special constitution and properties of the BBB will be summarized after a short historical review.

1.1 History of the Blood-Brain Barrier

Before more than 100 years, Paul Ehrlich (1854-1915) injected defined dyes into the vascular system in 1885, which were quickly taken up by the organs. Only the brain and the spinal cord had been pictured as a special case where no drugs had been found and Ehrlich misinterpreted his findings as a lack of affinity of the nervous system for these dyes [2]. At a later date same dyes had been injected into the cerebrospinal fluid by Ehrlich's associate Edwin Goldman. He discovered that only the nervous tissues were stained and something prevented the dyes from gaining access to the blood circulation.

The term „blood-brain barrier“ was first characterised by Lewandowsky. In 1890, he had performed experiments showing that potassium-hexacyanoferrate (II) only affected brain function when directly injected into the brain but not when injected into the vascular system. Nearly at the same time Biedl and Kraus demonstrated the similar effects with bile acid in the brain. Approximately after further 70 years the capillary endothelial cells within the brain had been identified as the main component of the „barrier“ by electron-microscopic studies from Reese and Karnovsky (1967) and Brightman and Reese (1969).

1.2 Components of the Blood-Brain Barrier

1.2.1 Endothelial cells

In contrast to endothelial cells (EC) of the peripheral circulation brain microvascular endothelial cells (BMEC) (Fig. 1.1) are characterised by structural components called tight junctions (TJ) [3]. A very small pinocytotic activity, lacks of fenestration and an increased amount of cytosolic mitochondria are further typical features of the BBB [3, 4]. Moreover an enzymatic barrier that is capable of metabolizing drugs and nutrients could be found in BMEC as γ -glutamyl-transpeptidase (GGTP), alkaline-phosphatase (AP) and aromatic acid decarboxylase. The distribution and functionality of a variety of transporters as P-glycoprotein (P-gP) at the BBB play also an important role in protecting the brain of possibly harmful xenobiotica.

1.2.2 Astrocytes

Astrocytes (AC) are glial cells that envelop ~99% of the BBB endothelial cells [3]. Generally, astrocytes support neurones with nutrients through contacts to the blood vessel, since neurons never encounter the bloodstream. Specific characteristics of astrocyte end-feet are high concentrations of the water channel aquaporin 4 (AQP4) and the K^+ channel Kir4.1, which are important for the fluid regulation in the brain and in the potassium-household [4].

Moreover, recent in vitro studies showed influence of astrocytes on BMEC, which resulted in tighter TJ, the expression and polarized localization of transporters as P-gP and GLUT1 and specialized enzyme systems [5, 6]. A few of those studies also showed evidence, that a direct interaction between endothelial cells and astrocytes was not necessary to induce BBB properties in BMEC because astrocyte conditioned medium (ACM) alone revealed similar but weaker beneficial effects.

1.2.3 Pericyte

Pericytes (PC) are cells that cover about 20-30% of endothelial cells from microvessels including capillaries, venules and arterioles. Their appearance is restricted to every second

to fourth BMEC, whereby PCs prefer to be close to a contact-spot of two EC. Although PCs are separated through a basal lamina from BMEC, a direct contact is possible through gap junctions. It's been suggested that PC can also influence the regulation of EC proliferation, survival, migration, differentiation and vascular branching by those contacts [3]. Under pathological conditions like hypoxia or traumatic brain injury PC can migrate away from brain microvessels which lead to an increased BBB permeability. Therefore, probably also PC play a major and beneficial role – similar effects were already seen with AC – in maintaining the tightness and structural integrity of the BBB [3,7].

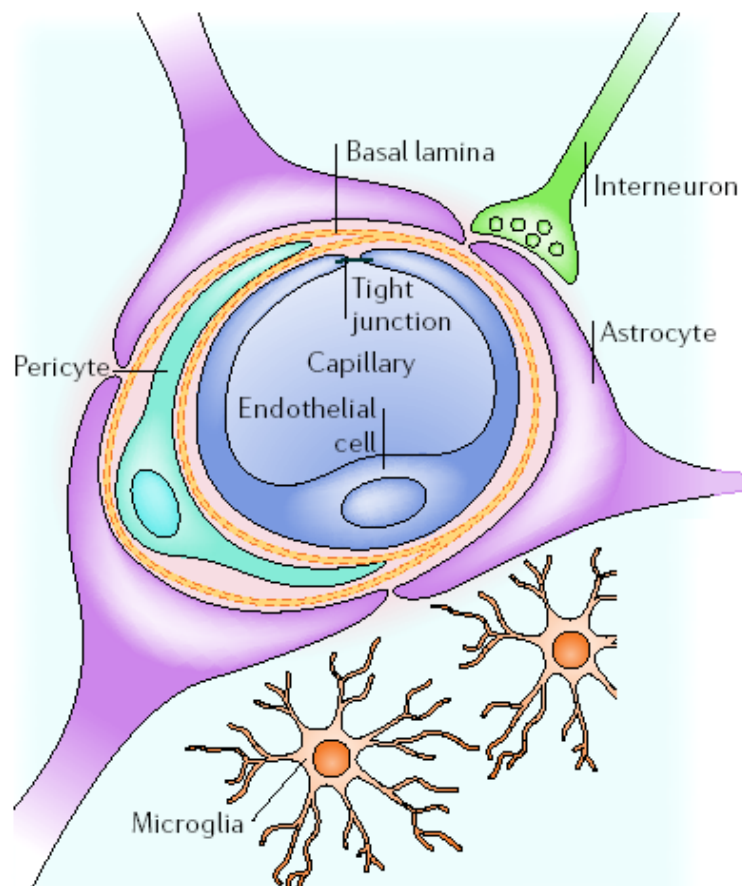


Fig. 1.1: Cellular constituents of the blood-brain barrier [5]

1.2.4 Basal lamina

The basal lamina is an about 40-50 nm thick layer of proteins that surrounds the endothelial cells and pericytes. Moreover, it represents a non-cellular component of the BBB. Assemble of type IV collagen, fibronectin, laminin and different proteoglycans, the basal lamina build up some sort of specialized extracellular matrix. Pathological conditions like ischemic stroke can cause an increased BBB permeability by disappearance of important components like type IV collagen, fibronectin and laminin [11].

1.3 Physiology of blood-brain barrier junctional complexes

BMEC are connected by a strong cell-cell-association that is characterized by a junctional complex including adherens junctions (AJ), tight junctions (TJ) and possibly gap junctions (Fig. 1.2) [7].

1.3.1 Adherens junctions

AJ are protein complexes that occur between cell-cell-associations, mediating adhesion of vascular EC to each other, contact inhibition during vascular growth and remodelling, initiation of cell polarity, and some participation in the regulation of paracellular permeability. The main component of AJ is vascular endothelial cadherin (VE-cadherin), that is connected through the catenin-binding region over other AJ including α -catenin, β -catenin, plakoglobin (γ -catenin), p120 (δ -catenin) to the actin cytoskeleton. Even though studies showed that TJ were predominantly responsible for the low paracellular permeability and a high electrical resistance, a disruption of AJ can also cause an increased permeability [7].

1.3.2 Tight junctions

As already mentioned, the interactions of TJ-proteins between BMEC primarily play the important role in the maintenance of BBB tightness. Therefore, this fusion will nearly

exclude every paracellular transport and force substances to permeate transcellularly through the membranes and the cytosol (Fig. 1.3).

A few plasma membrane proteins have been identified as TJ proteins such as claudins, occludin and junctional adhesion molecules (JAM). Those transmembrane TJ-proteins are linked by cytoplasmatic TJ anchoring proteins like ZO-1, ZO-2, ZO-3 (zonula occludens) and cingulin to actin [8].

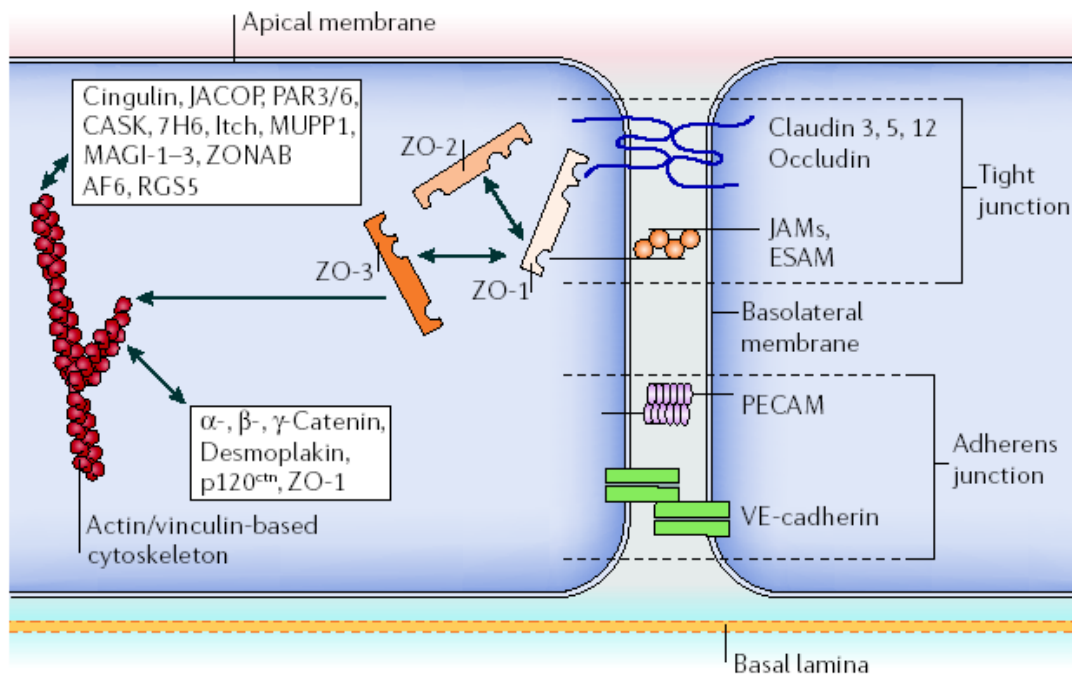


Fig. 1.2: Molecular composition of endothelial tight junctions [5]

1.3.2.1 Occludin

In 1993, Occludin was the first identified integral membrane protein of the tight junctions. With his 65 kDa this phosphoprotein is considerably bigger than Claudins [12], moreover it also shows no sequence similarity to this protein. From the structural point of view Occludin has four transmembrane domains with a long carboxyl and a short amino terminal directed to the cytoplasm. Two extracellular loops spanning the intercellular cleft form together with claudin one part of the paracellular barrier of the BBB. The

cytoplasmatic C-terminal domain of occludin is directly associated with the cytoplasmatic anchoring proteins ZO-1 and ZO-2 and provides the connection to the cytoskeleton [7].

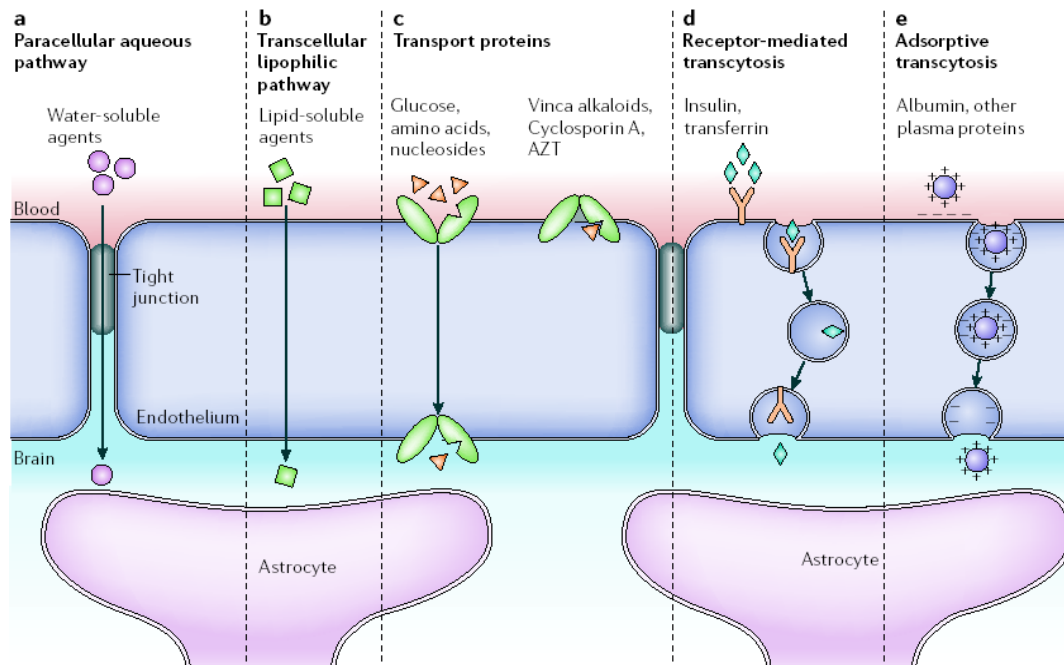


Fig. 1.3: Pathways across the BBB [5]

1.3.2.2 Claudins

Since 1998 at least 18 proteins of the claudin – family have been identified in human. All of those 20–24 kDa phosphoproteins have their own specific sequence. Nevertheless similar predicted foldings and a high sequence homology among the first and fourth transmembrane domain and their extracellular loops exist [3]. Homophilic and heterophilic interactions of those extracellular loops provide a tight contact between the cells. Moreover, it is assumed that claudins are responsible for generating the primary TJ – connection between each cell, whereas occludin subsequently improve the tightness of TJ [7]. It is assumed that Claudin-3, Claudin-5 and Claudin-12 are expressed primarily in the endothelial cells of the BBB.

1.3.2.3 Junctional adhesion molecules (JAM)

Until now the function of junctional adhesion molecules (JAM) in the mature BBB is still largely unclear. JAM-1, an about 40 kDa protein, is a member of the IgG superfamily. It consists of single membrane-spanning chains that have a large extracellular domain, mediate – probably through homophilic interactions – the early attachment of adjacent cell membranes in the BBB [12].

1.3.2.4 Cytoplasmatic TJ anchoring proteins

Besides transmembrane components of TJ, there are several anchoring proteins, including zonula occludens (ZO-1, ZO-2, ZO-3), cingulin, AF-6 and others that connect with them in the cytoplasm [12]. The association with TJ was firstly proven for ZO-1, a 220 kDa phosphoprotein [7]. It belongs with ZO-2 and ZO-3 to the membrane-associated guanylate kinase (MAGUK) proteins that are also accessory elements for the transmembranous components of TJ in the cytoplasm. However, most is known about ZO-1 which connects the transmembrane proteins of TJ to the actin cytoskeleton – e.g. the C-terminus from occludin binds over ZO-1 to actin filaments. An increased BBB permeability is also associated with the dissociation of ZO-1 from the complex of tight junctions with the cytoskeleton [3].

1.4 Calcium signalling and calcium metabolism

The divalent cation calcium (Ca^{2+}) acts as intracellular second messenger controlling many essential cellular processes including muscle contraction, secretion, metabolism, neuronal excitability, cell proliferation and cell death. Former studies on BBB regulation of tightness and its decrease, demonstrated the importance of this second messenger. Moreover extracellular Ca^{2+} depletion and/or an intracellular increase were known to increase BBB disruption of TJ, even before some of those specific proteins were well characterized [13].

Two main pathways for Ca^{2+} signalling in living cells are possible, whereas either an influx from the extracellular space through channels in the plasma membrane or a release from internal stores occur. The Ca^{2+} level of cells at rest are kept between 10–100 nM,

stimulation lead to increased cytosolic concentrations up to 1 μM or even more [14]. Since only stimulations will cause cell-damage after a period of time, a counter-regulation is needed to ensure balance. Such counter-regulations should reduce high Ca^{2+} concentration and adjust again to a normal concentration in the nM range. Those “On” and “Off” mechanism – characterized by the increase or decrease of cytosolic Ca^{2+} concentrations – are so coordinated that they produce brief spikes and waves to generate different signals for cell regulation (figure 1.4).

1.4.1 Ca^{2+} – “On” mechanism

1.4.1.1 Plasma membrane channels

A diversity of Ca^{2+} influx channels at the plasma membrane are known that can be grouped by the way of their activation.

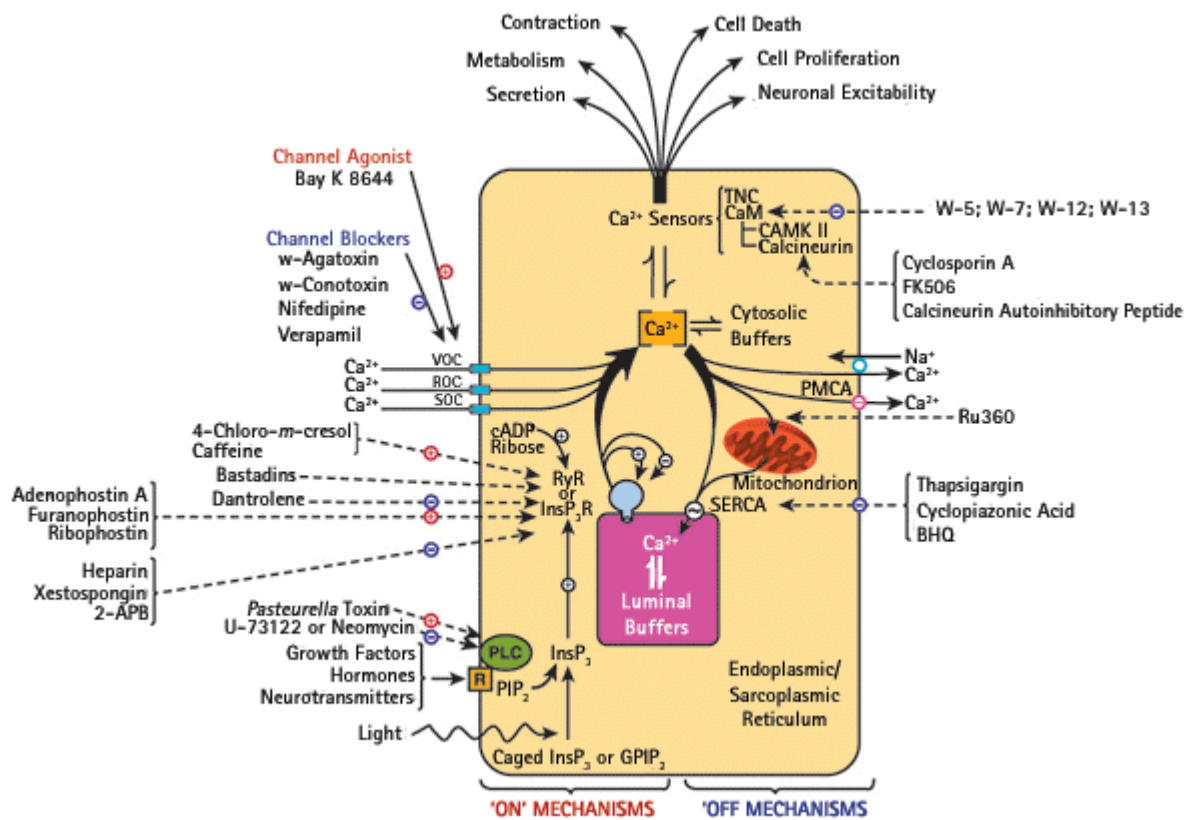


Fig. 1.4: Overview of the “On”- and “Off”-mechanisms and modulations of intracellular calcium level [14]

Voltage-operated channels (VOC): Depolarization of the plasma membrane triggers a selective influx of calcium ions into the cell. This family is divided in L-, T-, N-, P/Q- and R-type channels that vary in the basis of their kinetics and pharmacological properties.

Receptor-operated channels (ROC): This group of receptors like NMDA-receptor or AMPA-receptor needs specific binding of an agonist whereby the channel opens and a Ca^{2+} entry takes place.

Store-operated channels (SOC): These channels were activated when the calcium of the internal stores deplete. However, the interaction between internal stores with SOC is still unclear. A communication over a calcium-influx factor (CIF) and/or over direct protein-protein interactions is assumed.

1.4.1.2 Intracellular Ca^{2+} channels

Inositol 1, 4, 5-trisphosphate receptors and Ryanodine receptors are those substitutes for the merging of different signalling pathways. Activation of these channels are possible by numerous factors like phosphorylation, adenosine-nucleotides, thiol-reactive compounds, pH and the Ca^{2+} load of the endoplasmatic reticulum or sarcoplasmatic reticulum (ER/SR) [9].

Inositol 1, 4, 5-trisphosphate (InsP_3) receptor: Specific receptor like G-protein-linked or tyrosine kinase-linked receptors leads to activation of phospholipase C that produce the second messenger (InsP_3). This messenger diffuses into the cell interior to release stored Ca^{2+} from the ER/SR by binding on InsP_3 receptors.

Ryanodine receptor (RZR): These receptors have similar structural and functional properties compared to InsP_3 receptors; also their sensitivity to cytosolic Ca^{2+} concentrations are related to those, although RZR were generally activated and inhibited by higher concentrations [9].

1.4.2 Ca^{2+} – “Off” mechanism

In order to avoid cell damage, an increased cytosolic calcium signal has to be decreased again through those counter-regulations or so called “Off” mechanism.

Sodium-calcium exchangers are pumps on the surface of the cell membrane that are mainly expressed in the heart and brain. During each reaction cycle an influx of three sodium ions was performed while one Ca^{2+} ion is effluxed. The energy needed for this pump is

generated by the Na^+/K^+ ATPase and the activity of the $\text{Na}^+/\text{Ca}^{2+}$ exchanger is dependent on factors as Na^+ , Ca^{2+} , intracellular pH and ATP.

The ubiquitous Ca^{2+} -ATPase (PMCA), found on the plasma membrane, is another “Off” mechanism controlled by a diversity of factors including calmodulin, acidic phospholipids and protein kinases A and C. Together with the $\text{Na}^+/\text{Ca}^{2+}$ exchanger the PMCA is the main regulator for intracellular down-regulation of calcium concentrations.

Structurally similar to PMCA the uptake from the cytoplasm to the internal stores is characterized by a sarco/endoplasmic reticulum Ca^{2+} ATPase (SERCA).

1.5 The NMDA-receptor

The NMDA receptor is a specific type of ionotropic glutamate receptor. The name is derived from its selective agonist N-methyl-D-aspartate (NMDA). The majority of the literature sees the NMDA receptor being present as a key signalling protein with complex roles in the physiology of the central nervous system (CNS). There this channel is needed consistently for synapse formation, maintenance and is involved in brain functions like learning, memory and certain behaviours [10]. More and more studies also reported the presence of this target in extra-synaptic locations like the spinal cord, osteoblasts, osteoclasts and their progenitors, but their physiological role there is still not clarified. Also the presence and participation in major regulatory mechanisms at the BBB had been reported [18, 20, 21].

The importance of this receptor seems to become clear, when someone considers that this receptor is indispensable to life for normal brain function and probably also other functions in the body. However, an extra activation or over-stimulation of this target by a diversity of disease processes and conditions such as Alzheimer’s disease, epilepsy or stroke – although they are caused by different mechanism – can subsequently cause cell death [15, 16].

1.5.1 Organization and functionality of the NMDA receptor

In contrast to other members of the glutamate receptor family, the NMDA receptor requires NR-1 as well as NR-2 subunits to form a functional ion channel, whereby

literature sees this target currently as a heterotetramer, being assembled of combinations of two NR-1 and two NR-2A through -2D. NR-1 subunits are needed in every functional receptor, unlike the other subtypes. For example, presence of different NR-2 subunits varies in specific regional expression patterns [16]. Although many of this information is mostly based on the analysis of rodents, more and more reports also claim similar, but not identical expression patterns by the human.

Various studies also dealt with the functionality of the subunits or specific subunit combinations (Fig. 1.5). Thus, the NR-1 subunit possesses the binding site for glycine (or D-serine), which must be occupied before binding of glutamate on the NR-2 subunits which then leads to an opening of the NMDA receptor. Even though, glycine and glutamate opened under physiological conditions the channel, the passage is still blocked by an Mg^{2+} ion at rest. Only after sufficient depolarization, the Mg^{2+} -block is alleviated in a voltage-dependent manner and lead to a permeation of calcium, sodium and potassium. This needed depolarization can vary depending on the formation of the receptor; NR-2A or NR-2B subunits leads to high-conductance channel openings, whereby NR-2C or NR-2D subunits form receptors with low-conductance channel openings. Another interesting characteristic of NR-1 subunits is that they can form homo-dimers on their own and it is also hypothesized that such dimers were formed even before the receptor is created. Some of those studies also show that the constitution of the NMDA receptor is a complex process requiring time for forming the functional receptor [17].

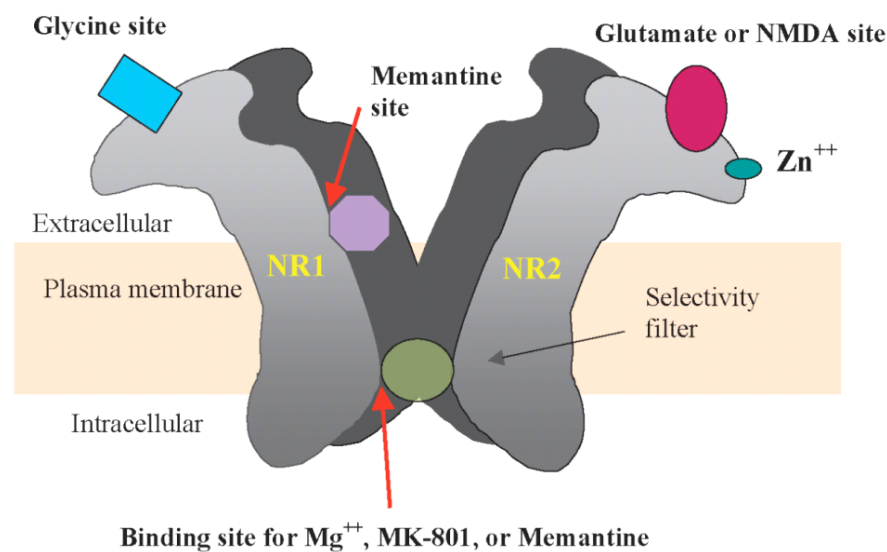


Fig. 1.5: Model of the NMDA receptor illustrated with some important binding-sites [16]

1.5.2 Role of the NMDA receptor on the BBB

A failure of the protective and regulative function of the blood-brain barrier must be seen as a critical event in the development and progression of several diseases that affect the CNS. More and more often the NMDA-receptor becomes the center of attention although the role on the BBB is still not clear. However, the participation of this target in a diversity of diseases on the blood-brain barrier was reported in several studies. During pathological conditions like ischemia and stroke the abundant excitatory amino acid glutamate increases dramatically [18]. This increased level of extracellular glutamate could result in an overstimulation of several types of glutamate receptors that are expressed on cerebral endothelial cells [18, 19]. This overstimulation of especially the NMDA receptor causes a loss in BBB properties and also results in a disruption of the barrier. Increased permeability of BBB-models due to glutamate overstimulation were already seen before [18, 20], but the cause of this disruption were not fully understood. However, a clue was given by András et al. [21], who showed glutamate- induced alterations of tight junction

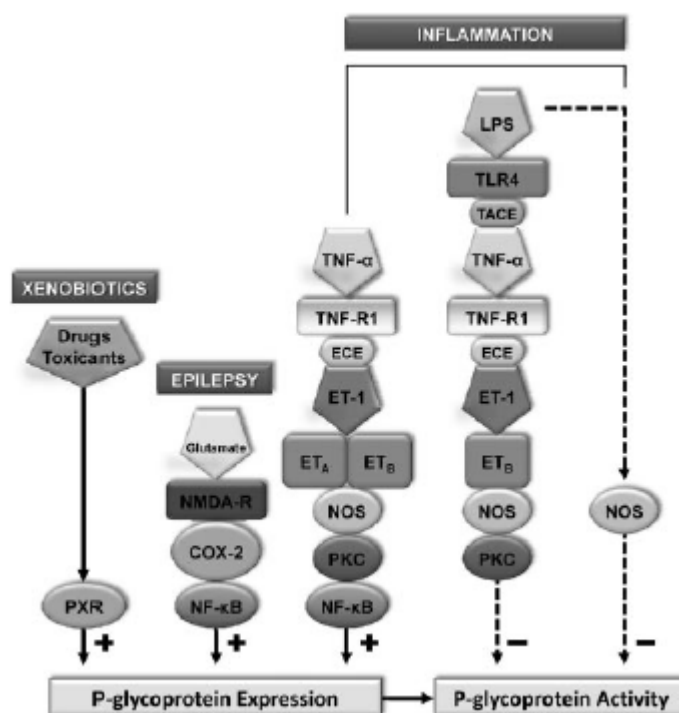
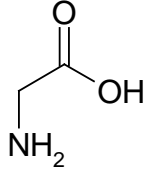
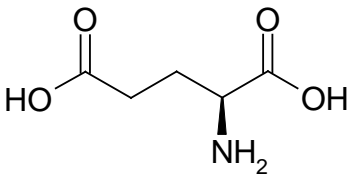
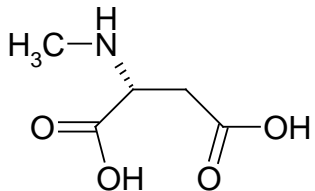
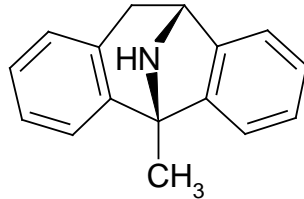


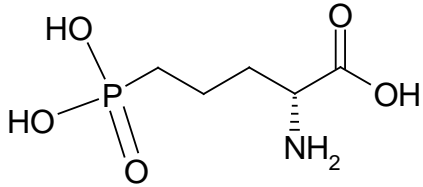
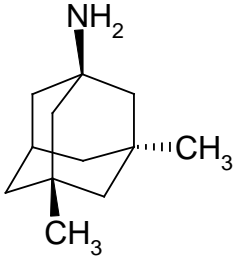
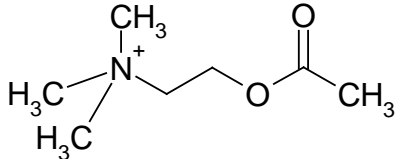
Fig. 1.6: Signaling Mechanisms that modulate P-gp activity in rodent brain capillaries [23]

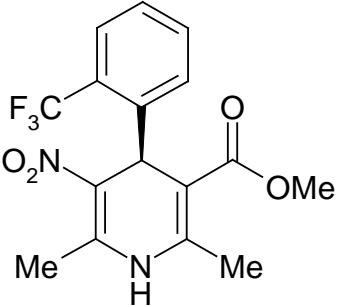
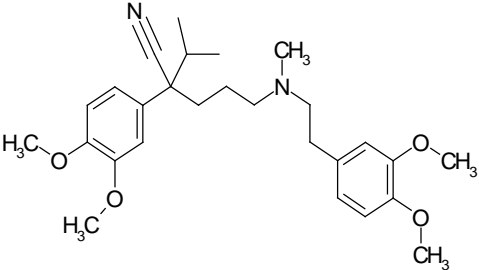
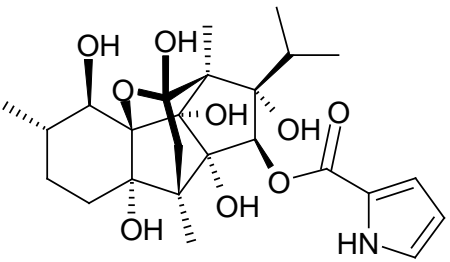
protein expression. Not only an increased BBB permeability and a decreased expression of tight junctions were results of an overstimulation of the NMDA receptor by glutamate. A major problem in the therapy of many brain disorders is also the resistance to the drug treatment [22]. The probably most intensively studied resistance mechanisms are caused by drug transporters [22, 23, 24]. Studies also already showed that overstimulation of the NMDA-receptor during diseases like epilepsy is one possible pathway (Fig. 1.6) that lead to an up-regulation of efflux transporter P-gP [25, 26], what could also prevented by NMDA-receptor antagonists.

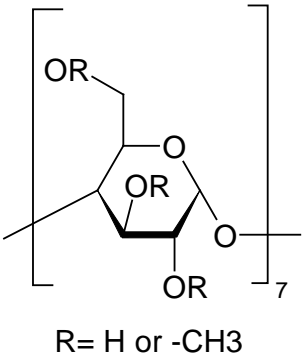
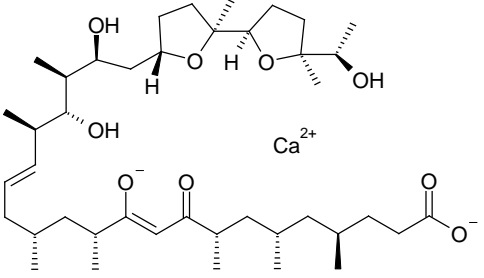
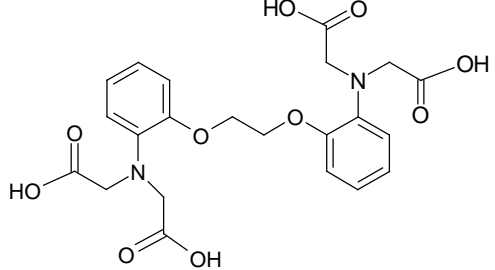
In summary the NMDA-receptor seems to be important at the blood-brain barrier, although his real functions are still not clear yet. However, a participation of this target during different pathological disorders was already reported and it remains to be followed if new therapy approaches could be found targeting NMDA-receptor dependent pathways.

Following tables provide an overview of the substances used in this diploma thesis including molecular structures and kinetic data related to the NMDA-receptor and other targets.

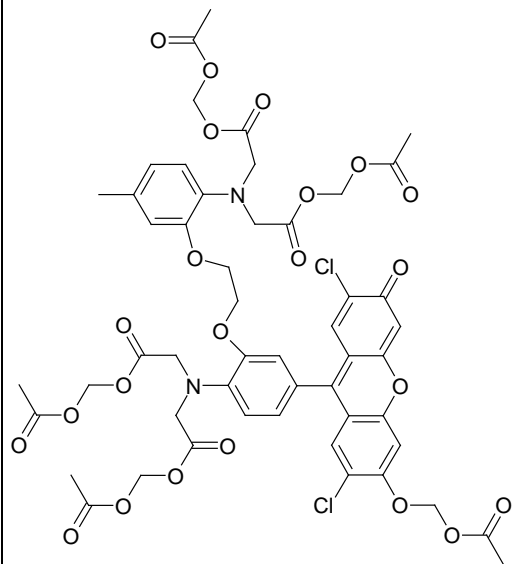
Substance	Structural formula	EC ₅₀ /IC ₅₀ -values	Cells/Cell-line	Method and Target	Reference
Glycine		EC ₅₀ = 27 μM	Cerebral cortices from Sprague-Dorley rats	LDH-release assay over NMDA-receptor	[27]
L-Glutamate acid		EC ₅₀ = 50 μM	Isolated neurohypophysiol nerve terminal from male Sprague-Dorley rats	Ca ²⁺ -influx assay over NMDA-receptor	[28]
NMDA N-methyl-D-aspartic acid		EC ₅₀ = 364 μM EC ₅₀ = 30 μM EC ₅₀ = 5.7 μM	Cerebral cortices from Sprague-Dorley rats Isolated neurohypophysiol nerve terminal from male Sprague-Dorley rats Mesencephalic tissue from Wistar rat fetuses	LDH-release assay over NMDA-receptor Ca ²⁺ -influx assay over NMDA-receptor Ca ²⁺ -influx assay over NMDA-receptor	[27] [28] [29]
(+)-MK801 Dizocilpine (+)-5-methyl-10,11-dihydro-5H-dibenzo[a,d]cyclohepten-5,10-imine maleate		IC ₅₀ = 120 nM (Hippocampus) IC ₅₀ = 270 nM (Striatum)	Isolated hippocampus or striatum of 12-14 days old Wistar rats	Patch-clamp assay of NMDA-receptor	[30]

<p>D-APV 2-amino-5-phosphonopentanoic acid</p>		<p>IC₅₀ = 3.7 μM</p>	<p>Cerebral cortical neurons</p>	<p>Binding-studies assay of NMDA-receptor</p>	<p>[31]</p>
<p>Memantine 3,5-dimethyltricyclo[3.3.1.1.3,7]decanamin</p>		<p>IC₅₀ = 1.4 μM (Hippocampus) IC₅₀ = 2.93 μM (Striatum) IC₅₀ = 170 nM</p>	<p>Isolated hippocampus or striatum of 12-14 days old Wistar rats Mesencephalic tissue from Wistar rat fetuses</p>	<p>Patch-clamp assay of NMDA-receptor Ca²⁺-influx assay over</p>	<p>[30] [29]</p>
<p>Acetylcholine</p>		<p>EC₅₀ = 30 μM</p>	<p>Xenopus laevis</p>	<p>Voltaged-clamped assay of nACh-receptor</p>	<p>[32]</p>

<p>(S)-(-)-BayK 8644</p> <p>(4S)-1,4-dihydro-2,6-dimethyl-5-nitro-4-[2-(trifluoromethyl)phenyl]-3-pyridinecarboxylic acid methyl ester</p>		<p>EC₅₀ = 30 μM (at -80 mV)</p>	<p>Guineapig ventricular tissue</p>	<p>Patch-clamp assay of voltage-dependent calcium channel</p>	<p>[33]</p>
<p>Verapamil</p> <p>(RS)-2-isopropyl-2,8-bis(3,4-dimethoxyphenyl)-6-methyl-6-azaoctanitril</p>		<p>(+/-)IC₅₀ = 1.8 μM (-) IC₅₀ = 900 nM (+)IC₅₀ = 3.6 μM</p>	<p>NCB-20 cells</p>	<p>Ca²⁺-uptake assay of voltage-sensitive calcium channels</p>	<p>[34]</p>
<p>Ryanodine</p> <p>1H-Pyrrole-2-carboxylic acid, (3S,4R,4aR,6S,7S,8R,8aS,8bR,9S,9aS)-dodecahydro-4,6,7,8a,8b,9a-hexahydroxy-3,6a,9-trimethyl-7-(1-methylethyl)-6,9-methanobenzo[1,2]pentaleno[1,6-bc]furan-8-yl ester</p>		<p>IC₅₀ = 10 nM (skeletal muscles) IC₅₀ = 2.8 μM (cardiac muscles) IC₅₀ = 2.7 μM</p>	<p>NCB-20 cells</p>	<p>Ca²⁺-uptake assay of voltage-sensitive calcium channels</p>	<p>[35] [34]</p>

Methyl- β -cyclodextrine	 <p>R= H or -CH₃</p>		Removes plasma membrane Ca ²⁺ -ATPase (PMCA) from the membrane
Ionomycin	 <p>Ca²⁺</p>		Positive control of the Ca ²⁺ -measurement
BAPTA			Negative control of the Ca ²⁺ -measurement

Fluo3-AM



Fluorescence-dye of the
 Ca^{2+} -measurement

2 Aims of the thesis

The NMDA-receptor is a key player for synapse-formation, -maintenance and is involved in brain functions like learning, memory or certain behaviours. However, an overstimulation of this target is also involved in the induction of apoptosis due to neurotoxic effects. At present time such incidents could increasingly be seen in the light of pathological conditions like neurodegeneration. Recent studies now also reported the presence and participation of this glutamate-gated ion-channel in major regulatory mechanisms at the blood-brain barrier [18, 20, 21, 25]. Therefore, the work of our research group aids in investigating the hypothesis of an important role of the BBB in neurodegeneration, to develop possible therapeutic interventions based on this assumption. Following aims were preassigned or accordingly amended during this diploma thesis:

- The confirmation of the presence of the NR-1 subunit in our human BBB *in vitro* model based on the work of Kuhlmann et al. [20] by methods as western blot analysis and immunofluorescence microscopy. Furthermore, the presence of NR-2A, -2B and – 2C subunits should be checked, in order to get an impression of possible compositions of a functional NMDA receptor in cell line ECV304.
- The major aim of this thesis was to establish a 96-well plate fluorescence-assay for measuring the intracellular Ca^{2+} -level for determining the influence of different NMDA-receptor agonists and antagonists onto it. Thus pathological conditions should be simulated or prevented, whereby the change in intracellular calcium could be used as a functional parameter to predict BBB stabilization or disruption.
- Furthermore, methods as the measurement of the transendothelial electrical resistance (TEER) and western blotting should be performed, in order to investigate the influence of over-stimulation or inhibition of the NMDA-receptor on specific BBB properties.

3 Material and Methods

3.1 Chemicals

3.1.1 Antibodies (AB)

Actin (C-11) (A2066), rabbit polyclonal AB, Sigma-Aldrich

Cox-1 (5F6/F4) (sc-52971), mouse monoclonal AB IgG₁, Santa Cruz Biotechnology

Cox-2 (5E10/D10) (sc-52972), mouse monoclonal AB IgG₁, Santa Cruz Biotechnology

Human E-Selectin/CD62E (BBA16), mouse monoclonal AB IgG₁, R&D Systems

ICAM-1 (G-5) (sc-8439), mouse monoclonal AB IgG_{2a}, Santa Cruz Biotechnology

Mdr (C-19) (sc-1517), goat polyclonal AB, Santa Cruz Biotechnology

MRP-1 (IU2H10) (sc-53130), mouse monoclonal AB IgG₁, Santa Cruz Biotechnology

NMDAR1 (ab52177), NMDAR-NR-1, rabbit polyclonal AB, AbCam

NMDA ϵ 1 (sc-9056), NMDAR-NR-2A, rabbit polyclonal AB, Santa Cruz Biotechnology

NMDA ϵ 2 (sc-9057), NMDAR-NR-2B, rabbit polyclonal AB, Santa Cruz Biotechnology

NMDA ϵ 3 (sc-50437), NMDAR-NR-2C, rabbit polyclonal AB, Santa Cruz Biotechnology

NMDA ζ 1 (sc-9058), NMDAR-NR-1, rabbit polyclonal AB, Santa Cruz Biotechnology

Occludin (33-1500), mouse monoclonal AB, Zymed, Molecular Probes® Invitrogen

ZO-1 (33-9100), mouse monoclonal AB, Zymed, Molecular Probes® Invitrogen

Secondary donkey anti-goat IgG-HRP (sc-2020), Santa Cruz Biotechnology

Secondary goat anti-mouse IgG-HRP (sc-2005), Santa Cruz Biotechnology

Secondary goat anti-rabbit IgG-HRP (sc-2004), Santa Cruz Biotechnology

Secondary goat anti-rabbit IgG-Alexa Fluor 546 (A-11010), Molecular Probes® Invitrogen

Human cerebellum (ab30078), whole cell lysate, adult normal tissue, AbCam

Mouse cerebellum extracts tissue (sacsc-2403), Santa Cruz Biotechnology

3.1.2 Chemicals

1,2-Bis(2-aminophenoxy)ethane-N,N,N',N'-tetraacetic acid tetrasodium salt (14513),
Sigma-Aldrich

(+)-MK801 hydrogen maleate (M107), Sigma-Aldrich
(S)-(-)-Bay K 8644 (1546); Tocris Bioscience
Acetylcholine chloride (A2661), Sigma-Aldrich
Acrylamide 2x (10675), Serva Electrophoresis GmbH
Albumin from bovine serum (A8022), Sigma-Aldrich
Ammonium persulfate (13375.01), Serva Electrophoresis GmbH
Amphotericin B (A2942), Sigma-Aldrich
Bicarbonate (25080-060), sterile, 7.5 %, Invitrogen Life technologies
Bromphenol blue (15375), Na-salt, Serva Electrophoresis GmbH
BSA (A-8806), fraction V powder, Sigma-Aldrich
CHAPS (17038), Serva Electrophoresis GmbH
Collagen bovine (150703), MP Biomedicals
Coomassie Brilliant Blue G250 pure (17524), Serva Electrophoresis
D(-)-2-Amino-5-Phosphono-pentanoic acid (A8054), D-APV, Sigma-Aldrich
DMEM (41966), plus 4.5 g/L glucose, L-glutamine and pyruvate, Gibco™
DMSO (1.02952.1000), MerckKGaA
DTT, research grade (20710), Serva Electrophoresis GmbH
Fluo-3-AM (F14218), 1mM solution in DMSO, Invitrogen
Fluorsave™ Reagent (345789), Calbiochem®, Merck Biosciences
Gelatin from bovine skin, Type B (G9391), Sigma-Aldrich
Glycerol (23390), Serva Electrophoresis GmbH
Glycine anal. Grade (23390), Serva Electrophoresis GmbH
Ham's F12 (21765-029), sterile, Invitrogen Life technologies
HBSS (H4641), 10x, sterile filtered, Sigma-Aldrich
HBSS (H6648), modified, without phenol red, calcium chloride and magnesium sulphate, Sigma-Aldrich
HBSS (H8264), modified with sodium bicarbonate, without phenol red, Sigma-Aldrich
Heparin sodium salt from porcine intestinal mucosa (5151), Fluka
Hepes (15630-049), 1 M, sterile, Invitrogen Life technologies
IMDM (21980-032), sterile, Invitrogen Life technologies
Ionomycin calcium salt from Streptomyces conglobatus (I0634), Sigma-Aldrich
L-Glutamic acid monosodium salt hydrate (G1626), Sigma-Aldrich
L-glutamine (25030-024), 200mM, sterile, 10x, Invitrogen Life technologies
MeOH (8404), HPLC-grade, Malinchrodt Baker B.V.

Methyl- β -cyclodextrin (C4555), Sigma-Aldrich
Milk powder (Art.-Nr.: T145.2) blotting grade, Carl Roth GmbH & Co.KG
Molecular weight standard (161-0373), all blue stained, Precision Plus Protein™, Biorad Laboratories
N,N'-methylenebisacrylamide 2x (29195), research grade, Serva Electrophoresis GmbH
NCS (26010-74), sterile, Invitrogen Life technologies
N-Methyl-D-aspartic acid (M3262), NMDA, Sigma-Aldrich
PageRuler Prestained Protein Ladder (#SM0671), Fermentas Life Science
Paraformaldehyde (P-6148), Sigma-Aldrich
PBS (14190-094), sterile, Invitrogen Life technologies
Penicillin/Streptomycin (15140-122), 100x, sterile, Invitrogen Life technologies
Pluronic F-127 (P3000MP), 20% solution in DMSO, Invitrogen
Probenecid (P8761), p-(Dipropylsulfamoyl)benzoic acid, Sigma-Aldrich
Propidium iodide (P4170), Sigma-Aldrich
Protease inhibitor cocktail (P8340), Sigma-Aldrich
Ryanodine (1329), Tocris Bioscience
TEMED research grade (35925), Serva Electrophoresis GmbH
Thiourea (88810), Serva Electrophoresis GmbH
Transferrin holo (T-0665), for cell culture, Sigma-Aldrich
TRIS research grade (37190), Serva Electrophoresis GmbH
Triton X-100 pure (37240) Serva Electrophoresis GmbH
Trypsin/EDTA solution (15400-054), sterile, 10x, Invitrogen Life Technologies
Tween 20 (37470), Serva Electrophoresis GmbH
Urea (24524), anal. Grade, Serva Electrophoresis GmbH
Verapamil hydrochloride (94837), Fluka Biochemika

Other chemicals as H₂O bidest, H₃PO₄ (85 % (v/v), HCl (6 N), NaOH (2 N), NaCl, CaCl₂, were made of analytical grade

3.2 Materials

3.2.1 Materials

96-well cell culture plate (655180), sterile, crystal-clear, F-bottom, Greiner bio-one
96-well microplate (655090), sterile, black with transparent bottom, F-bottom, Greiner bio-one
12-well plates (353503), BD Biosciences
6-well plates (353046), BD Biosciences
6-well Transwell inserts (353102), BD Biosciences
Autoclave band (84-200-048-CC), steam A, Schinko-Neuroth
Biofuge tubes (Cellstar 188271), 15 mL, Greiner Bio-One GmbH
Biofuge tubes (Cellstar 227261), 50 mL, Greiner Bio-One GmbH
Blottingpads (1703966), extra thick blot paper, 7x 8.4 cm Bio-Rad Laboratories
Cell culture tissue flasks (690160, 658170, 660160) surface area 25 cm², 75 cm², 175 cm², Greiner Bio-One GmbH
Cell scraper (541080), sterile, Greiner Bio-One GmbH
Cover slips, diameter 15 mm, Assistant
Eppendorf vials (616201), 1.5 mL, Greiner Bio-One GmbH
Immun-Star WesternC™ (170-5070), Chemiluminescent Kit, Biorad Laboratories
Microscope slides (02 1102), 76 x 26 mm, Menzel-Gläser
Pipette tips (1-111-96-0, 1-201-96-0), 1-200 µL, 1000 µL, Ahn
PVDF membrane, Immuno-Blot™ (162-0177), Biorad Laboratories
Stericups (SCGPU11RE, SCGVU05RE), 1000 mL, 500 mL, Millipore
Sterile filter (P666.1), sterile, 0.22 µm pore size, Carl Roth GmbH
Sterile syringes (300910, 300812, 3001229), 3 mL, 10 mL, 30 mL, BD Biosciences

3.2.2 Devices and softwares

-20 °C freezer, Öko super, Liebherr-International AG
-80 °C freezer, VX 490 F, Jouan, purchased from Ehret Labor & Pharmatechnik
Automatic wet developing machine (Type 5270), Classic E.O.S, Agfa Medical

Fluorescence microscope Eclipse 50i equipped with an EXFO X-Cite 120 fluorescence illumination system, Nikon

Gel apparatus: Mini-Protean® 3 with a Power Pack 1000 controller unit, Biorad Laboratories

LAS 3000™, Fujifilm, Tokyo, Japan

Image Reader Las 3000™ 2.0, Fujifilm, Tokyo, Japan

Incubator Napco 6101-C CO2 (51201015) Ehret Labor & Pharmatechnik

Laminar air flow sterile working bench Biosafe 3, Ehret Labor & Pharmatechnik

Light microscope TMS, Nikon

Microplate reader Polarstar galaxy, BMG Labtechnologies

Microplate reader Tecan Infinite M200i, Tecan

Microplate reader TECAN GeniosPro™, Tecan

Millicell Electrical Resistance System ERS, Millipore

Semi-dry plotter, Trans blot SD semi dry transfer cell, Biorad Laboratories

Shaker GFL, G. Albrechts's WTW.Nachf.

Thoma chamber superior, Paul Marienfeld GmbH & CoKG

Ultrasound bath Sonorex RK255H, Bandeline

Software Quantity One 4.1.0, Biorad Laboratories

Software Fluostar 4.10, BMG Labtechnologies

Aida – Advanced Image Data Analyser v4.06, Raytest Inc.

Magellan 5.03, Tecan, Mannedorf Switzerland

3.3 Cell lines

3.3.1 Rat glioma cell line C6

Rat cell line C6 was obtained from the German Cancer Research Center Heidelberg (DKFZ Heidelberg, Germany). C6 cells were grown at passages 20 to 65 in 175 cm² gelatin coated tissue flasks in C6 medium in order to obtain corresponding astrocyte conditioned media.

3.3.2 ECV304

The ECV304 cell line was obtained from the European Collection of Cell Cultures (ECACC, Wilthshire, United Kingdom). The ECV304 cell line, which was introduced by Takahashi et al. [36] as a spontaneously transformed human umbilical vein cell line, exhibits increased TEER when grown in astrocyte conditioned medium (ACM). Moreover, ECV304 developed many other BBB characteristics including P-glycoprotein (P-gP) or the expression of tight junctions [6]. ECV304 cells were grown between passages 145 to 190 in 25 cm² or 75 cm² gelatine coated tissue flasks in PBMEC medium.

3.4 Cell culture media and solutions

3.4.1 Trypsin/EDTA solution (200 mL)

10x Trypsin/EDTA solution	20 mL
10x HBSS	20 mL
sterile PBS	154 mL
1 M Hepes	2 mL
7.5 % (v/v) bicarbonate	2 mL
10,000 Units/mL penicillin; 10 mg/mL streptomycin	2 mL

3.4.2 C6 medium (1000 mL)

Ham's F12	439 mL
IMDM	439 mL
NCS	75 mL
200 mM L-glutamine solution	35 mL
10,000 Units/mL penicillin; 10 mg/mL streptomycin	10 mL
250 µg/mL amphotericin B	1 mL
10mg/mL humane holo-transferrin	500 µL
1000 U/mL heparin	500 µL

3.4.3 Astrocyte conditioned medium (ACM) of C6 medium

To obtain astrocyte conditioned medium (ACM) the supernatant of C6 cultures was collected every other day (25 mL/day). For further uses the collected ACM (500 mL) were sterile filtered and stored at 4° C.

3.4.4 PBMEC medium (500 mL)

ACM	250 mL
Ham's F12	103.75 mL
IMDM	103.75 mL
NCS	19 mL
200 mM L-glutamine	17.5 mL
10,000 Units/mL penicillin; 10 mg/mL streptomycin	5 mL
250 µg/mL amphotericin B	500 µL
10 mg/mL holo-transferrin	250 µL
1000 U/mL heparin	250 µL

3.4.5 Gelatine solution 1%

Gelatin from bovine skin, Type B	4 g
Aqua bidest	ad 400g

Before use, the gelatine was dissolved for 2 h at >50° C and was then autoclaved.

3.4.6 C6 medium (250 mL), without serum and heparin

IMDM	119,1875 mL
Ham's F12	119,1875 mL
200 mM L-glutamine	8,75 mL
10,000 Units/mL penicillin; 10 mg/mL streptomycin	2,5 µL
250 µg/mL amphotericin B	250 µL
10 mg/mL holo-transferrin	125 µL

3.5 Cell culture work/protocol

3.5.1 Coating of cell culture flasks or 96-well plate

Before cell culture flasks are used, they were coated with a 1 % sterile gelatin solution for 20-30 min at RT under the laminar.

T25 flasks	à	2 mL 1% gelatin solution
T 75 flasks	à	6 mL 1% gelatin solution
T175 flasks	à	10 mL 1% gelatin solution
96-well plate	à	50 µL/well 1% gelatin solution

It should be noted that the whole surface was covered with the gelatin solution. After the incubation period the remaining supernatant was removed and the plate/flask was ready for use.

3.5.2 Subculturing of ECV304 or C6 cells

The consumed medium was removed from a confluent cell layer and was washed with sterile PBS twice. Further on, Trypsin/EDTA solution was put into the flask and the confluent cells were incubated for about 3-5 min (ECV304) at room temperature (RT). During this the cell-shape changed from a cobble-stone morphology to a nearly spherical morphology which was controlled microscopically. For C6 cells the Trypsin/EDTA solution was only for about 10 sec on the surface because C6-cells detach very fast. When ECV304 cells nearly reached this spherical state, Trypsin/EDTA solution was removed. Then the flask was knocked for a few times on a table to detach the spherical cells from the surface. Afterwards growth medium was added again into the flask over the whole surface on nine specific points to detach the remaining cells. To get a homogeneous cell suspension the solution with the detached cells was pulled up and down for about 20 times. For further subculturing an appropriate volume of this suspension was put in a new gelatin-coated flask and was filled with growth medium to the adequate volume of the flask. For further cultivation the flask was shaken a little to distribute the cells on the whole surface before it is placed again into the incubator at 37° C, 5 % CO₂ and 96 % humidity.

T25 flask	à	2 mL PBS or Trypsine/EDTA solution
T75 flask	à	6 mL PBS or Trypsine/EDTA solution
T175 flask	à	10 mL PBS or Trypsine/EDTA solution

ECV304 or C6 cells were normally subcultured in a ratio of 1:10 or 1:20.

T25 flask	à	5 mL growth medium
T75 flask	à	15 mL growth medium
T175 flask	à	25 mL growth medium

3.5.3 ECV304 culture in a Transwell™ model and measurement of the transendothelial electrical resistance (TEER)

Before ECV304 cells were seeded, transwell inserts had to be coated with collagen. Therefore 150 µL of a 0.14 mg/mL collagen solution were distributed on a transwell-surface of 4.2 cm². It should be taken care that the whole surface of the insert is covered in the collagen solution. Then the 6-well plates with the inserts were put for one hour into the incubator (at 37° C, 5 % CO₂ and 96 % humidity). Afterwards the remaining supernatant of the collagen solution was removed and the inserts were ready for seeding the ECV304 cells.

ECV304 cells were seeded at a density of 80 000 cells/cm² on the Transwell filter inserts. Cells were counted by using a thoma chamber after they had been detached from the surface of T25 or T75 flasks with Trypsin/EDTA solution and resuspended in an adequate amount of growth medium. It is now beneficial for getting a uniform attachment on the inserts, to prefill each well with 3 mL, the inserts were filled with a certain amount of medium according to the counted cell number that was subtracted from a total volume of 2 mL. Then the cell suspension was added to the inserts and shaken afterwards to get a uniform distribution and subsequent attachment on the surface of the insert. ECV304 cells were cultured for 14 days in an incubator at 37° C, 5 % CO₂ and 96 % humidity, whereby the medim was changed every other day.

After the cells were cultured for 7 days, the transendothelial electrical resistance (TEER) was measured with a Millipore Millicell Electrical Resistance System. Based on Ohm's law – $V = I \times R$ (V = voltage, I = current, R = resistance) – the resistance reflects the

tightness of the cell–surface against small ions. Following protocol was used for the measurements:

- (a) During the days when the measurement electrode was not used, it was stored in 70 % (v/v) ethanol
- (b) 6-well plates were removed from the incubator and put under the laminar air flow (LAF). Afterwards the old medium was changed immediately and replaced with new, pre-warmed medium. Since the electrical resistance is temperature dependent, the measurements were carried out after incubation at RT for 1 hour.
- (c) Electrodes were plugged in a 15 mL Biofuge tube with an adequate amount of growth medium to equilibrate them at RT for at least 30 minutes.
- (d) Before measurement, plug the electrode for about 10 seconds in 70 % (v/v) ethanol, tap hanging drops off and dip it then into the growth medium.
- (e) Afterwards the electrodes were placed into the first well. Insert was oriented probably in the middle of the well, so that no liquid film was formed due to capillary forces between the walls of the insert and the well. Half of the distance between the boarder of the well and the boarder of the insert the electrode was situated, so that one part extended into the well reaching the ground and one into the insert not touching the insert membrane.
- (f) The electrode should be oriented as vertical as possible and only touched on the blue top by the fingers. When the correct vertical position was found, the measurement-button was pressed and the value of the display was read.
- (g) Blank inserts had been coated at the same time as the inserts, on which the cells were cultured, and were measured in the same series.
- (h) After every measurement the electrodes were put into 70 % (v/v) ethanol for 10 seconds and dipped afterwards in growth medium again.
- (i) After finishing the measurements, the electrodes were put in 70 % (v/v) ethanol for storage again.

To calculate the TEER following formula was used:

$$\text{TEER [Ohm * cm}^2\text{]} = (\text{TEER}_{\text{cell}} - \text{average TEER}_{\text{blank}}) * \text{surface area}$$

3.5.4 Influence of glutamate on the TEER

Cells were cultured in 6-well plates with inserts and TEER was measured as it is described in 3.5.3. After the cells were cultured for 14 days the experiment was performed under following parameters:

- (a) Electrode was stored in 70 % (v/v) EtOH when it was not used.
- (b) 6-well plates were removed from the incubator and put under the LAF. Without a medium change before, the plates were incubated for 1 hour at RT for temperature adjustment.
- (c) – (h) are similar to working streams as in 3.5.3 (c-h) to measure the TEER.
- (i) After this measurement series, the electrode was plugged into 70 % (v/v) ethanol for 10 seconds and stored afterwards in serum- and heparin- free C6-medium for equilibration.
- (j) Now the 6-well plates and inserts were washed twice with sterile PBS.
- (k) Afterwards serum- and heparin- free C6-medium was added into the wells and inserts (3 mL per well, 2 mL per insert). After another 30 min. incubation at RT TEER was measured again. In those wells where an antagonist / channel blocker was added, this incubation time for RT adjustment was also used as pre-incubation step with the channel blockers. Therefore, serum- and heparin- free C6-medium was supplemented with the antagonist at the appropriate concentration.
- (l) Serum- and heparin- free medium or pre-incubation (in the case of glutamate + MK801) medium were replaced with the experimental medium at RT in the wells and the inserts.
- (m) Now the wells were incubated at RT under the LAF and TEER was measured every hour for at least 3 hours.
- (n) Afterwards wells and inserts were washed with sterile PBS twice and were refilled with serum- and heparin- free C6-medium and incubated in an incubator at 37° C, 5 % CO₂ and 96 % humidity for further 21 hours.
- (o) On the next day, one hour before a total experimental time of 24 hours was reached, the 6-well plates were taken out of the incubator and put under the LAF to adjust at RT again.
- (p) Electrodes were plugged into a Biofuge tube with serum- and heparin- free medium to equilibrate it.
- (q) TEER was measured again after 24 hours.

- (r) Afterwards the medium was aspirated and the cell layers onto the inserts were then washed twice and prepared for cell-lysis prior subsequent western blot analysis.

3.5.5 Protein analysis

Cell lysis stock buffer was stored at -20°C in corresponding aliquots and only thawed shortly before use. 400 μL stock lysis buffer were mixed with 2 mg DTT and 4 μL protease inhibitor cocktail. 6-well plates with inserts were placed on ice, growth- or experimental- medium was exhausted and washed twice with PBS. 50 μL of the modified cell lysis buffer were distributed on the cell surface of each insert. Cell disruption was monitored by light microscopy and cells were gently threadbared with the aid of a scraper. 25 μL of this lysis solution containing the cell fragments were immediately stored at -80°C , the remaining solution was centrifuged at 12,000 rpm for 10 minutes. Now the supernatant was also stored at -80°C until further protein analysis.

Cell lysis stock buffer:	8 M Urea
	2 M Thiourea
	0.5 % Trition X-100
	2 % Chaps
	5 mM EDTA

3.5.5.1 Bradford protein determination

In order to determine the protein concentration in a solution – needed for the appropriate volume of a protein solution for western blot analysis – Bradford protein assays were carried out using following protocol:

- Protein samples and a BSA standard (1 mg/mL) were thawed on ice.
- On each measurement day a new calibration curve had to be made. Therefore, BSA standard (1 mg/mL) was diluted to concentrations of 0.1, 0.05 and 0.025 mg/mL.
- 100 μL of each BSA dilutions were added to 1 mL of a pre-warmed (RT) Bradford solution and mixed gently into Eppendorf vials.
- After an incubation at RT for five minutes, the solution was put into a semi-microcuvette and absorption was measured at 595 nm against a blank consisting of 1 mL Bradford solution and 100 μL H_2O bidest. (instead of 100 μL protein solution).

- (e) Afterwards protein samples were measured the same way. Samples had to be diluted with H₂O bidest. in order to receive absorption values within the linear absorption range from 0.2-0.7. BSA dilutions were measured in triplicates and protein samples were measured in duplicates (when values were related).
- (f) Through the equation obtained by linear regression analysis of the calibration curve, concentrations of protein samples could be calculated.

Bradford solution (100 mL):

Coomassie Brilliant Blue G250	10 mg
96 % (v/v) Ethanol	5 mL
85 % (v/v) H ₃ PO ₄	10 mL
H ₂ O bidest.	85 mL

Coomassie brilliant blue G250 was weighted and mixed with circa 40 – 60 mL H₂O bidest. Then, 10 mL of 85 % (v/v) H₃PO₄ was added followed by 5 mL of 96 % (v/v) EtOH. Afterwards it was filled to a total volume of 100 mL with H₂O bidest. and stirred afterwards for 30 – 60 minutes. Finally, the solution was filtered and stored at 4° C.

3.5.5.2 SDS-polyacrylamide gel electrophoresis (SDS-PAGE)

Two different SDS-PAGE separation gels consisting of either 12.5 % acrylamide solution (NMDAR-subunits, Cox-1, Cox-2, E-selectin, ICAM, Occludin, ZO-1) or 7.5 % acrylamide solution (Mdr, MRP-1) were used. Electrophoretic separation were undertaken in a Mini-Protean® 3 apparatus at 125 V controlled by a Power Pack 1000 unit for 75 minutes and was based on following protocol (volume-composition of gels is referred for making two gels):

- (a) Prepare separation buffer, acrylamide buffer and APS before any gel is casted.

Separation buffer 4x (500 mL):

Tris (1.5 M)	90.8 g
SDS (0.4 % (w/v))	2 g
H ₂ O bidest.	ad 500 mL

pH = 8.8 with 6 N HCl, storage at RT

Acrylamide (400 mL):

Acrylamide (30 % (w/v))		120 g
N,N'-methylenebisacrylamide (0.8 % (w/v))		3.2 g
H ₂ O bidest.	ad	400 mL

Storage at 4° C

APS (50 mL):

Ammonium persulfate		5 g
H ₂ O bidest.	ad	50 mL

Storage in 1 mL aliquots at -20° C

Separating gel 12.5 % (v/v) (16 mL):

H ₂ O bidest.		5.42 mL
Separation buffer 4x		4 mL
Acrylamide solution		6.49 mL
TEMED		10 µL
APS		75 µL

Separating gel 7.5 % (v/v) (16 mL):

H ₂ O bidest.		8.1 mL
Separation buffer 4x		4 mL
Acrylamide solution		3.9 mL
TEMED		10 µL
APS		75 µL

(b) It should be noted that the solution should be degassed by ultrasonication before TEMED and APS were added. An appropriate volume of the complete solution was quickly filled into the Mini-Protean® 3 apparatus and covered afterwards with app. 0.5 cm H₂O saturated n-butanol to ensure a straight upper edge of the separation gel. After the separation gel has polymerized the n-butanol was removed. Now the edge was

washed twice with H₂O bidest.. Afterwards it was dried with a small sheet of a filter made of paper.

- (c) The stacking gel was then prepared, as it is described following.

Stacking gel buffer 4x (100 mL):

Tris (0.5 M)		6.06 g
SDS (0.4 % (w/v))		0.4 g
H ₂ O bidest.	ad	100 mL

Storage at RT

Stacking gel (5 mL):

H ₂ O bidest.	3.05 mL
Stacking gel buffer 4x	1.25 mL
Acrylamide solution	0.65 mL
TEMED	5 µL
APS	50 µL

Similar to the preparation of the separation gel, the solution could be degassed before TEMED and APS were added. Now the remaining space in the Mini-protean® 3 chamber was filled with the stacking gel and the combs were placed quickly before the gel was polymerized (it should be tried to prevent any air bubbles when adding the combs).

- (d) Laemmli buffer was thawed and mixed with 6.2 mg DTT/mL. Then, a determined volume of the samples (determined through Bradford-Protein assay) were mixed with the Laemmli/DTT buffer to reach a total volume of 20 µL and 20 µg total amount of protein.

Laemmli buffer (50 mL):

Tris (250 mM), pH = 6.8	1.514 g
SDS (8 %)	4 g
Glycerol (20 %)	10 mL
Bromphenol blue (1 % stock solution)	1 mL
H ₂ O	ad 50 mL

The needed amount of Tris was weighted in, dissolved it in circa 20 mL H₂O and adjusted to a pH = 6.8 (circa 3 mL of a 6 N HCl) and was then filled with missing H₂O. Carefully 4 g of SDS was added, followed by adding glycerol and bromphenol blue (1 % stock solution while stirring constantly until everything is dissolved).

1 mL aliquots are stored at -20° C
before use 6.2 mg DTT/mL was added

- (e) Now the mixture consisting of protein sample and Laemmli/DTT was heated up to 95° C for 10 minutes and put directly afterwards on ice.
- (f) Cathode and anode buffer (1x) were prepared from the stock solutions, while the samples were heated.

Cathode buffer 10x (1000 mL):

Tris (250 mM)		30.2 g
SDS (1 % (w/v))		10 g
Glycine (1.92 M)		144.2 g
H ₂ O bidest.	ad	1000 mL

Storage at RT, 1:10 dilution shortly before use

Anode buffer 10x (1000 mL):

Tris (250 mM)		30.2 g
SDS (1 % (w/v))		10 g
H ₂ O bidest.	ad	1000 mL

Storage at RT, 1:10 dilution shortly before use

- (g) The combs were carefully removed from the polymerized stacking gel and the pockets were filled with cathode buffer. Afterwards the chilled samples and an internal standard (either 2-4 µL of PageRuler Prestained Protein Ladder or Molecular weight Precision Plus Protein™ were used) as a reference were added into the pockets.
- (h) Mini-Protean® – system was build together, adequate volume of anode buffer (300 mL) was added to the exterior chamber and cathode buffer was filled in the interior chamber. Now the system was started at 125 V controlled by a Power Pack 1000 unit for 75 minutes.

3.5.5.3 Western blotting

Following protocol was used, after samples were separated by electrophoresis (described in 3.5.5.2):

- (a) PVDF membrane was given into a dish with methanol and soaked there for a few seconds. Afterwards the membrane and blotting pads were stored in a dish with Towbin blotting buffer for 15 – 30 minutes.

Towbin blotting buffer (1000 mL):

Tris (25 mM)		3.3 g
Glycine (192 mM)		14.4 g
Methanol (20 % (v/v))		200 mL
H ₂ O bidest.	ad	1000 mL

Storage at 4° C, reuseable for about 10 times

- (b) After the electrophoretic separation was finished (~ 75 minutes). The stacking gel was carefully removed with a knife and discarded afterwards.
- (c) Two wet blotting pads were put into a semi-dry blotter, followed by the wet PVDF blotting membrane and afterwards carefully the gel was put upon it. Another two wet blotting pads were put at top of this to complete the sandwich-assembly. Possible air bubbles were removed and little blotting buffer was distributed on the surface. Now the semi-dry blotter was closed, for each gel 50 mA were set up (100 mA for two gels) and the blotting process was started for one hour.
- (d) Afterwards the semi-dry blotter was opened and as a control the migration of the standard into the PVDF membrane was checked. If nearly everything migrated, the PVDF membrane was washed for two times with H₂O bidest. and soaked into a dish with milk powder solution over night (shaking at 10 % at 4° C).

Milk powder solution (100 mL):

Milk powder (5% (w/v))		5 g
TBS 10x		10 mL
Tween 20		0.1 mL
H ₂ O bidest.	ad	100 mL

Freshly prepared

TBS 10x (1000 mL):

Tris		30.12 g
NaCl		84 g
H ₂ O bidest.	ad	1000 mL

pH = 7.8 with HCl, storage at RT

- (e) On the next day the PVDF membrane was washed with 0.1 % TBS-T solution for three times. Each washing step was performed for 10 minutes and shaken at 10 %.

TBS-T 0.1% (1000 mL):

TBS 10x		100 mL
Tween 20 (0.1 % (v/v))		1 mL
H ₂ O bidest.	ad	1000 mL

Storage at RT

- (f) Now the solutions for the primary antibody should be prepared. Primary antibody for Cox-1, Cox-2, ICAM-1, MRP-1, NMDAR-subunits, Occludin and ZO-1 was diluted 1:200, for Mdr and E-selectin 1:100, and for Actin 1:1666.7 in 10 mL (for 2 membranes) milk powder solution.
- (g) If it's necessary, the membrane was cut in appropriate parts, so that each part can be incubated with the different antibodies. Therefore 5 mL of each primary antibody solution was added to the appropriate part of the PVDF membrane and incubated for one hour (shaking at 10 %).
- (h) Afterwards the primary antibody solution was removed and the membrane was washed three times with 0.1 % TBS-T solution for 10 minutes (shaking at 10 %).
- (i) During the washing process the secondary antibody could be prepared. Secondary antibodies for anti-mouse, anti-goat and anti-rabbit were diluted 1:5000, and the secondary anti-rabbit antibody for Actin 1:10000 in 10 mL (for two membranes) milk powder solution. 5 mL secondary antibody solution was added to each membrane and every membrane part was incubated at 10 % shaking for 1 hour.
- (j) After the incubation with the secondary antibody, the membrane parts that were separated just a few steps earlier were fitted together again and were then treated with the Immun-Star WesternC™ chemiluminescent kit. Referred to two membranes, 1.5 mL of solution A were mixed with 1.5 mL of solution B and afterwards 1.5 mL were applied to each membrane to visualise where the secondary antibody had bound. Shake

gently for about 5 minutes, to ensure that the whole surface of the membrane was covered in the chemiluminogen solution.

- (k) Compatible membrane parts were covered in a transparent foil, air bubbles were removed and everything were developed in either a BioRad imager or the image reader Las 3000™.

3.5.6 Immunofluorescence microscopy

Cover slips with a diameter of 15 mm were put under the LAF by means of a tweezer into each well of a 12-well plate. Following 2 mL of sterile filtered 70 % (v/v) ethanol was added into each well for disinfection for at least 30 – 60 minutes. Ethanol was removed afterwards and cover slips were then washed with 2 mL (per well) sterile PBS 2-3 times. Please note that residual ethanol should be removed with a pipette. Optionally, the 12-well plate could now be put with its lid into a drier to ensure everything of the ethanol was evaporated (please note that the top cover shouldn't be removed during this step, otherwise the plate would be contaminated). Afterwards the 12-well plate was put again under the LAF and ECV304 cells could be seeded at a density of 80,000 cells/cm² (please note that no coating was necessary for the attachment and growth of ECV304 cells). Cells were grown for 7 or 10 days prior to immunofluorescence staining, medium was changed every other day. Following two protocols were used for staining and preparation for immunofluorescence microscopy.

3.5.6.1 Protocol using methanol (MeOH)

- (a) MeOH was put into a 50 mL Biofuge tube and precooled at –20° C for at least 30 – 60 minutes.
- (b) 12-well plates with cultured ECV304 cells on the cover slips were washed for three times with 2 mL/well PBS. After the last washing step all residues of PBS should be removed as good as possible with a pipette. Following 2 mL of the precooled (–20° C) MeOH were given into each well for cell fixation and then stored at –20° C for 20 minutes.

- (c) After incubation at -20° C MeOH was removed and washed for 2 times with 2 mL PBS, afterwards it was refilled with 2 mL PBS and incubated at RT for 20 minutes for rehydratisation.
- (d) The PBS was removed and residuals were aspirated with a pipette. Now the cell layer was incubated with 400 μ L of the primary antibody solution (1:100 in 1 % BSA/PBS) at 37° C for 1 hour.
- (e) The primary antibody solution was then removed and washed for three times with 2 mL/well PBS (please note that after each washing step possible solution leftovers are removed with a pipette).
- (f) Then 400 μ L of the secondary antibody solution (1:100, either FITC or IgG-Alexa Fluor 546 was used, in 1 % BSA/PBS including 1 μ g/mL propidium iodide) was incubated at 37° C for 30 minutes.
- (g) After the incubation, the cell layer was washed again with 2 mL PBS per well for three times.
- (h) Slides were cleaned with 70 % (v/v) EtOH before the cover slips were mounted.
- (i) One cover slip after another were removed from the wells, remaining PBS was carefully absorbed by a paper towel and mounted afterwards using a drop of FluorSave on a slide.
- (j) Then the slides with the mounted cover slips were dried over night in the dark at RT
- (k) Before slides are used for immunofluorescence microscopy they were gently cleaned with 70 % (v/v) EtOH to remove salt crystals onto the glass surface.

3.5.6.2 Protocol using paraformaldehyde and 0.1 % Triton-X 100

- (a) A 2 % paraformaldehyde (P-FA) solution (protocol see below) and a 50 mM NH_4Cl -solution in PBS were prepared.
- (b) 12-well plates with cultured ECV304 cells on cover slips were washed for two times with 2 mL/well PBS, whereas after the last washing step all leftovers of PBS should be removed completely with a pipette.
- (c) 750 μ L – 1000 μ L of the 2 % P-FA solution in PBS were added into each well for cell fixation and incubated for 10 – 15 minutes at RT.
- (d) The P-FA solution was efficiently removed and washed afterwards two times with 2 mL/well PBS (leftovers of the solution should be removed with a pipette).

- (e) Afterwards 750 μ L – 1000 μ L of a 50 mM NH_4Cl solution in PBS were added to each well and incubated for 10 – 15 minutes
- (f) The solution was removed and washed again twice with PBS
- (g) Optional: If cells should be permeabilized, add 750 μ L – 1000 μ L of a 0.1 % Triton-X 100 solution in PBS to each well and incubate for 7 minutes. Afterwards wash again twice with 2 mL/well PBS and remove leftovers with a pipette. Meanwhile this permeabilisation step, slips with cells which should not be permeabilized can be left in PBS.
- (h) Now the cell layer was incubated with 400 μ L of the primary antibody solution (1:100 in 1 % BSA/PBS) at 37° C for 1 hour.
- (i) The primary antibody solution was removed and washed for three times with 2 mL/well PBS (please note that after each washing step possible solution leftovers were removed with a pipette).
- (j) Then 400 μ L of the secondary antibody solution (1:100, either FITC or IgG-Alexa Fluor 546 was used, in 1 % BSA/PBS including 1 μ g/mL propidium iodide) were added to each well and incubated at 37° C for 30 minutes.
- (k) Again each well was washed for three times with 2mL PBS
- (l) Then the slides had been cleaned with 70 % (v/v) EtOH before slips were mounted.
- (m) One cover slip after another were removed from the wells, remaining PBS was carefully absorbed by a paper towel and mounted afterwards using a drop of FluorSave on a slide.
- (n) Then the slides with the mounted cover slips were dried over night in the dark at RT
- (o) Before slides are used for immunofluorescence microscopy they were gently cleaned with 70 % (v/v) EtOH to remove salt crystals onto the glass surface.

Preparing a 2 % P-FA solution in PBS:

Paraformaldehyde	600 mg
1 mM NaOH	3 drops
10x PBS	3 mL
Aqua bidest.	~27 mL

600 mg of P-FA were laced with ~20 mL H_2O in an appropriate Erlenmeyer flask and then 3 drops of a 1 mM NaOH solution were added to this. A small magnetic stir bar was given into the Erlenmeyer flask, the opening was sealed with parafilm and placed

afterwards on a magnetic stirrer with an adjusted temperature of 60° – 70° C. It was waited until everything was dissolved – this will take for about 1 hour – and then cooled down to RT again. 3 mL of a 10x PBS were added into the Erlenmeyer flask and refilled afterwards with H₂O to a total volume of 30 mL.

3.5.7 Intracellular Ca²⁺ - level assay

As a consequence of the activation of NMDAR, a calcium influx into the cell takes place. Therefore one of our aims was to measure the change of the intracellular calcium level as a functional parameter of the NMDA receptor activation by a fluorescence method in a 96-well plate format. A steady-state as well as a kinetic-like protocol had been developed to determine changes in the intracellular Ca²⁺-level. Both finally developed protocols were described in the following paragraphs. Differences in the experiments in comparison to these protocols were described later in the appropriate result part.

3.5.7.1 Culturing ECV304 cells in a 96-well plate

Cells were seeded on a black, gelatine coated 96-well plate at a density of 50,000 cells/cm². Mostly the ECV304 cells were cultured for 7 days (experiments where cells had been cultured for 4 or 14 days were also performed), whereby medium was changed every other day.

A membrane-permeable form of the fluorescence dye Fluo-3 called Fluo-3-AM was chosen, thus cells could be loaded via incubation. However, due to a relatively low water solubility of the AM ester Pluronic F-127 was also added as a dispersing agent to facilitate the loading. Inside the cells Fluo-3-AM was hydrolyzed to the active Ca²⁺-binding form by endogenous esterases. In order to minimise efflux of the cleaved Fluo-3 out of the cells, mediated by MRP or OAT transporters, the inhibitor Probenecid (2.5 mM) was added.

Three different multiplate readers were tested in order to investigate the differences between each system and to find the optimum one. The instrument and appropriate settings were given below.

3.5.7.2 Steady-state protocol

- (a) Appropriate amounts of Probenecid were weighted in and solutions were made by dissolving the Probenecid in HBSS/20 mM Hepes to reach a solution of 2.5 mM. Either HBSS with Mg^{2+} and Ca^{2+} were used (H8264), or HBSS (H6648) without Mg^{2+} and Ca^{2+} , in which Ca^{2+} was added afterwards.

To dissolve Probenecid completely in HBSS, everything was given into a ultrasonic bath for at least 1 hour (shaking or vortexing sometimes during this process would be helpful).

F1:	Probenecid	18.8 mg
	HBSS with Mg^{2+} and Ca^{2+} (H8264)	25.8111 mL
	1 M Hepes (20 mM)	526.7 μ L

F2:	Probenecid	18.8 mg
	HBSS without Mg^{2+} and Ca^{2+} (H6648)	25.8111 mL
	1 M Hepes (20 mM)	526.7 μ L

à Then 7.6 mg $CaCl_2$ were weighted in and dissolved in 25.84 mL of the prepared F2 solution.

This step could also be performed one day before the experiment and solutions were stored at 4° C overnight, since the dissolving process lasts quite long.

- (b) 1 % Albumin from bovine serum (A8022) was added to the Probenecid/Hepes/HBSS solutions. Solutions were then gently mixed by a vortex to avoid too much foam formation.
- (c) pH value was adjusted with 2 N NaOH to pH = 7.4
- (d) A 100 μ L aliquote of Pluronic F-127 was incubated at 37° – 40° C for at least 1 hour.
- (e) Fluorescence loading solution was prepared. Therefore 76 μ L of Fluo3-AM was mixed with 76 μ L of Pluronic F-127 and vortexed afterwards. Then 18.848 mL of F1-solution (with Mg^{2+} and Ca^{2+}) was added and stored at RT in the dark until its use.
- (f) 96-well plate with cells were taken out of the incubator and washed three times with 200 μ L HBSS (H8264) per well using a multichannel pipette.
- (g) 200 μ L of the F1-solution were given into each well of row 1 from the 96-well plate as a blank value. All other wells (rows 2 – 12) were filled with 200 μ L of the fluorescence loading solution prepared in (e). Then the whole plate was incubated at RT in the dark for one hour.

- (h) Unless the experimental mediums were not prepared until now, this should be finished during the incubation time. It should be noted that all solutions had to be prepared as 4x concentrated in F2-solutions, since the solutions will be diluted 1:4 in the addition step (m). Then ~60 μ L of experimental mediums were pre-pipetted into defined wells of an transparent 96-well plate, so that these solutions could then easily taken out with the multichannel pipette. The 96-well plate was then incubated at 37° C.
- (i) After the loading the black 96-well plate with cells was washed again for two times with HBSS (8264) and refilled with 75 μ L per well of the F2-solution. Then, the 96-well plate was incubated at 37° C in the dark for 30 minutes (preferably in a CO₂-incubator).
- (j) The plate reader should be turned on now, if it's not done until yet and heated to 37° C. Also the used measurement-protocol could be loaded.

Microplate reader Tecan Infinite M200i:

Measurement Mode: Fluorescence Bottom Reading

Excitation Wavelength: 485 nm

Excitation Bandwidth: 9 nm

Emission Wavelength: 535 nm

Emission Bandwidth: 20 nm

Interval Time: Minimal

Gain: 180 – 190

Number of Reads: 25

Integration Time: 25

Lag Time: 0 μ s

Microplate reader TECAN GeniosPro™:

Mode: Fluorescence Bottom Reading

Excitation Wavelength: 485 nm

Excitation Bandwidth: 20 nm

Emission Wavelength: 535 nm

Emission Bandwidth: 25 nm

Gain: 62 nm

Number of Reads: 20

Integration Time: 20

Lag Time: 0 μ s

Time between move and flash: 40 ms

Microplate reader Polarstar galaxy:

Excitation filter: 485 nm – P

Emission filter: 520 nm – 535 nm

Gain: 128

Number of flashes: 20

Reading direction: horizontal

- (k) After the incubation the 96-well plate with the cells were given into the analyzer and the base-fluorescence was measured. Therefore 2x 4 Cycles were measured in order to get a good baseline for the starting-point (~10 minutes).
- (l) Now 25 μL of the experimental medium of the prepared 96-well plate from step (i) were quickly pipetted in reverse mode into the defined wells (this step accords to a 1:4 dilution, therefore the experimental medium was 4x concentrated with the applied substances in step (i).
- (m) The measurement was carried out for 25-35 cycles.
- (n) Now a solution of HBSS/1 % Triton X-100 was prepared for subsequent cell lysis.
- (o) After the experiment was finished the experimental medium was removed from the cells and replaced with 100 μL HBSS/1 % Triton X-100 to check the loading capacity.
- (p) The measuring was started 5 minutes after adding the solution from step (p) by using 4 cycles.

3.5.7.3 Kinetic-like protocol

- (a) Appropriate amounts of Probenecid were weighted in and solutions were made by dissolving the Probenecid in HBSS with Mg^{2+} and Ca^{2+} (H8264) to get a 2.5 mM solution. To dissolve Probenecid completely in the HBSS, everything was given into a ultrasonic bath for at least 1 hour (shaking or vortexing sometimes during this process would be helpful).

F1: Probenecid	32.5 mg
HBSS (8264)	45.55 mL

This step could also be performed one day before the experiment and solutions were stored at 4° C overnight, since the dissolving process lasts quite long.

- (b) Add 1 % Albumin from bovine serum (A8022) to the Probenecid/Hepes/HBSS solutions and mix it gently on a vortex to avoid too much foam formation.
- (c) pH was adjusted then with 2 N NaOH to pH = 7.4
- (d) A 100 μ L aliquote of Pluronic F-127 was incubated at 37° – 40° C for 1 hour.
- (e) Fluorescence loading solution was prepared. Therefore 42 μ L of Fluo3-AM was mixed with 42 μ L of Pluronic F-127 and vortexed afterwards. Then 10.416 mL of F1-solution (with Mg²⁺) was added and stored at RT in the dark until its used.
- (f) Prepare all solutions needed for the experimental medium and pre-pipette them into a 96-well plate.
- (g) 96-well plate was taken out of the incubator. First, row 1 – 4 were washed three times with 200 μ L HBSS per well, followed by adding 200 μ L F1-solution to row 1 and 2, then 200 μ L of the fluorescence loading solution were added into the wells of row 3 and 4. The addition of fluorescence solution equals to the starting point of the loading period.

Seven minutes after Fluo3-AM solution was given to row 3 and 4, row 5 and 6 were washed three times with HBSS (this will take for about 3 minutes). After the washing step 200 μ L Fluo3-AM was given to row 5 and 6.

Repeat this step again for row 7 and 8, during the time when nothing is done with the 96-well plate; store it at RT in the dark.

- (h) Turn the analyzer on and set the parameters

Microplate reader Tecan Infinite M200i:

Measurement Mode: Fluorescence Bottom Reading

Excitation Wavelength: 485 nm

Excitation Bandwidth: 9 nm

Emission Wavelength: 535 nm

Emission Bandwidth: 20 nm

Intervaltime: Minimal

Gain: 180 – 190

Number of Reads: 25

Integration Time: 25

Lag Time: 0 μ s

- (i) One hour after row 3 and 4 were loaded with the fluorescence dye, wells of row 1-4 were washed with HBSS twice, followed by adding 75 μ L of F1-solution to row 1-4 and incubating at RT in the dark for 30 minutes.

One hour after row 5 and 6 were loaded the wells were equally treated as row 1-4.

Same steps were repeated with row 7 and 8.

- (j) A few minutes after 75 μL were added to row 7 and 8, measuring of the baseline from row 1 and 2 was started by measuring 2x 4 cycles. 25 μL of the control medium were given into row 1 and 2 (this was performed while the 96-well plate still stands close to the analyzer) and as fast as possible the change in fluorescence was measured during 20 cycles.
- (k) After 30 minutes incubation of row 3 and 4 the fluorescence-baseline was determined by measuring 4 cycles. Then 25 μL of an experimental medium was given into each well of row 3 and 4, followed by measuring the change in the fluorescence level by 20 cycles (whole step (l) takes about 8-9 minutes).
- (l) Now this steps were repeated with row 5/6 and 7/8 as well, since a time interval of 10 minutes was set between the incubation of the paired rows 3/4, 5/6 and 7/8.
- (m) After measurements of rows 7/8 were finished, the measuring of the whole plate from row 1-8 with 20 cycles was carried out.
- (n) After the experiment was finished the experimental medium was removed from the cells and replaced by 100 μL HBSS/1 % Triton X-100 to check the loading capacity.
- (o) 5 minutes after the solution from step (n) was added the measuring started by using 4 cycles.

3.5.7.4 Variable parameters in the calcium influx protocol

- Instead of Albumin also NBS was used in some experiments.
- It was checked if Probenecid is needed for the experiment to prevent Fluo-3 bleeding out from the cells.
- The fluorescence dye Ca-green-AM was also tested.
- Experiments were performed at RT and at 37° C analyzer temperature.
- Cells were loaded with the fluorescence dye Fluo3-AM for 30 minutes instead of normally 1 hour.
- Experiments were performed where cells were cultured for 4 or 14 days, instead of normally 7 days.
- The buffer Hepes wasn't used in every experiment.

- At the beginning of the experiments, one complete row was filled with one substance (n=8), this means:

Row 1 = cells without fluorescence dye

Row 2 = control

Row 3 = positive control (= Ionomycin)

By-and-by this was changed to following distribution on the 96-well plate (only steady state experiments). The blank, where cells were not loaded with any fluorescence dye, was always distributed in row 1; all the other substances and controls were distributed in a pre-defined sequence between rows 2 – 12. Starting with the first substance/control in the first well of row 2, followed by the next substance added to the second well of row 2 and so on. So a variable and random distribution could be achieved by this way, what probably resulted in more accurate results.

4 Results

4.1 Presence of the NMDA receptor in cell line ECV304

Kuhlmann et al. [20] already showed the presence of the glycine binding NR1 subunit on ECV304 cells and also assumed this target to be functional. We wanted to check in more detail and also tried to find, next to the NR1 subunit, the glutamate/NMDA binding NR2 subunits. Immunofluorescence microscopy and western blotting were used in order to detect the NMDA receptor on the protein level.

Primary polyclonal antibodies were purchased from Abcam (NR-1) and Santa Cruz Biotechnology (NR-1, NR-2 A-C). The Abcam antibody binds at a cytoplasmatic region, whereas all selected Santa Cruz Biotechnology antibodies bind extracellularly.

4.1.1 Western blot analysis of the NMDA receptor subunits

Primary antibodies from Santa Cruz Biotechnology were chosen for western blotting, since they should work for immunofluorescence microscopy as well as western blot analysis, according to the supplier's information. Moreover, lysates of the human (NR-2B) and mouse (NR-2A, NR-2C) cerebellum were used as a positive control for specific NR-2 subunits. Western blot analysis were performed using the protocol described in materials and methods (3.5.5).

Figures 4.1.1-1.3 show the western blot results for the presence of NMDAR subunits NR-1, NR-2 A-C in ECV304 cells. Therefore two different lysates were used as samples for this experiment. One lysate (in figures sample mostly A or E, in figure 4.1.3 it is B) was gained of ECV304 cells cultured on the surface of a 6-well plate (P149, 8th generation in PBMEC-FIB growth medium), the second lysate (in figures sample C or G) is from ECV304 cells cultured on an Transwell insert of an 6-well plate (P156, 15th generation in PBMEC-FIB growth medium).

Actually a band of the NR-1 subunit was assumed at a molecular weight of 115 kDa, but only the positive control seems to have such a band in this area. However, many other bands at lower molecular weights of our samples matched to bands of the mouse cerebellum sample, thus some sort of degradation during sample preparation is assumed.

Bands of NR-2A were visible in both ECV304 samples close to the expected molecular weight of 177 kDa (Fig. 4.1.2 [A, C]), but no band was seen in this area in the positive control (Fig. 4.1.2 [B]). However, strong bands were seen at same lower molecular weights both in samples as well as in the positive control. No bands were visible in the human cerebellum (Fig. 4.1.2 [D]), indicating, that no NR-2A subunits had been expressed there.

The expected molecular weight of the NR-2C subunit is 135 kDa. However, according bands were only found in one of the two samples (Fig. 4.1.2 [G]) and slightly in the positive control (Fig. 4.1.2 [F]). The positive control showed a strong band at a molecular weight of ~72 kDa, which matched to a band of the same sample [G]. Strong bands were found for NR-2C in the positive control, although these fragments possessed a distinct lower molecular weight, which matched to bands at the same height of our samples. As already mentioned for the NR-1 subunit, some sort of degradation during our working process was suggested. Differences between the two different samples were also seen when we checked for NR-2C subunits. This we assume was maybe due to slightly different culture conditions of the ECV304 cells before they were lysed.

Somehow the image of the NR-2B subunit (figure 4.1.3) was blurred and western blot repeats showed similar results. Unfortunately, no clear bands could be seen at 178 kDa, where the molecular weight for NR-2B was expected. But again, bands lower than 72 kDa could be seen in the positive control [A] as well as in two different samples [B/C] and in the mouse cerebellum [D] indicating that the primary antibody probably targeted a degraded fragment of the NMDA receptor.

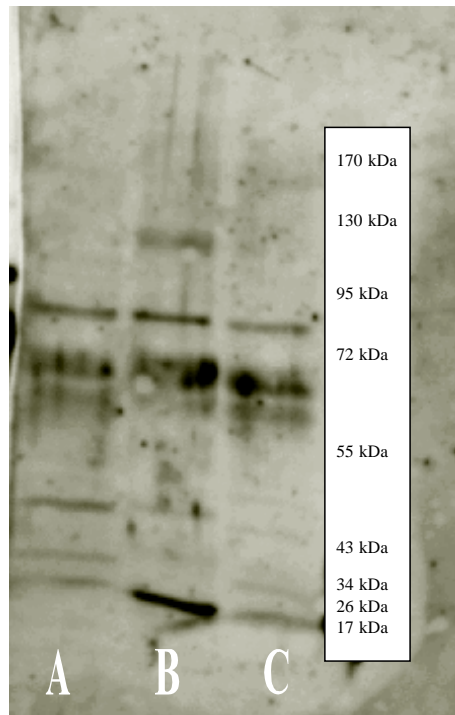


Fig. 4.1.1: Western blot analysis of the expression of NMDA NR-1 in two different samples of ECV304 cells [A, C]. Lysate of the mouse cerebellum was used as a positive control [B].

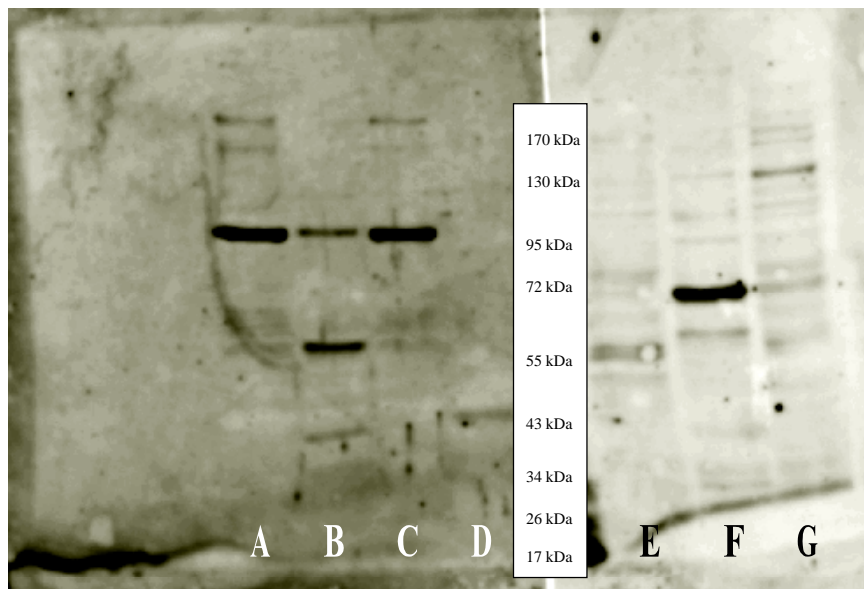


Fig. 4.1.2: Western blot analysis of the expression of NMDA NR-2A and -2C in two different ECV304 samples [A/E and C/G]. Lysate of the mouse cerebellum [B/F] was used as a positive control for NR-2A and -2C, also human cerebellum lysate was checked for NR-2A.

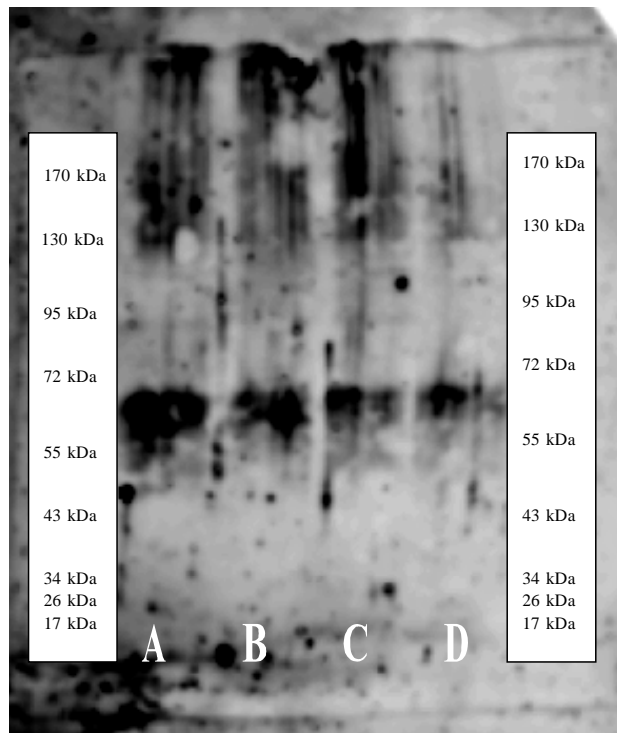


Fig. 4.1.3: Western blot analysis of the expression of NMDA NR-2B in two different samples [B/C]. Moreover, the lysate of a human cerebellum was used as one positive control [A] and a lysate of the mouse cerebellum as a second positive control [D].

4.1.2 Immunofluorescence microscopic analysis of the NMDA receptor subunits

Two different protocols, described in materials and methods were used for the staining, but it was decided to present only the results of the protocol with paraformaldehyde due to comparability reasons. Intensity of the fluorescence signals were detected for propidium iodide at level 2 with an exposure time of 2/3 seconds and for the NR-subunits at level 3 with an exposure time of 4 seconds.

Figures 4.1.4-4.1.8 show the immunofluorescence images after Triton-X 100 permeabilisation for NMDA subunits NR-1, NR-2A – 2C. For NR-1 stainings two antibodies from different sources were compared. Also according blank images with only the secondary antibody were shown in the figures in order to facilitate the comparison and to show the significant stainings for NMDA-subunits. Cells were seeded at a density of 80,000 cells/cm² and cultured for 10 days under optimal growth conditions with medium

exchange every second day. Used protocol for the preparation was already described in 3.5.6.2.

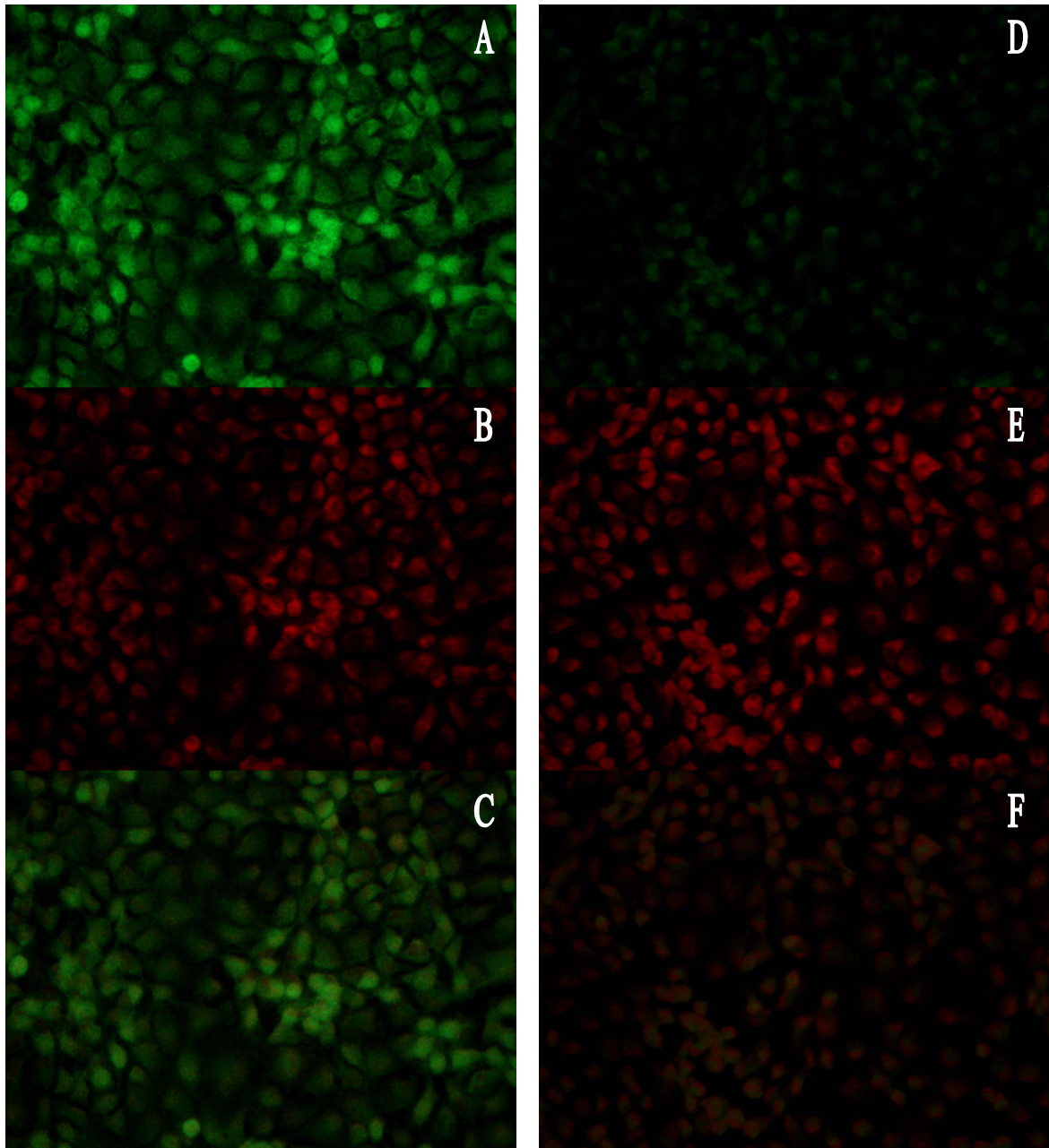


Figure 4.1.4: Immunofluorescence images of NR1 subunits of ECV304 cells using the primary antibody from Abcam [A], with the appropriate cell nuclei stain (propidium iodide) as control [B] and the merge of A and B [C]. This could be compared to control images, where only the secondary antibody was used (green fluorescence [D], cell nuclei [E], merge of D and E [F]).

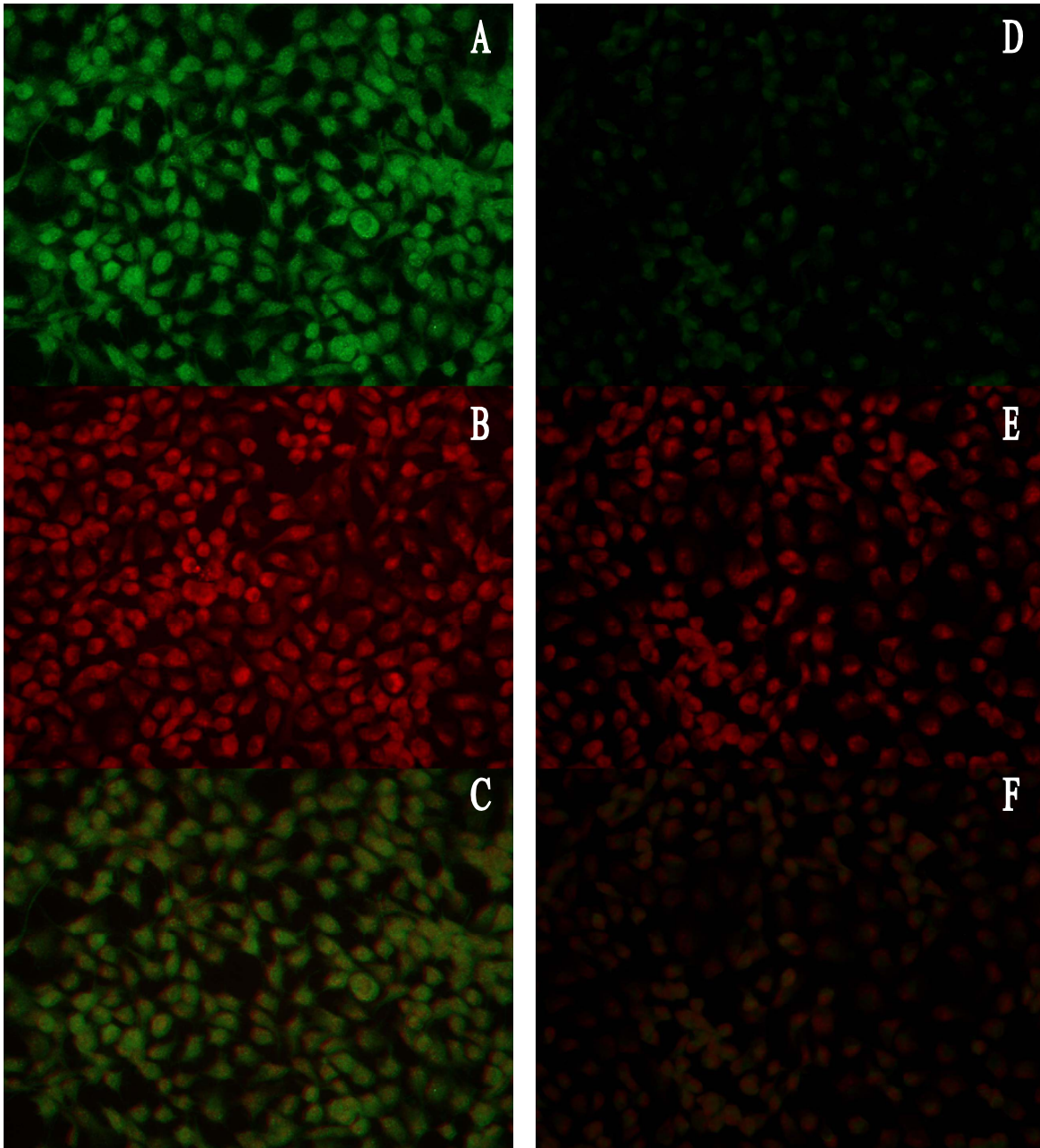


Figure 4.1.5: Immunofluorescence images of NR1 subunits of ECV304 cells using the primary antibody from Santa Cruz Biotechnology [A], with the appropriate cell nuclei stain (propidium iodide) as control [B] and the merge of A and B [C]. This could be compared to control images, where only the secondary antibody was used (green fluorescence [D], cell nuclei [E], merge of D and E [F]).

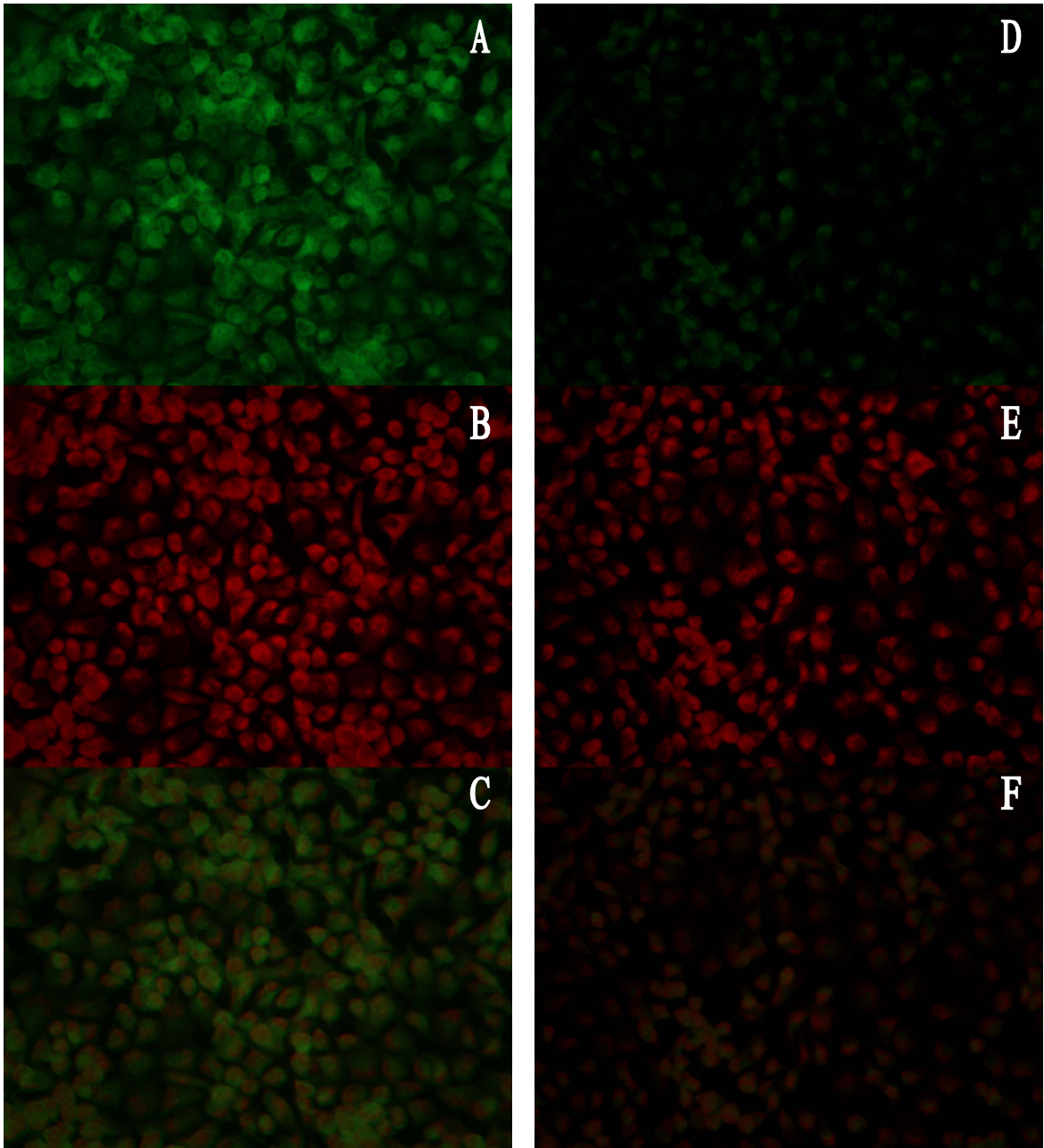


Figure 4.1.6: Immunofluorescence images of NR-2A subunits of ECV304 cells using primary antibody from Santa Cruz Biotechnology [A], with the appropriate cell nuclei stain (propidium iodide) as control [B] and the merge of A and B [C]. This could be compared to control images, where only the secondary antibody was used (green fluorescence [D], cell nuclei [E], merge of D and E [F]).

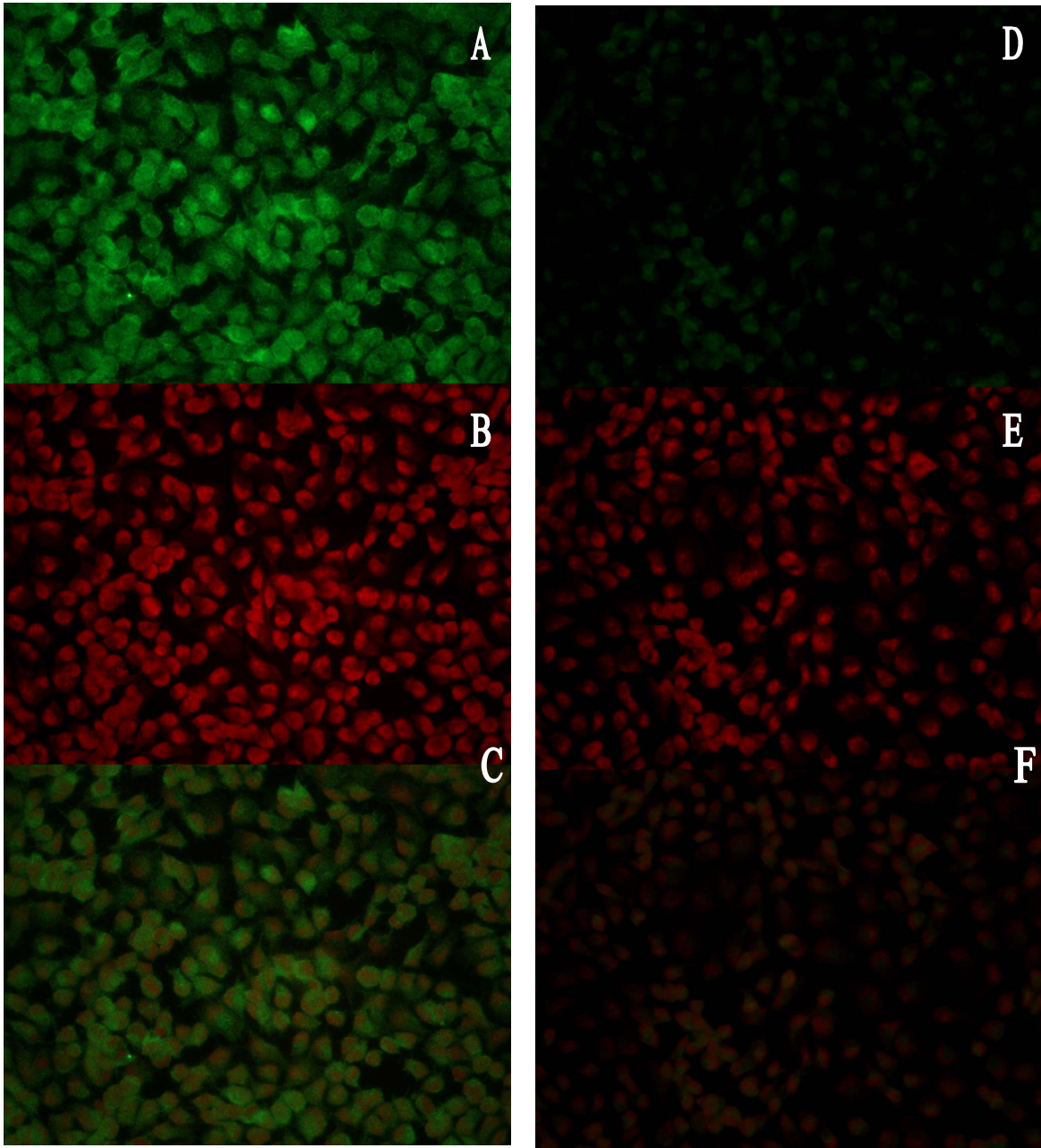


Figure 4.1.7: Immunofluorescence images of NR-2B subunits of ECV304 cells using primary antibody from Santa Cruz Biotechnology [A], with the appropriate cell nuclei stain (propidium iodide) as control [B] and the merge of A and B [C]. This could be compared to control images, where only the secondary antibody was used (green fluorescence [D], cell nuclei [E], merge of D and E [F]).

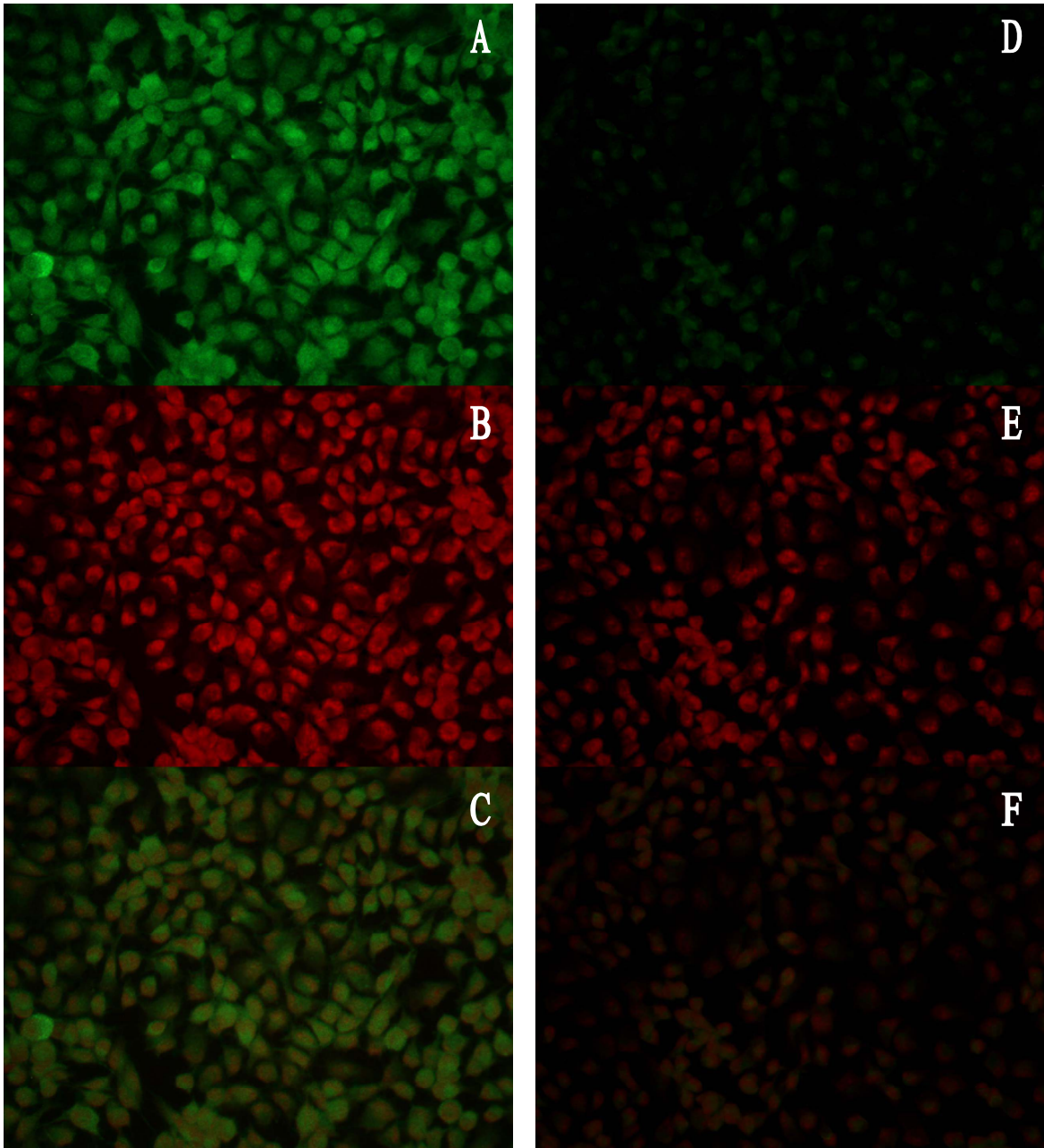


Figure 4.1.8: Immunofluorescence images of NR-2C subunits of ECV304 cells using primary antibody from Santa Cruz Biotechnology [A], with the appropriate cell nuclei stain (propidium iodide) as control [B] and the merge of A and B [C]. This could be compared to control images, where only the secondary antibody was used (green fluorescence [D], cell nuclei [E], merge of D and E [F]).

In summary, western blotting and immunofluorescence microscopy suggested the presence of NMDAR subunits NR-1, NR-2A, -2B and possibly -2C in cell line ECV304. Their presence is a prerequisite for further functional tests with regard to the NMDA receptor.

4.2 Measurement of the intracellular calcium level

Activation of the NMDAR leads to a permeation of calcium ions into the cell. Consequently, one of our major aims was to measure this change of the intracellular calcium level as a first functional parameter of the activation of the NMDA-receptor by establishing a fluorescence method using a 96-well plate system.

4.2.1 Development of a 96 well-plate assay.

The basic principles of this assay were based on different other protocols that determine the change in calcium level by confocal laser microscopy, flow cytometric measurement or measurement by a multiplate reader [37, 38, 39]. Finally we decided to measure changes of the intracellular calcium level by a 96-well plate fluorescence method since recording of many data over a longer time interval should be possible.

4.2.1.1 Comparison of different plate reader devices

The first experiments were performed on the microplate reader Polarstar Galaxy (figure 4.2.1). Concentration-dependent signals of Fluo3-AM (1, 4, 10 μ M) were best seen using the positive control Ionomycin. However, the fluorescence intensity in general was quite unsatisfactory (figure 4.2.1), since the intensity level did not rise above 250 fluorescence units at the maximum gain. Neither any effect of the control, 1 mM Glutamate, nor 1 mM Glutamate/10 μ M MK801 could be seen or interpreted in the graph due to stronger up- and downturns and the lack of any detectable differences between agonists/antagonists compared to the control. The obtained negative fluorescence resulted of a high self-fluorescence of cells without Fluo3-AM, whose intensity was subtracted of those ECV304 cells that were loaded with the dye. In summary due to those results we assumed that the Polarstar Galaxy microplate reader was not appropriate for this kind of experiments.

As a result of this two other multiplate reader from Tecan were tested that were not as old as the Polarstar Galaxy:

- Microplate reader Tecan Infinite M200i with a monochromator
- Microplate reader Tecan GeniosPro™ with filters for specific wave-lengths.

Already the first measurement with the Tecan Infinite M200i showed that the differences in fluorescence intensity between blank and Fluo-3-AM loaded cells could easily be more than 100 times higher compared to the Polarstar Galaxy (figure 4.2.2). Again only the measuring points and not the real timescale were showed due to overview reasons. Moreover, it should be noted that gain-changes were performed after the first measuring point in the experiment depicted in figure 4.2.2, although the test substances were just applied and again after 18 measuring points since the absolute fluorescence was still increasing and probably would rise over the detection limits (since the first experiments were just tests to adjust the settings of the microplate reader and to see if the assay work we didn't mind changes described before). However, the concentration-dependent differences of Fluo3-AM were seen well. Therefore it was decided, based on the concentration-dependent effect and on different protocols, to use a concentration of 4 μM Fluo3-AM for all following experiments, since 10 μM fluorescence dye would be maybe an unnecessary waste of money [38, 39, 40].

Also experiments with the Tecan GeniosPro showed that the fluorescence intensity is much higher (figure 4.2.3) compared to the Polarstar Galaxy microplate reader, indicating that both Tecan microplate readers could be used. In the experiment depicted in figure 4.2.3 already a concentration of 4 μM Fluo3-AM was used and mixed with different combinations of Ca^{2+} -channel agonists and/or antagonists. It should be noted that in all experiments Ionomycin was used as positive control resulting in a quite high fluorescence level and BAPTA as a negative control resulting in a decreased intracellular calcium level. The actual interesting measurement changes of the intracellular calcium level by different Ca^{2+} -channel modulators were inbetween the controls and in a much smaller range.

In summary, it was observed that both Tecan microplate readers were able to measure the change in intracellular calcium level over a period of time, whereby such a measuring method could not be performed on the Polarstar Galaxy. The only differences, except little adjustment-differences between the microplate readers, were seen by the curve-progression. In this context, it seemed that results from the Tecan Infinite M200i oscillated more compared to the GeniosPro.

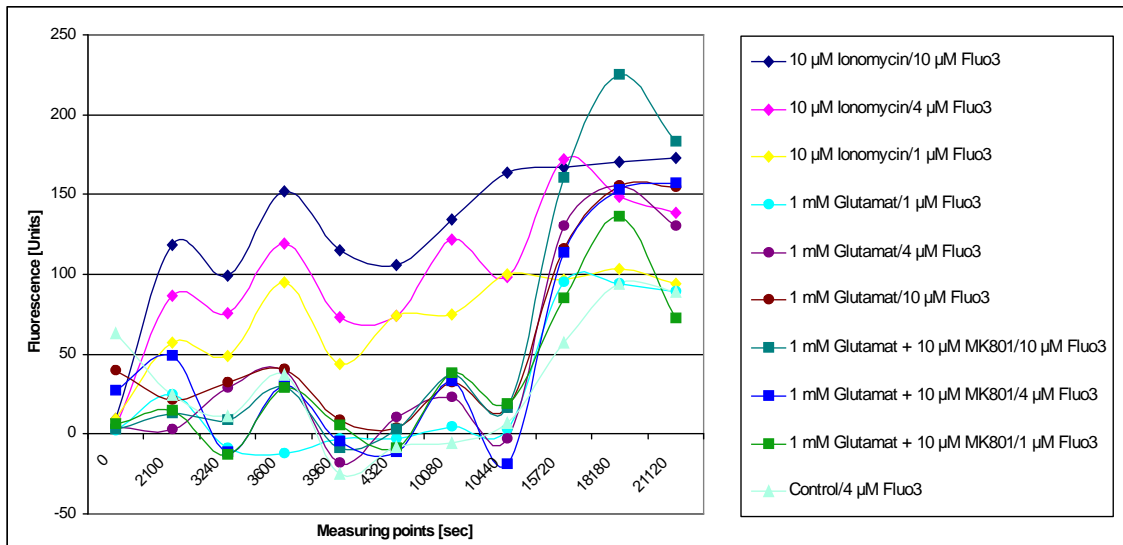


Fig.4.2.1: Change in intracellular calcium level. Concentration-dependent differences of Fluo3-AM were only seen with Ionomycin. After 10.440 seconds cells were lysed with 100 μ L HBSS/1 % Triton-X 100 to control the uptake of the fluorescence dye into the cell. Due to overview reasons only the measuring points were showed, the real timescale was ignored.

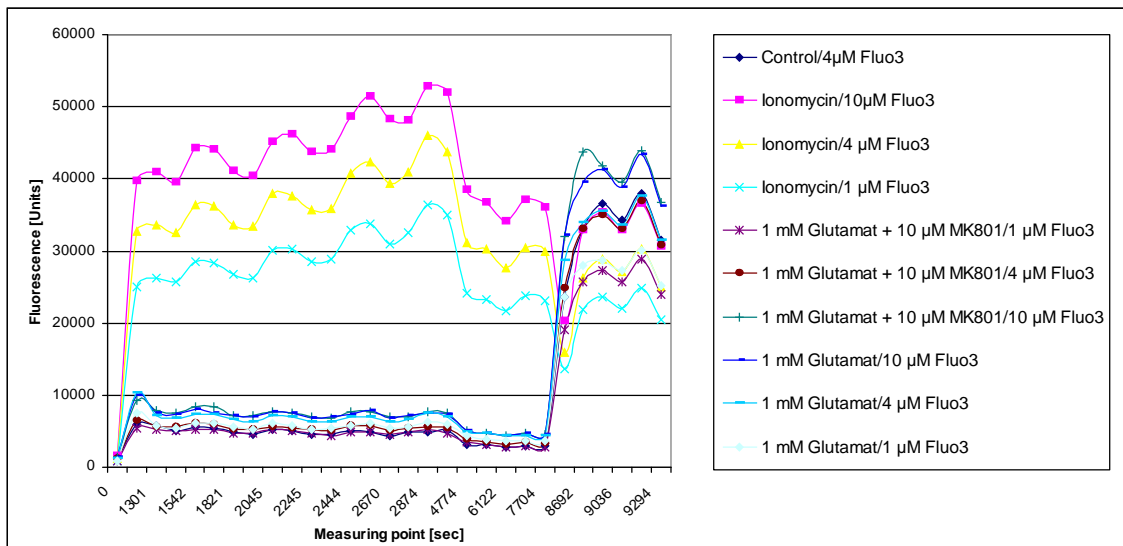


Fig.4.2.2: Change in intracellular calcium level on the Tecan Infinite M200i. Concentration-dependent differences were seen at Ionomycin, 1 mM Glutamate and 1 mM Glutamate/10 μ M MK801. Timescale was ignored and only the measuring points were showed.

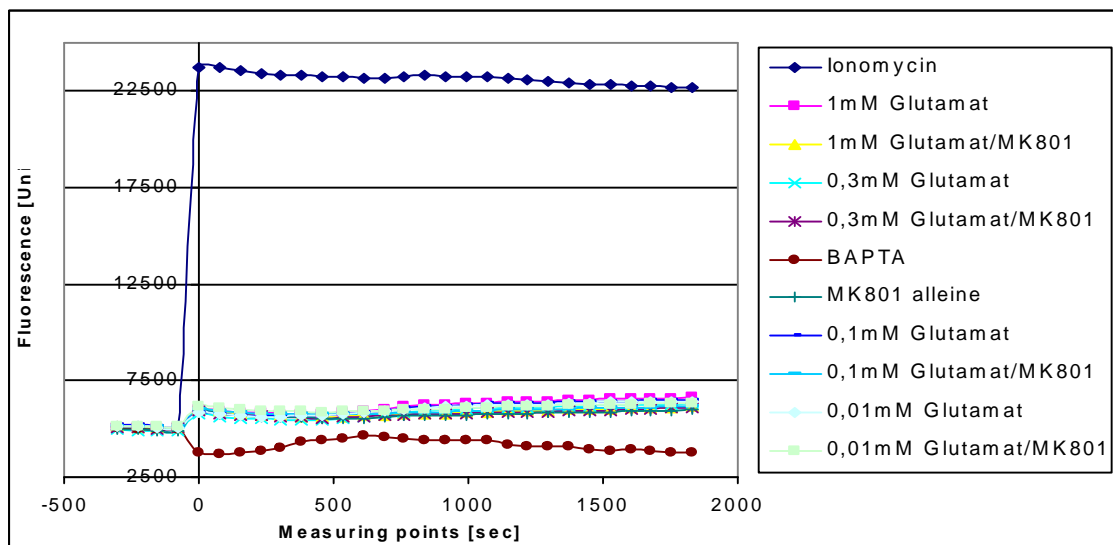


Fig. 4.2.3: Change in intracellular calcium level, performed on the Tecan GeniosPro, was detected by using 4 μ M Fluo3-AM.

4.2.1.2 Influence of different cell culture durations (4, 7, 14 days)

As next step optimum cultivation times to use ECV304 cells for the assays were investigated. Therefore, cells were seeded at a density of 50,000 cells/cm² per well of an 96-well plate and cultured in an incubator at 37° C, 5 % CO₂ and 96 % humidity. In order to find a good culture time for cell growth, the change of the intracellular calcium level by agonists such as glutamate or NMDA with or without antagonists like MK801 or D-APV were determined after 4, 7 or 14 days cultivation. Experiments were performed in Mg²⁺ free medium and test-substances were dissolved in water (glycine, glutamate, MK801, D-APV), directly in the HBSS/Probenecid/Albumin solution (BAPTA), or DMSO (Ionomycin) to the needed stock solutions. Afterwards experimental medium was prepared by diluting the stocks to the needed 4x concentrations. All of those experiments were performed on the Tecan GeniosPro at 37° C. Due to overview reasons of the diagram, percentage of the fluorescence of the positive control Ionomycin and the negative control BAPTA were not shown, but discussed at a later point.

Figure 4.2.4 showed the results of ECV304 cells that were cultured in a 96-well plate for 4 days. Observation by a light microscope showed that the surface area was completely

covered with cells. However, the ECV304 cells were not so compact populated than in 96-well plates that were cultured for 7 days or longer. This reduced culture time caused probably the resulting fluctuating curve-progression and their high standard deviations, where no clear differences or tendencies between agonist- with/without antagonists could be seen.

It seems that a surface completely covered in ECV304 cells is not enough to perform this sort of experiment. In fact, it probably also take some time until the needed transporters were fully expressed on the surface.

Another experiment where ECV304 cells were cultured in a 96-well plate for 7 days was performed. Observation with the light microscope revealed that the cells grew tighter together compared to the cells that were only cultured for 4 days. Moreover it was observed that ECV304 already developed multilayer in the wells of the 7 day cultured 96-well plate. Figure 4.2.5 showed the results of ECV304 cells that were cultured in a 96-well plate for 7 days. Differences between agonists with/without antagonists could clearly be seen over a period of time, whereby the effects of those Ca^{2+} -level modulators were discussed at a later point (4.2.2). The graph in general showed a good curve-progression characterised by a low standard deviation.

Figure 4.2.6 shows the curve progression of a 96-well plate that was cultured with ECV304 cells for 14 days. Before the experiment was performed the wells were observed microscopically and a tight surface with ECV304 cells was seen which developed more multilayer than a 7 day plate. Differences between agonists with/without antagonists that modulate the Ca^{2+} -level were seen. However, results were quite similar to 7 day old cells, but bigger multilayers were developed by 14 days cultured ECV304 cells. Thus, it was decided to perform all following experiments with cells cultivated for 7 days onto 96-well plates.

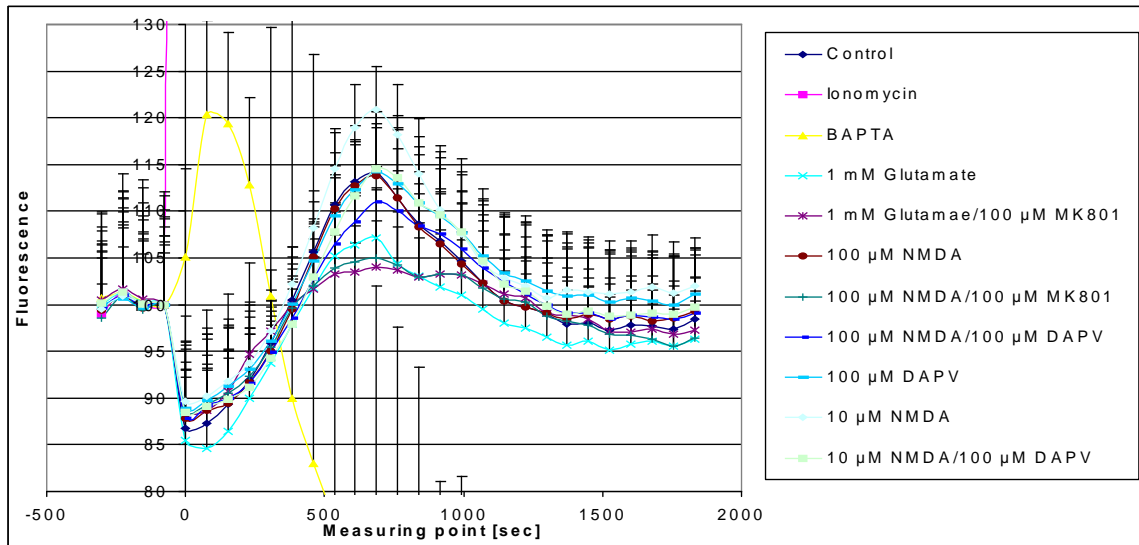


Fig. 4.2.4: Change in intracellular calcium level of a 96-well plate that was cultured for 4 days. Values are expressed as means \pm SEM (n=8).

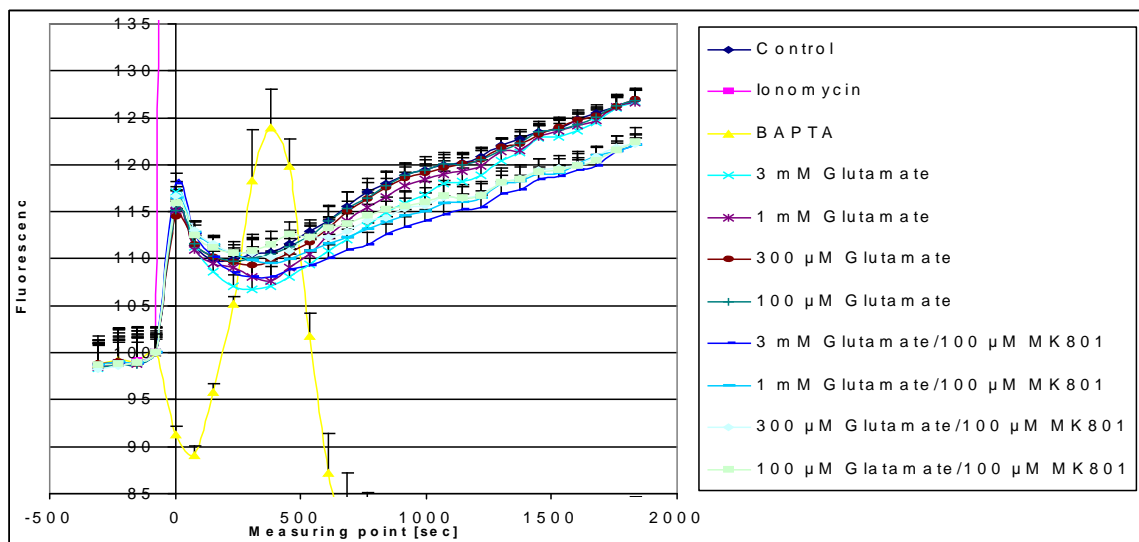


Fig. 4.2.5: Change in intracellular calcium level of a 96-well plate that was cultured for 7 days. Values are expressed as means \pm SEM (n=8).

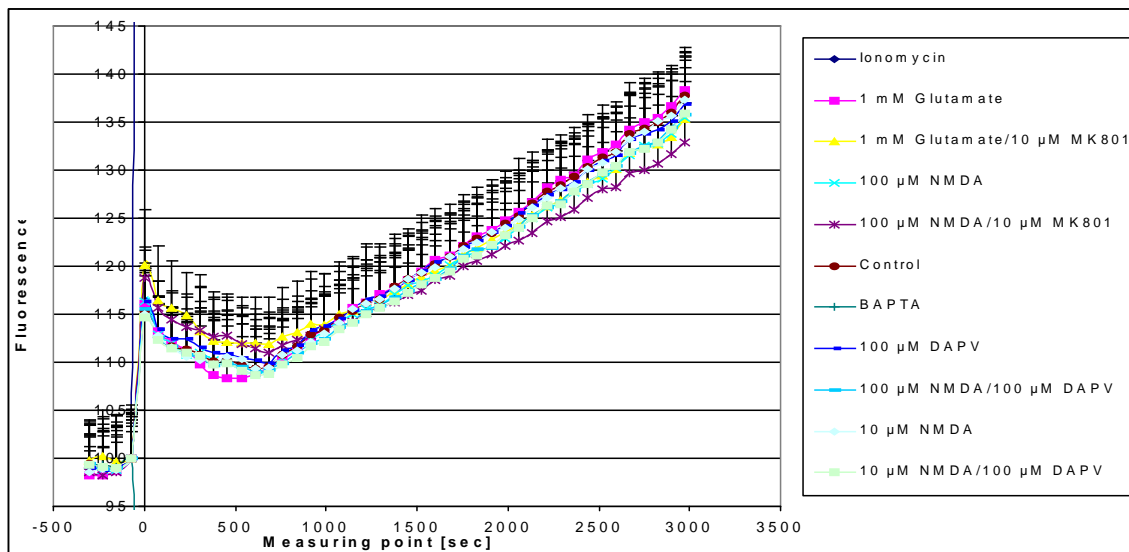


Fig. 4.2.6: Change in intracellular calcium level of a 96-well plate that was cultured for 14 days. Values are expressed as means \pm SEM (n=8).

4.2.1.3 Kinetic-like- versus steady-state-studies

Besides the steady-state studies an assay for kinetic-like experiments were developed and performed, in order to see the influence on the intracellular calcium level directly after test-substances were administered. The experiment is based on the protocol described in materials and methods (3.5.7), whereby medium containing Mg^{2+} was always used. The substances which were needed to perform the experiment were dissolved in water (glycine, NMDA, D-APV), or DMSO (Ionomycine) to the needed stock solutions. Afterwards the experimental medium was prepared by diluting the stock to the needed 4x concentrations. All experiments were performed on the Tecan Infinite M200i at 28° C. Due to the overview of the diagram, percentage of the fluorescence of the positive control Ionomycin were not shown, but discussed at a later point. Although several kinetic-like experiments were performed, only the results of a few specific were shown and their outcome was then compared with the steady-state experiments.

Since always two rows were loaded in the same step with the fluorescence dye (as described in materials and methods), it was supposed that those were comparable with other rows because of similar starting conditions. The curve-progression of the first

performed kinetic-like experiments seemed to demonstrate plausible results at the first sight. As seen in figure 4.2.7, NMDA (10 μM) was able to increase intracellular Ca^{2+} -level compared to the control. Moreover, more significant effects were seen when 10 μM NMDA was mixed with different concentrations of glycine (100, 10, 1 μM), the co-agonist on the NMDA receptor, whereby 10 μM and 1 μM glycine seemed to have the strongest effects. By that high expectations were put in this measurement until experiments with D-APV, a potent and specific NMDA receptor antagonist, were performed. As seen in figure 4.2.8, 10 μM NMDA caused a higher intracellular calcium level compared to the control, by what an activation a calcium channel like the NMDA receptor was assumed. Such a result was already also shown in figure 4.2.7, but interestingly common concentrations of D-APV (100, 10, 1 μM) were not able to decrease the intracellular calcium level, moreover it seemed that the calcium level increases as lower the D-APV concentration was. This result indicates that either no functional NMDA receptor is available on the ECV304 cell line, or the concentration of D-APV was still too low. Though it was noticeable, that again those values that were obtained at the same time had related curve progressions of the intracellular calcium level (figure 4.2.7, 4.2.8), indicating adulterated results due to the measuring method. Therefore, this experiment was repeated, whereby just the order in which the test-substances were applied, was changed, by adding and measuring the control as the last value. As seen in figure 4.2.9 the control had one of the highest intracellular calcium levels, moreover it is also very close to the row (10 μM NMDA/1 μM D-APV) that was measured at the same time. Unfortunately 10 μM NMDA/10 μM D-APV had a high calcium level, which could be explained because of the smaller fluorescence in the raw-data compared to the other rows, where same changes in [%] had a bigger effect. Although all rows should be treated the same, the factor „time“ that is needed between two pairs of rows, seems to have an important influence which adulterate the values. Due to this outcome, kinetic-like experiments with this protocol were stopped, since the results were questionable.

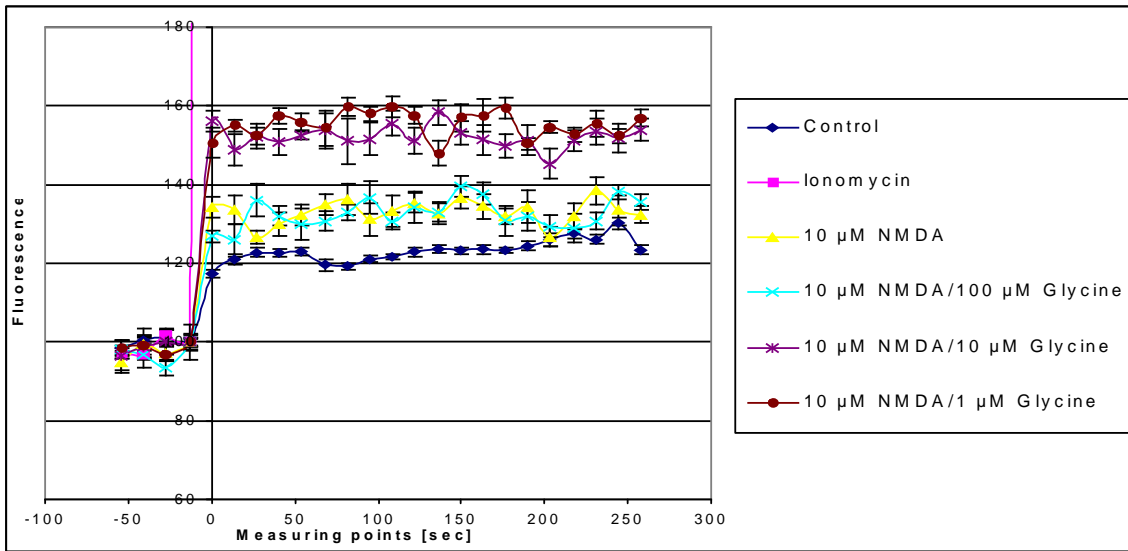


Fig. 4.2.7: Influence of 10 μM NMDA with/without different concentrations of glycine on the intracellular calcium level, compared to the control. Values are expressed as means +/- SEM (n=8).

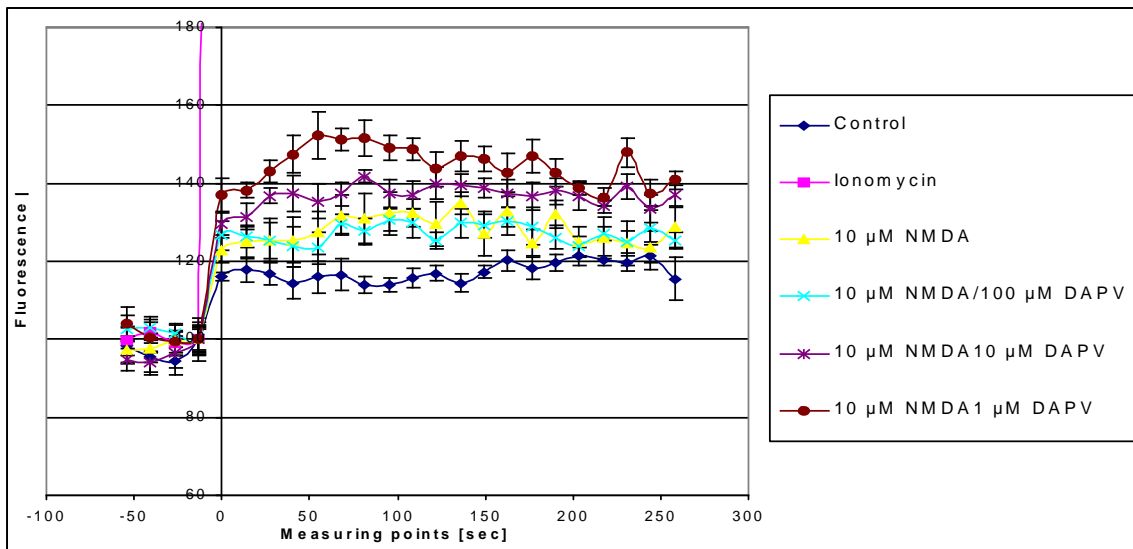


Fig. 4.2.8: Change in intracellular calcium level by 10 μM NMDA with/without different concentrations of D-APV. Values are expressed as +/-SEM (n=8).

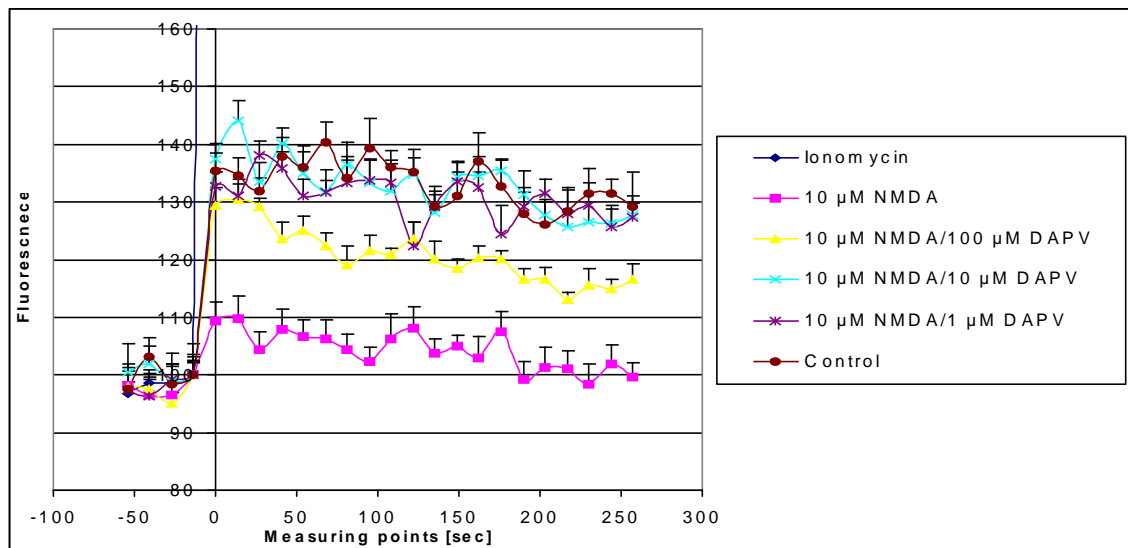


Fig. 4.2.9: Influence of a different application order on the intracellular calcium level. Values are expressed as means +/- SEM (n=8).

4.2.1.4 Influence of different tested parameters on the intracellular calcium level.

In order to optimise our fluorescence method to measure the change in intracellular calcium level, different parameters were changed and tested.

NBS vs. Albumin: In the first experiments NBS was used instead of Albumin (usage see materials and methods 3.5.7). In those experiments (data not shown) the control always showed one of the highest intracellular calcium levels of all tested values. Unfortunately the composition of the serum was not exactly known, why a change to albumin was chosen. However, also those experiments showed that the control always had one of the highest intracellular calcium levels. Although no differences between NBS and albumin were seen, it was decided that only albumin would be used for all following experiments. This decision was made due to the fact that defined concentrations of glycine and/or glutamate should be used since the exact composition of serum is not known, leftovers of those amino acids could still be in the serum.

Fluo3-AM vs. Calcium-Green-AM: Since this thesis is based on the work of Kuhlmann et al. [20] who used calcium-green as fluorescence dye for his experiments, also this indicator was tested in order to see possible advantages over Fluo3-AM which was normally used. In those experiments (data not shown) Fluo3-AM showed the differences in calcium level more precisely than Calcium-Green-AM. This was caused probably due to the fact that the fluorescence dyes possess different K_D -values. Fluo3-AM has a $K_D = 325$ nM [41] and Calcium-Green-AM a $K_D = 190$ nM [42] at 22° C. With the higher K_D -values of Fluo3-AM bigger intracellular concentrations of calcium could be measured, whereas it seemed that Calcium-Green-AM was faster saturated with Ca^{+2} .

Use of Probenecid: In order to minimise the efflux of the fluorescence dye of the cells, Probenecid, an anion channel blocker, was also implemented in our protocol (see materials and methods 3.5.7). Experiments where Probenecid was not used (data not shown) revealed a significant increase in fluorescence intensity by binding of the effluxed fluorescence dye Fluo3 with calcium in the medium. This increased leakage fits to the information given by the product information of the fluorescence dye [41].

Experiments using HBSS with/without Mg^{2+} : During this thesis, experiments were performed using HBSS with/without Mg^{2+} due to the advice of Dr. M. Berger. The outcome of those results will be discussed at a later point in 4.2.2.

Experiments with/without Hepes: The beneficial effects of Hepes, a buffer agent with a buffer capacity between pH 6.8-8.2 were tested in our solutions that were needed for the experiments. Those results revealed (data not shown) that no significant differences between experiments with solutions consisting the buffer agent or no Hepes were seen. Only the adjustment to pH 7.4 was a bit easier when Hepes was used. Since it was not seen that the adjusted pH-value really changed until the experiment ends, it could be chosen whether a buffer agent should be used or not.

Influence of shortening the loading time of Fluo3-AM to 30 minutes: In order to minimise the experimental time and work with maybe more vital cells it was tested to shorten the loading time of the fluorescence dye Fluo3-AM to 30 minutes instead of the normally 60 minutes. In those results it was seen that the base fluorescence was lower

compared to other experiments (data not shown) indicating that the uptake of Fluo3-AM into ECV304 were lower, but expressed in percent the fluorescence units fit again to the other results. The effects of the used test-substances will be discussed in more detail in 4.2.2. In order of a better comparison between the experiments a loading time of 60 minutes with Fluo3-AM was still maintained, although a loading of 30 minutes with the fluorescence dye also seemed to work.

4.2.2 Influence of Ca²⁺-level modulators

After establishment of the 96-well plate assay to measure the intracellular calcium levels, the influence of different Ca²⁺-level modulators was tested. Especially the change of intracellular calcium level by the activation or inhibition of an active NMDA receptor should be tested. Therefore, the steady-state-protocol described in materials and methods (3.5.7) was used unless deviations specified at the single experiment descriptions.

4.2.2.1 NMDA receptor modulators

Following the protocol described in 3.5.7, all experiments with NMDA receptor modulators were finally performed in Mg²⁺- and Ca²⁺-free HBSS (6648) supplemented with Ca²⁺. In this context it should be noted, that the fluorescence-dye solution for loading the ECV304 cells with Fluo3-AM was prepared with HBSS (4641) containing Mg²⁺- and Ca²⁺. The substances tested were dissolved in water (glycine, glutamate, NMDA, MK801, D-APV), directly in the HBSS/Probenecid/Albumin solution (BAPTA), or DMSO (Ionomycin, Verapamil) to the needed stock concentrations. Afterwards the experimental medium was prepared by diluting the stock solutions to the needed 4x concentration. Since the NMDA receptor also needs glycine as a co-agonist to be activated, it should be noted that in every solution must also be an appropriate final-concentration of it (10 µM glycine in our case). Experiments were performed on the Tecan GeniosPro at 37° C. Due to presentation reasons, Ionomycin and BAPTA curves were not completely shown in the graphs.

The influence of different glutamate concentrations (1 mM, 0.3 mM, 0.1 mM, 0.01 mM) on the intracellular calcium level and the change over a period of time was shown in figure 4.2.10. Different concentrations of glutamate displayed varying intracellular calcium level.

1 mM glutamate seemed to cause the highest intracellular calcium level which decreased at lower glutamate concentrations. Unfortunately the effects of 100 μ M MK801 alone (in combination with 10 μ M glycine, the co-agonist which was always present) were tested in order to see the influence on the intracellular calcium level, instead of a control-value. However, interestingly also MK801 alone was able to reduce the intracellular calcium level to nearly the same level as glutamate (and glycine) supplemented with the channel blocker MK801 did. Actually no big effect on the intracellular calcium level of the NMDA receptor blocker MK801 alone was assumed, since the receptor should only be activated by agonists like glutamate or NMDA in combination with the co-agonist glycine and not by glycine and MK801 alone. A retry of nearly the same experiment was carried out in order to check the influence of different glutamate concentrations (3 mM, 1 mM, 300 μ M, 100 μ M) on the intracellular calcium level, compared to a control-value (see figure 4.2.11a). Interestingly, a concentration-dependent effect, as it was seen in figure 4.2.10, could not be observed, instead all glutamate-values without the inhibitor MK801 had nearly the same intracellular calcium level. However, again all the values where glutamate was applied together with MK801 showed a lower intracellular calcium level. The differences between the endpoints of the glutamate-values and the glutamate/MK801-values compared to the control that is set to 100% were seen in the bar graph 4.2.11b. In both experiments Ionomycin displayed a fluorescence of about 445 % (4.2.10) and 413 % (4.2.11) and BAPTA of 75 % (4.2.10) and 82 % (4.2.11) after addition of the substances.

Figure 4.2.12a shows different concentrations of NMDA (3 mM, 1 mM, 300 μ M, 100 μ M, 30 μ M, 10 μ M) which were tested in order to see their influence on the intracellular calcium level. Again, controls exhibited highest intracellular calcium levels over a period of time, as it was already observed in the experiments where glutamate was added (see 4.2.11a). However, the effect of NMDA seemed more interesting, since the intracellular calcium level decreased at higher the NMDA concentrations.

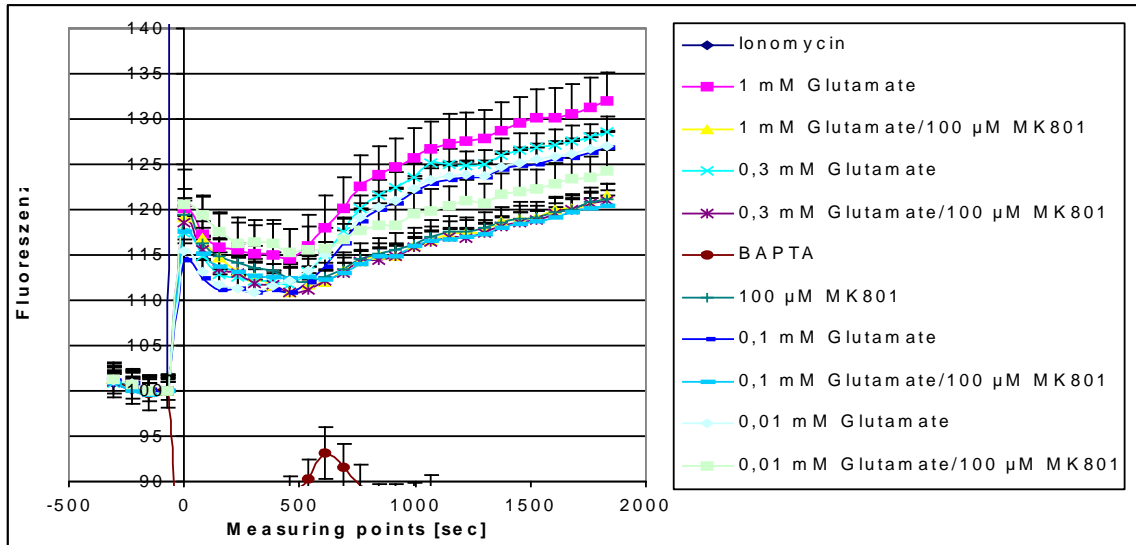


Fig. 4.2.10: Influence of different concentrations of glutamate on the intracellular calcium level. This effect could partially be inhibited by 100 μM MK801. ECV304 cells were used at passage 178. Values are expressed as means \pm SEM (n=8).

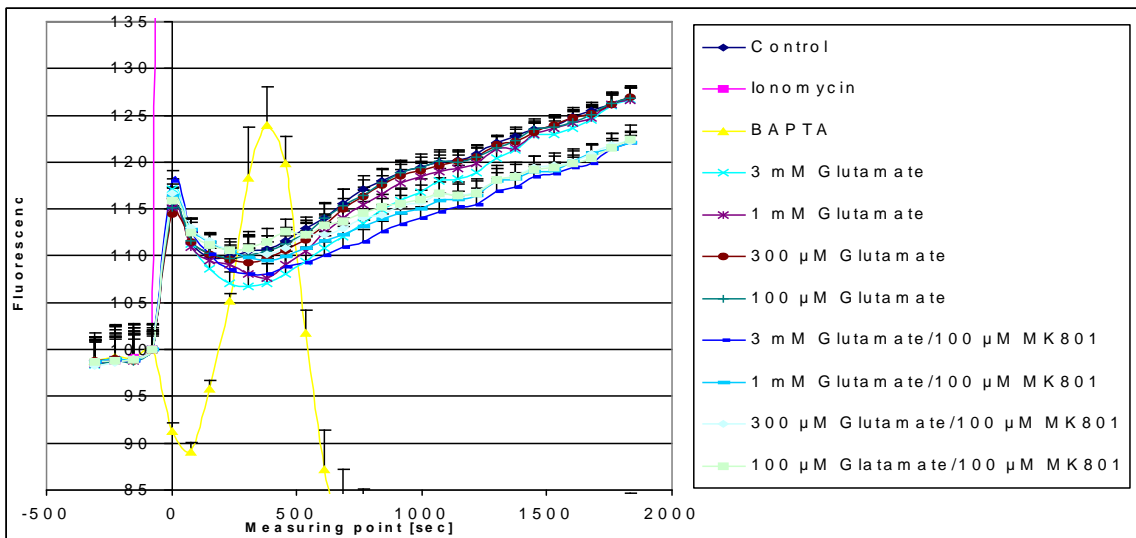


Fig. 4.2.11a: Repeat of the experiment about the influence of different concentrations of glutamate on the intracellular calcium level. ECV304 cells were used at passage 189. Values are expressed as means \pm SEM (n=8).

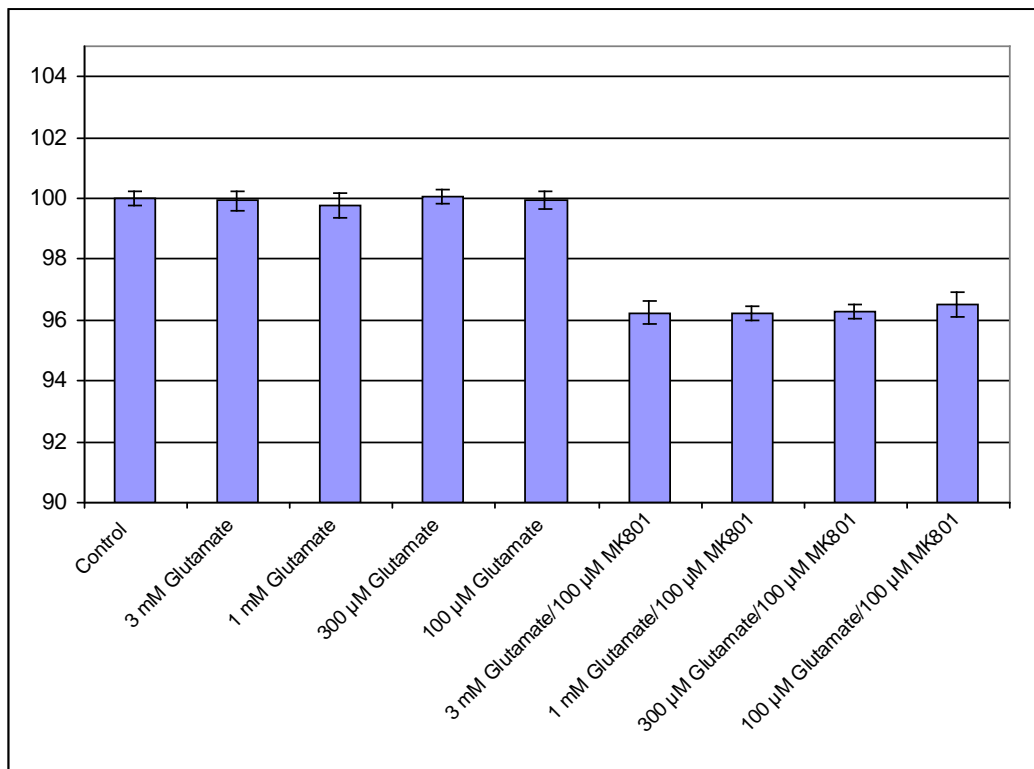


Fig. 4.2.11b: Difference between varying concentrations of glutamate with/without 100 μ M MK801 compared to the control after 33 minutes. Control values were set to 100 %. Values are expressed as means \pm SEM (n=8).

This was the completely opposite effect that was once observed in a glutamate experiment (see 4.2.10) and expected if the NMDA receptor was the main target of glutamate to increase the intracellular calcium level. Since the intracellular calcium level decreases as higher the NMDA concentration got, some sort of a strong counter-regulation, activated by the increasing NMDA concentration and the resulting overstimulation of the NMDA receptor, could be assumed. Interestingly, significant increasing of the NMDA concentration was necessary, since the concentration range between 10 μ M–100 μ M caused no detectable effects. However, NMDA is also said to be a specific agonist on the NMDA-receptor, whereby seen effects were assigned to NMDA receptor activation. The concentration-dependent effect of this experiment at the endpoint is shown in a bar graph in more detail (figure 4.2.12b). Quite interesting was also the effect of 3 mM NMDA since these concentrations seems to have a big influence on the intracellular calcium level. Those

values showed even a lesser intracellular calcium level than the values of 300 μ M NMDA/100 μ M MK801, whereas 3 mM NMDA/100 μ M MK801 once more was lower than 3 mM NMDA alone. However, in this context the difference between agonist with/without inhibitor was bigger at the 300 μ M NMDA concentration than it was observed at 3 mM NMDA concentration.

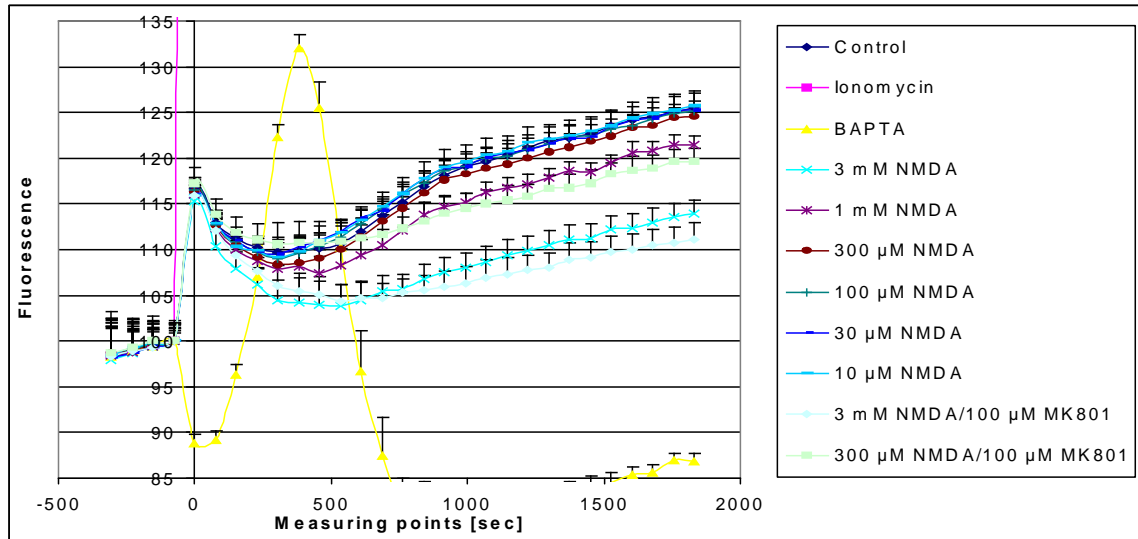


Fig. 4.2.12a: Influence of different NMDA concentrations partly with the channel blocker MK801 on the intracellular calcium level. ECV304 cells were used at passage 188. Values are expressed as means \pm SEM (n=8).

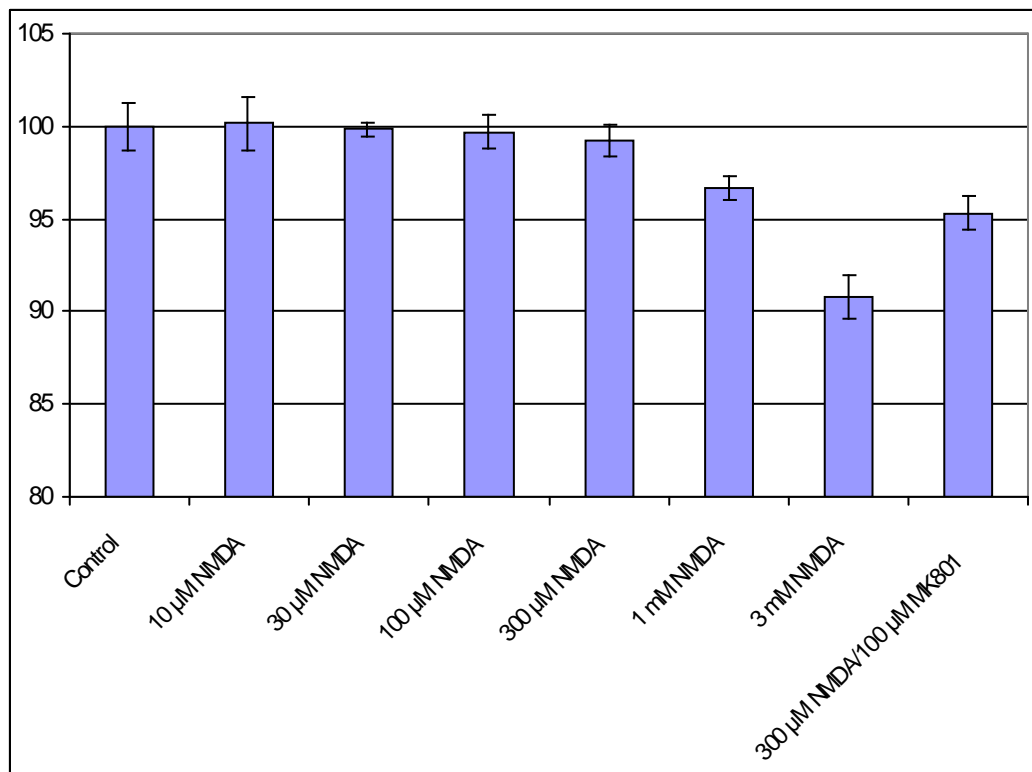


Fig. 4.2.12b: Difference between varying endpoint-concentrations of NMDA with/without the channel blocker MK801 compared to the control after 33 minutes. Control values were set to 100 % Values are expressed as means \pm SEM (n=8).

The experiment shown in figure 4.2.13a was already partly described in section 4.2.1, because of the influence of shortening the loading time of Fluo3-AM to 30 minutes. Now, the influence of the tested substances of this experiment on the intracellular calcium level will be presented. 1 mM glutamate was tested with/without different concentrations of the NMDA receptor channel blocker MK801. Moreover a pre-test with 100 µM Verapamil was performed. Figure 4.2.13a shows the results of this experiment, in which again the control had probably the highest intracellular calcium level over a period of time. Application of 1 mM glutamate did not change the intracellular calcium levels compared to the control (as it was once seen in 4.2.10). However, the goal of this experiment was to check a possible concentration-dependent effect of the NMDA receptor channel blocker MK801 onto the NMDA receptor activity, which should have been activated by the simultaneous addition of 1 mM glutamate and 10 µM glycine. As expected, different concentrations of MK801 showed in combination with 1 mM glutamate (and glycine)

varying intracellular calcium level, in which the highest concentration of the channel blocker resulted in the lowest observed intracellular calcium level. For a better overview, the endpoint-concentration of this experiment was also shown in a bar graph (4.2.13b). In this experiment also a pre-test with 100 μM Verapamil, a L-type calcium channel blocker, was accomplished since the high intracellular calcium levels of the control value was probably cause of a different Ca^{2+} -channel. In this experiment Ionomycin was again used as a positive control reaching an average fluorescence of about 372 % and BAPTA as negative control decreasing average fluorescence intensity to 55 % compared to the control.

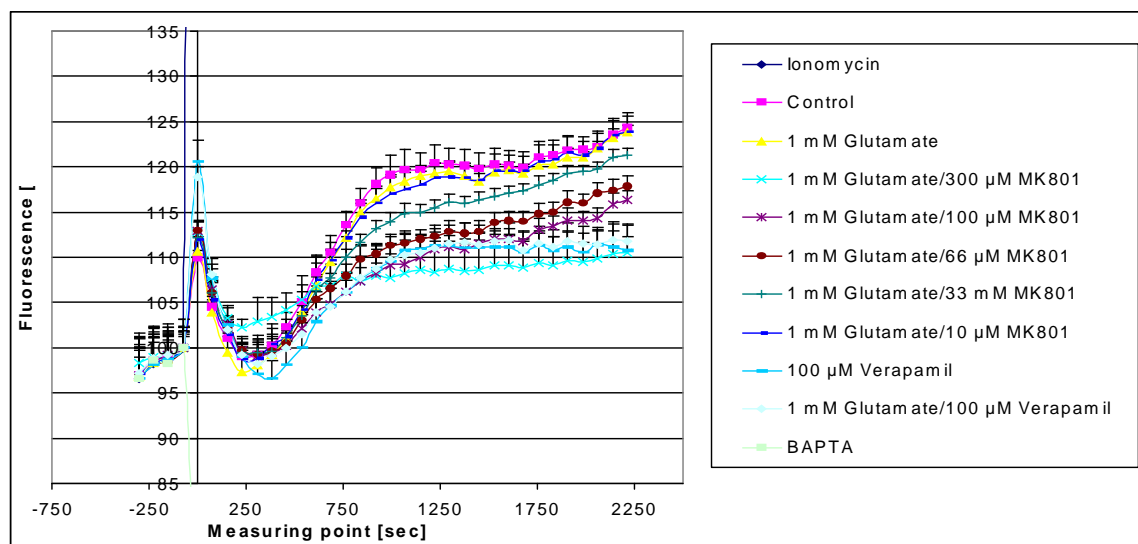


Fig. 4.2.13a: Change of the intracellular calcium level caused by different concentrations of the NMDA-receptor channel blocker MK801. ECV304 cells were used at passage 180. Values are expressed as means \pm SEM (n=8).

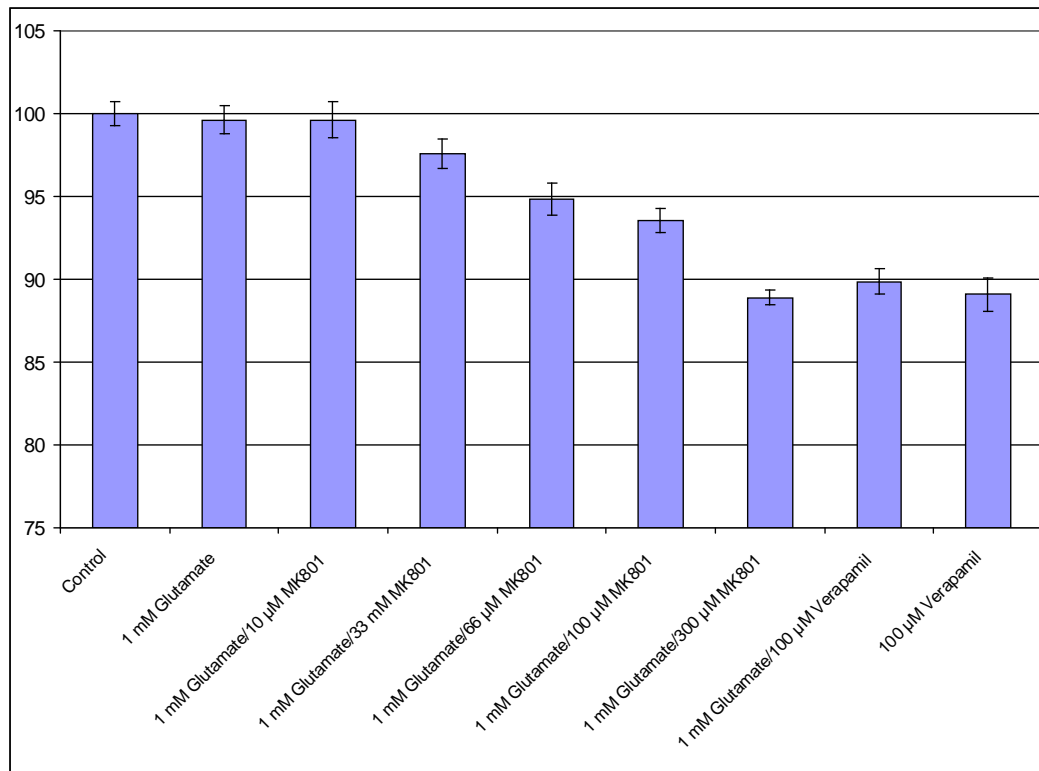


Fig. 4.2.13b: Difference between varying endpoint-concentrations of 1 mM glutamate with/without the channel blocker MK801 compared to the control after 39 minutes. Control values were set to 100 %. Values are expressed as means +/- SEM (n=8).

The influence of 100 and 10 μ M NMDA with/without 100 μ M D-APV on the intracellular calcium levels and the change over a period of time was shown in figure 4.2.1.14a. The experiment was performed with ECV304 cells that were cultured for 14 days. This was already partly described in 4.2.1.2. The results showed that 100 μ M D-APV was not able to lower the intracellular calcium level in any possible set-up compared to the control. This was somehow already expected due to the lack of effects during the kinetic-like experiments. However, further studies in our group showed that D-APV influenced the intracellular calcium level significant at higher concentrations of 1 to 3 mM. These high concentrations were not tested in this diploma thesis since literature based data indicated that D-APV effects should have been detectable at maximum 100-300 μ M interacting with a functional NMDA-receptor. As expected also NMDA did not show any distinct effects on the intracellular calcium level at the used concentrations. For a better overview, calcium

concentration at the endpoint of this experiment were also shown in a bar graph (4.2.14b). It should also be mentioned that the glutamate values which were also performed during this experiment (see graph from 4.2.1.2) were not shown here. In this experiment Ionomycin was again used as a positive control reaching an average fluorescence of about 334 % and BAPTA as negative control decreasing average fluorescence intensity to 53 % compared to the control.

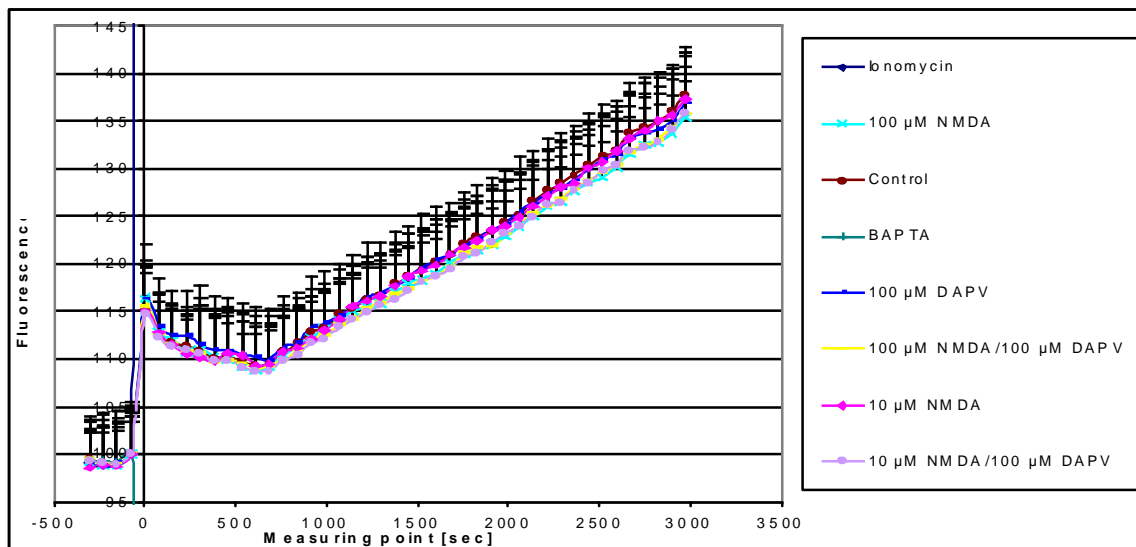


Fig. 4.2.14a: Influence of NMDA with/without D-APV on intracellular calcium levels. ECV304 cells were used at passage 178. Values are expressed as means \pm SEM (n=8).

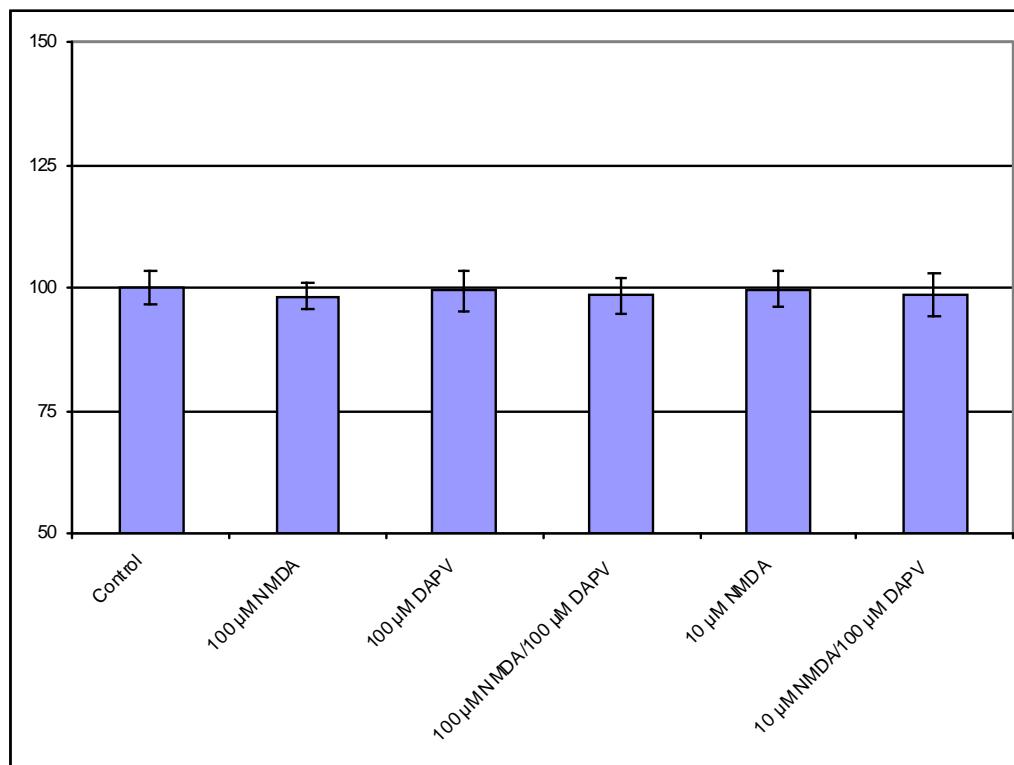


Fig. 4.2.14b: Difference between varying endpoint-concentrations of NMDA with/without D-APV compared to the control after 51 minutes. Control values were set to 100 %. Values are expressed as means +/- SEM (n=8).

4.2.2.2 Acetylcholine as calcium modulator

Following the protocol described in 3.5.7, all experiments with NMDA receptor modulators were finally performed in Mg^{2+} - and Ca^{2+} -free HBSS (6648) supplemented with Ca^{2+} . In this context it should be noted, that the fluorescence-dye solution for loading the ECV304 cells with Fluo3-AM was prepared with HBSS (4641) containing Mg^{2+} - and Ca^{2+} . Different concentrations of acetylcholine were tested in this experiment, although a direct link between acetylcholine, or acetylcholine-receptors and the NMDA receptor is not obvious at the first sight. However, the influence of MK801 on nicotinic acetylcholine receptors (nAChR) was already reported [43] and since neuronal nAChR could also be permeable for Ca^{2+} it was decided to investigate a possible influence of acetylcholine on the intracellular Ca^{2+} level. The substances were dissolved in water (acetylcholine,

MK801), directly in the HBSS/Probenecid/Albumin solution (BAPTA), or DMSO (Ionomycin) to the needed stock solutions. Afterwards the experimental medium was prepared by diluting the stock solutions to the needed 4x concentrations. Since the NMDA receptor was not the target in this experiment, it should be noted that no glycine was added as it was done during the experiments described in 4.2.2.1. Tests were performed on the Tecan GeniosPro at 37° C. Due to overview reasons fluorescence percentage of Ionomycin and BAPTA were not shown in the following graph. However, the positive control Ionomycin showed an increased fluorescence of 332 % (4.2.14a) or 392 % (4.2.14b) and the negative control BAPTA a of 52 % (4.2.14a) or 64 % (4.2.14b) after addition of the substances.

Since the functionality of the NMDA receptor as a Ca^{2+} channel in ECV304 cells is yet not fully confirmed, the influence of different concentrations of acetylcholine (0.001, 0.01, 0.1, 1, 10, 100 μM) on the intracellular calcium level compared to MK801 were tested in Mg^{2+} -free and Mg^{2+} -containing HBSS. The first experiment was performed in HBSS (4641) with Mg^{2+} and interestingly no effects or differences compared to the control could be seen. As in probably every performed experiment, the control had again one of the highest intracellular calcium levels over the period of time. Also the tested concentrations of acetylcholine nearly had the same curve progression as it was observed for the control indicating maybe no influence of Ach onto total intracellular calcium values.

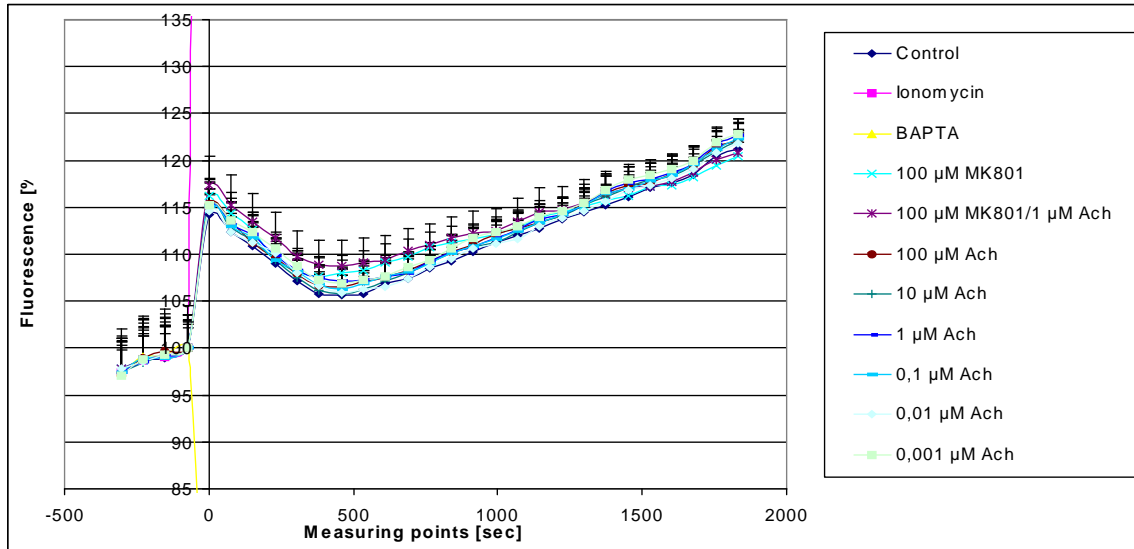


Fig. 4.2.14a: Influence of different concentrations of acetylcholine on the intracellular calcium level in HBSS with Mg^{2+} and Ca^{2+} , compared with 100 μM MK801 alone or in combination with 1 μM Ach. ECV304 cells were used at passage 186. Values are expressed as means \pm SEM (n=8).

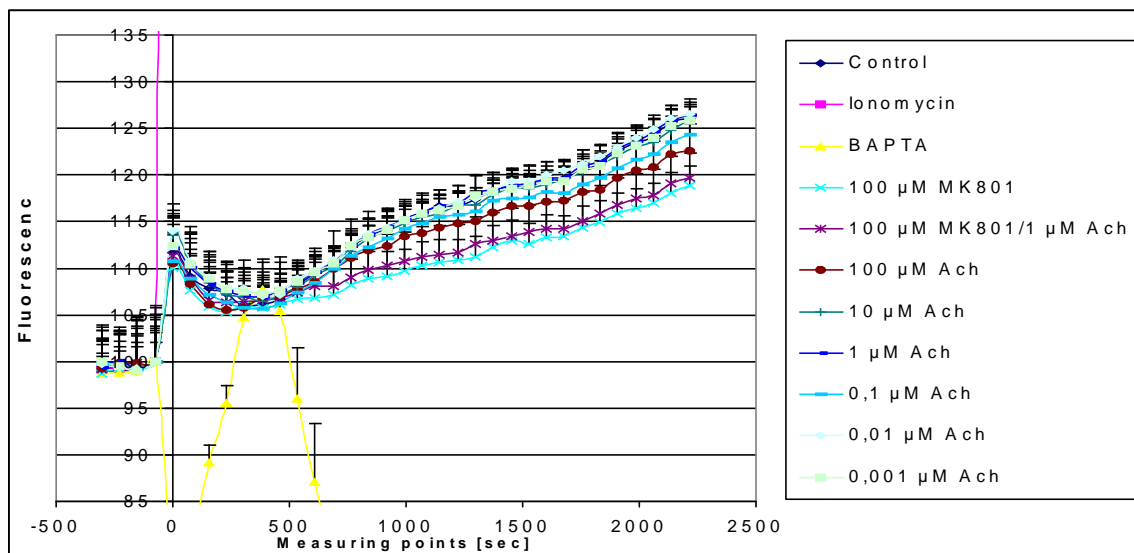


Fig. 4.2.14b: Influence of different concentrations of acetylcholine on the intracellular calcium level in Mg^{2+} - and Ca^{2+} -free HBSS supplemented with Ca^{2+} compared with 100 μM MK801 alone or in combination with 1 μM Ach. ECV304 cells were used at passage 187. Values are expressed as means \pm SEM (n=8).

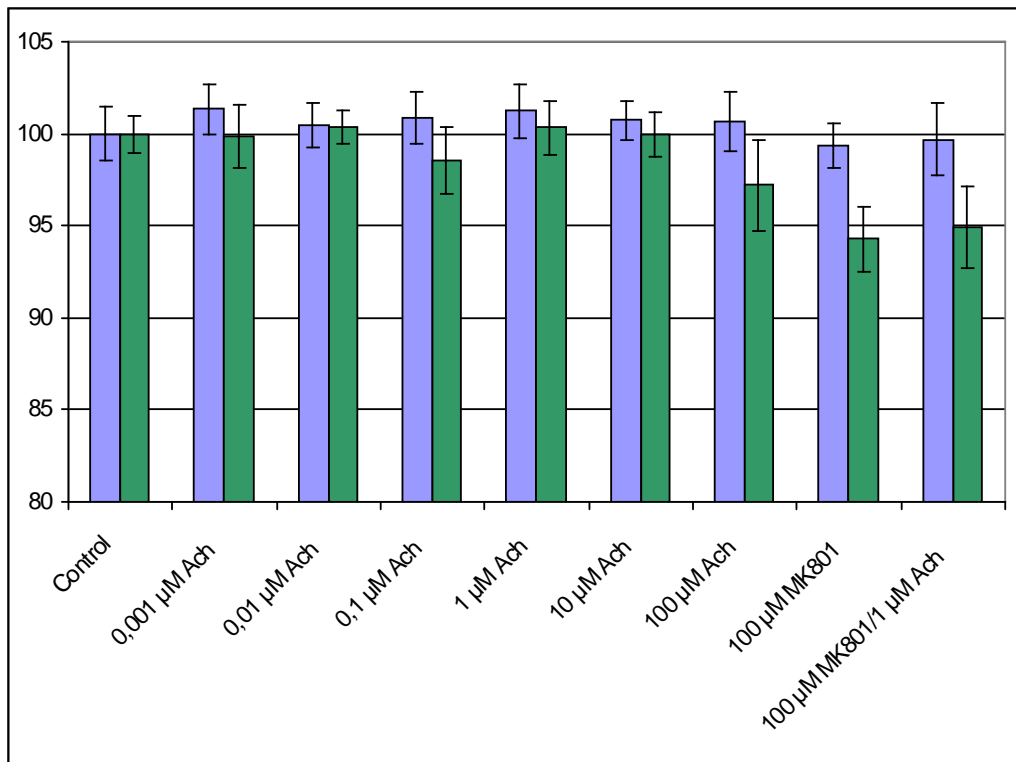


Fig. 4.2.14c: Difference between varying endpoint-concentrations of Ach and MK801 in Mg^{2+} -containing (blue) or Mg^{2+} -free (green) HBSS-solutions compared to the control after 33 minutes (blue) and 39 minutes (green). Control values were set to 100 %. Values are expressed as means \pm SEM (n=8).

However, interestingly no effect of 100 μ M MK801 on the intracellular calcium level was detected using Mg^{2+} -HBSS. Compared to experiments before, where only glycine and Mg^{2+} was not added. Since glycine was not assumed to modulate the intracellular calcium level alone the same test with acetylcholine was repeated in Mg^{2+} -free HBSS supplemented Ca^{2+} . The results revealed (figure 4.2.14b) that the control had one of the highest intracellular calcium level. Comparable to the experiment presented in figure 4.2.14a, acetylcholine seemed to have no detectable effect also in Mg^{2+} -free medium. Only 100 μ M acetylcholine could have shown a little effect, but due to the big standard deviation this wasn't significant. Perhaps following experiments should use increased concentrations of acetylcholine to investigate whether effects could be detected at higher acetylcholine concentrations. However, 100 μ M MK801 was again able to decrease the intracellular calcium level, which confirmed that Mg^{2+} free HBSS was necessary to detect

MK801 dependent changes in intracellular Ca^{2+} . For a better overview the endpoints of the different calcium concentrations were showed by a bar graph (see 4.2.14c) and the outcome of both experiments (blue = solutions with Mg^{2+} and Ca^{2+} , green = solutions with Ca^{2+} and without Mg^{2+}) could be compared with each other.

4.2.2.3 Bay-K 8664 and Verapamil as calcium modulators

Based on the protocol described in 3.5.7, the following described experiments were finally performed in Mg^{2+} - and Ca^{2+} -free HBSS (6648) supplemented with Ca^{2+} . In this context it should be noted, that the fluorescence-dye solution for loading the ECV304 cells with Fluo3-AM was prepared with HBSS (4641) containing Mg^{2+} - and Ca^{2+} . Different concentrations of (S)-(-)-BayK 8664, a L-type Ca^{2+} -channel activator, with/without the the L-type channel blocker Verapamil were the main tested substances in following described experiments in order to investigate their influence on the intracellular calcium level. The substances were dissolved directly in the HBSS/probenecid/Albumin solution (BAPTA), or DMSO (Ionomycin, BayK 8644, Verapamil) to the needed stock solutions. Afterwards the experimental medium was prepared by diluting the stock to the needed 4x concentrations. Since the NMDA-receptor was again not the assumed target in these experiments, glycine was not added as it was done during the experiments described in 4.2.2.1 Experiments were performed on the Tecan GeniosPro at 37° C. Due to the overview reasons percentage of Ionomycin and BAPTA were not shown in the graphs. However, the positive control Ionomycin reached a fluorescence of 443 % (4.2.15a) or 408 % (4.2.15b) and the negative control BAPTA showed fluorescence percentages of 61 % (4.2.15a) or 63 % (4.2.15b).

Since the L-type channel blocker Verapamil already showed to decrease the intracellular calcium level (figure 4.2.13a) and the cause of the increasing Ca^{2+} inside of the ECV304 cells of the control values was still unclear, the L-type Ca^{2+} -channel activator (S)-(-)-BayK 8664 was chosen as an additional assumed positive control which targets another Ca^{2+} -channel than the NMDA receptor. Figure 4.2.15a shows the effects on the intracellular calcium level observed after addition of 0.01, 0.1, 1, 10 μM BayK 8664 with/without 100 μM Verapamil in HBSS-solutions containing Mg^{2+} and Ca^{2+} . All values showed a time-dependent increase in the intracellular calcium level, but compared to the control the curves were quite similar or slightly decreased in case of higher concentrations of BayK

8664. This effect of BayK 8664 could be partially blocked by addition of 100 μM Verapamil. Nearly the same experiment was repeated with the only difference that HBSS-solution without Mg^{2+} was used. Tested concentrations of BayK 8664 were changed to 0.1, 1, 10, 100 μM in order to investigate a possible stronger concentration dependent effect. As it was assumed, the highest concentration of BayK 8664 (100 μM) caused the lowest intracellular calcium level over a period of time again. Interestingly, at the initial measuring phase 100 μM BayK seemed to cause nearly no change in intracellular calcium level which was then stable over the whole measuring period. In contrast to this, 100 μM BayK supplemented with 100 μM Verapamil showed a higher starting point after substance application which decreased rapidly to a similar calcium level as it was seen with 100 μM BayK only. These differences in the initial phase maybe reflected a regulatory phase in which intracellular Ca^{2+} were adjusted. As it was already seen in the experiments with $\text{Mg}^{2+}/\text{Ca}^{2+}$ containing HBSS-solutions, similar curve-progressions of 0.1 μM and 1 μM BayK were observed compared to the control, whereas 10 μM BayK showed a decreased intracellular calcium level. When 100 μM Verapamil were added in combination with BayK, the intracellular calcium levels were again lower compared to the values without Verapamil. For a better overview the fluorescence-endpoints of both experiments were presented as a bar graph (4.2.15c).

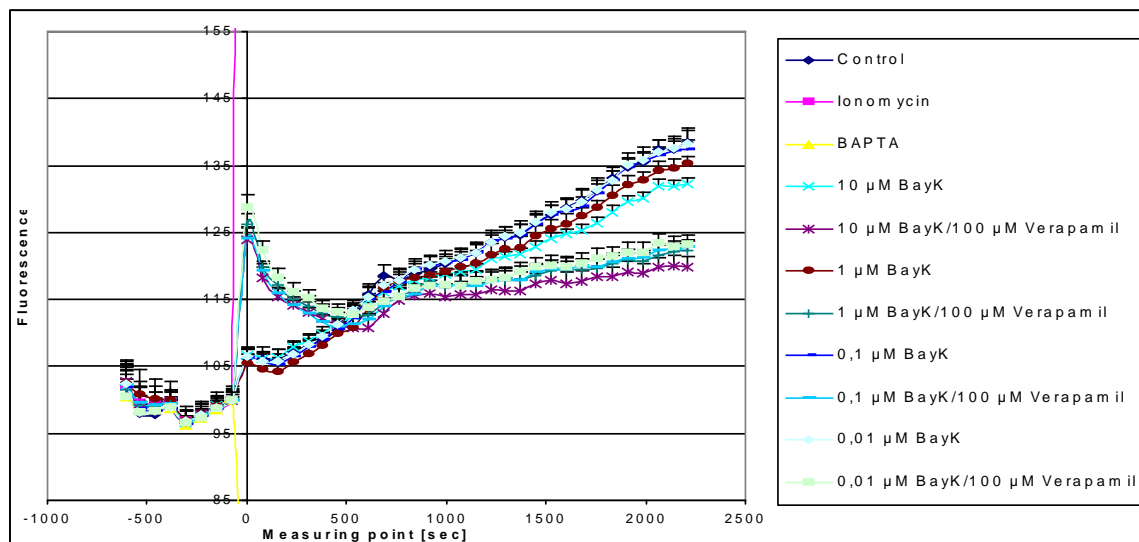


Fig. 4.2.15a: Influence of different concentrations of BayK 8664 with/without 100 μM Verapamil on the intracellular calcium level in solutions containing Mg^{2+} . ECV304 cells were used at passage 184. Values are expressed as means \pm SEM (n=8).

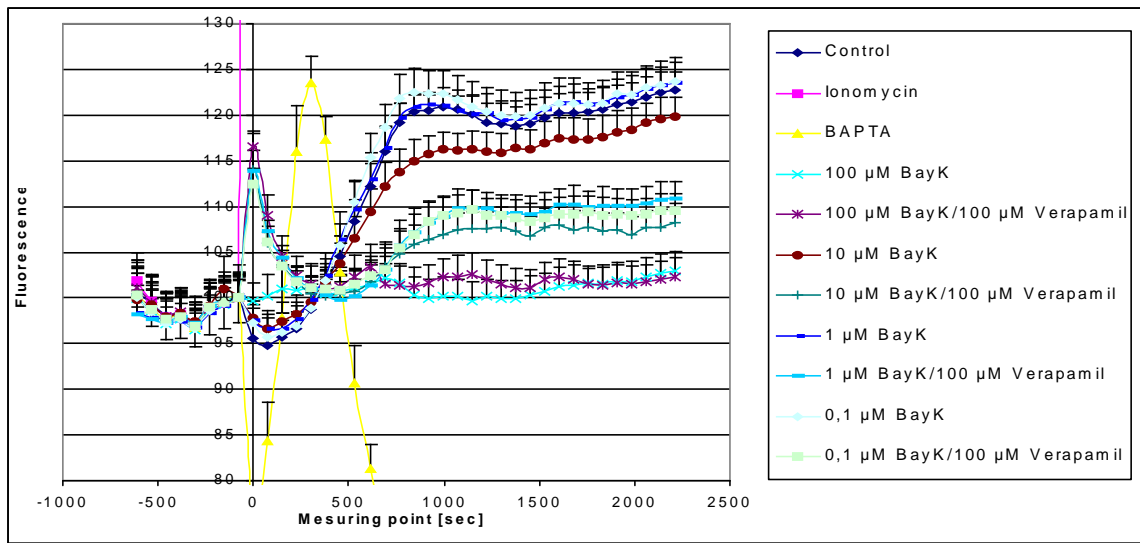


Fig. 4.2.15b: Inference of different concentrations of BayK 8664 with/without 100 μM Verapamil on the intracellular calcium level in solutions without Mg^{2+} . ECV304 cells were used at passage 182. Values are expressed as means \pm SEM (n=8).

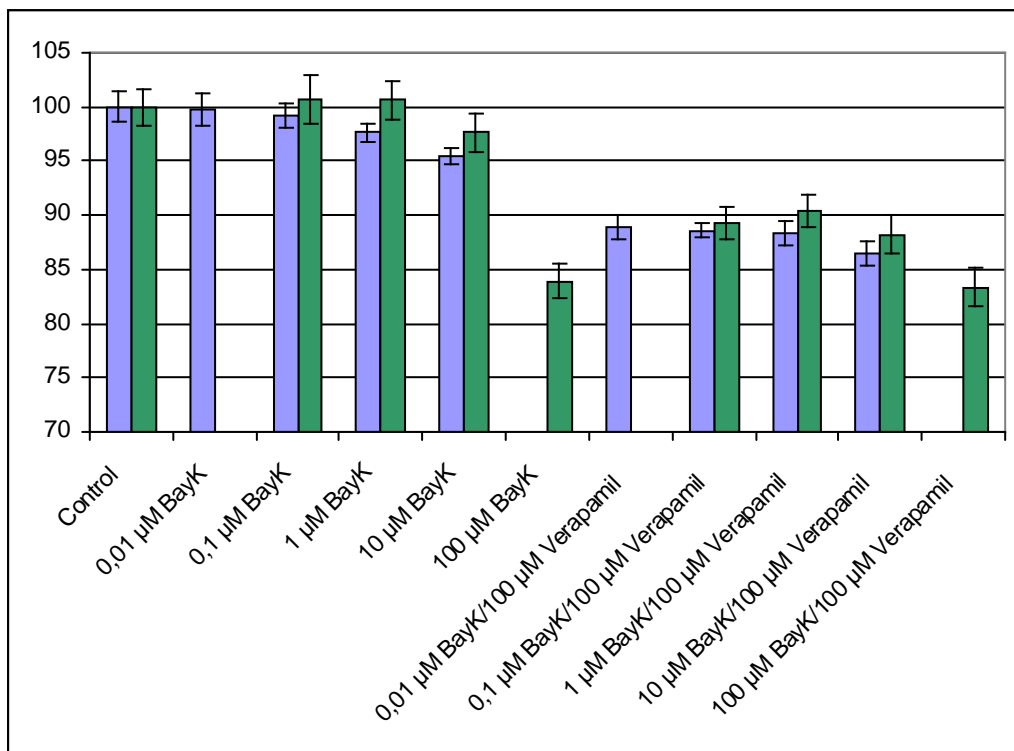


Fig. 4.2.15c: Difference between varying endpoint-concentrations of BayK 8664 with/without 100 μM Verapamil in Mg^{2+} -containing (blue) or Mg^{2+} -free (green) HBSS-solutions after 39 minutes. Values are expressed as means \pm SEM (n=8).

4.2.2.4 Influence of a plasma membrane Ca^{2+} -ATPase modulator and inhibition of the Ca^{2+} -release from the sarcoplasmatic reticulum

Based on the protocol described in 3.5.7, the following described experiment was performed in HBSS (4641) containing Mg^{2+} and Ca^{2+} . The substances were dissolved in water (glutamate, glycine), EtOH (Ryanodine), directly in the HBSS/Probenecid/Albumin solution (BAPTA, Methyl- β -Cyclodextrine), or DMSO (Ionomycin) to the used stock solutions. Afterwards the experimental medium was prepared by diluting the stock solutions to the needed 4x concentrations. Since the NMDA-receptor was also targeted, glycine was needed and added to every solution (final concentration 10 μM glycine). After cells were loaded with the Fluo3-AM-solution, defined wells were pre-incubated with 75 μL of a 10 mM or 50 mM methyl- β -cyclodextrin-solution at 37 °C for 30 minutes (=same pre-incubation step as described in the methods). Notedly, methyl- β -cyclodextrine was added in single pipetting steps to the wells after the baseline was measured. Experiment was performed on the Tecan GeniosPro at 37° C. Due to overview reasons percentage of the fluorescence of Ionomycin and BAPTA were not shown. However, the positive control Ionomycin raised to a fluorescence of 352 % and the negative control BAPTA yielded a fluorescence of 82 %.

Since almost every experiment showed a high intracellular calcium level of the control values over the period of time, tests about the Ca^{2+} -release from intracellular stores and the effect of blocking the plasma membrane Ca^{2+} -ATPase by Ryanodine were carried out. The result of this experiment is shown below (figure 4.2.15a). No significant differences between the values with Ryanodine and glutamate with/without each other were detected compared to the control. Every value with Ryanodine except those with 1 mM glutamate had a lower intracellular calcium level compared to the control. This could be interpreted as a little tendency. However, no effect of glutamate on the intracellular calcium level could be observed. Interestingly the pre-incubation with methyl- β -cyclodextrine had already a high influence on the absolute values of the base fluorescence at the starting point (figure 4.2.16b). Moreover, addition of 25 μL (to reach a total volume of 100 μL each well) of the single concentrated methyl- β -cyclodextrin-solutions even increased this effect, although the difference in the absolute fluorescence could not be recognised when the values were presented as percentages (figure 4.2.16a). 50 mM methyl- β -cyclodextrin even nearly reaches the same fluorescence values as it was observed for the positive control Ionomycin. This effect is probably caused due to the block of the PMCA by

dissolution out of the membrane. Further disintegration of the membrane maybe enables free calcium entry into the cells. For a better overview the fluorescence-endpoints of the absolute values were also presented as a bar graph (4.2.16c).

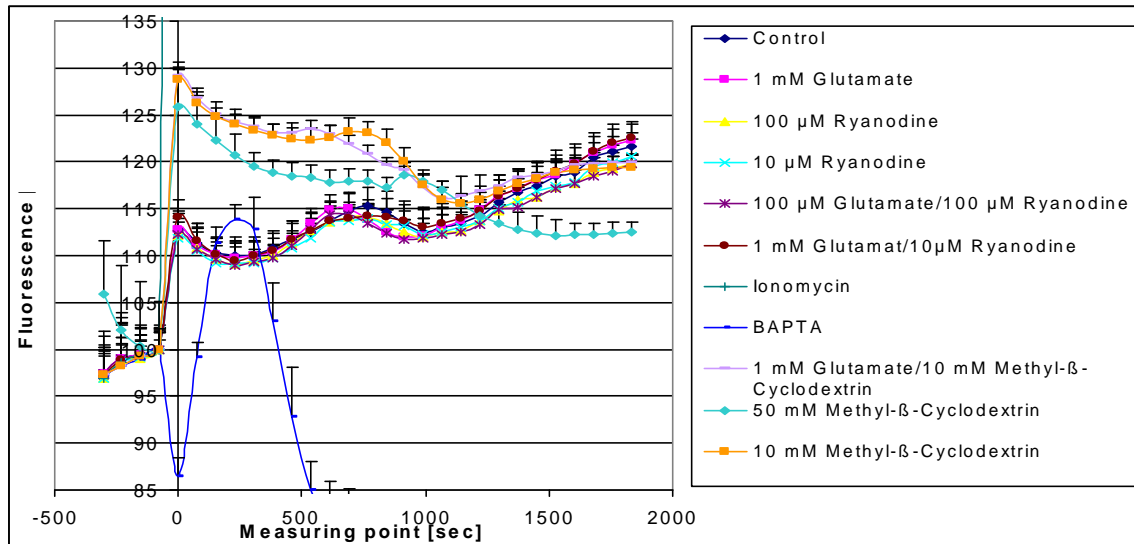


Fig. 4.2.16a: Influence of different concentrations of Ryanodine or methyl-β-cyclodextrine with/without 1 mM glutamate compared to a control or 1 mM glutamate alone. ECV304 cells were used at passage 190. Values are expressed as means \pm SEM (n=8).

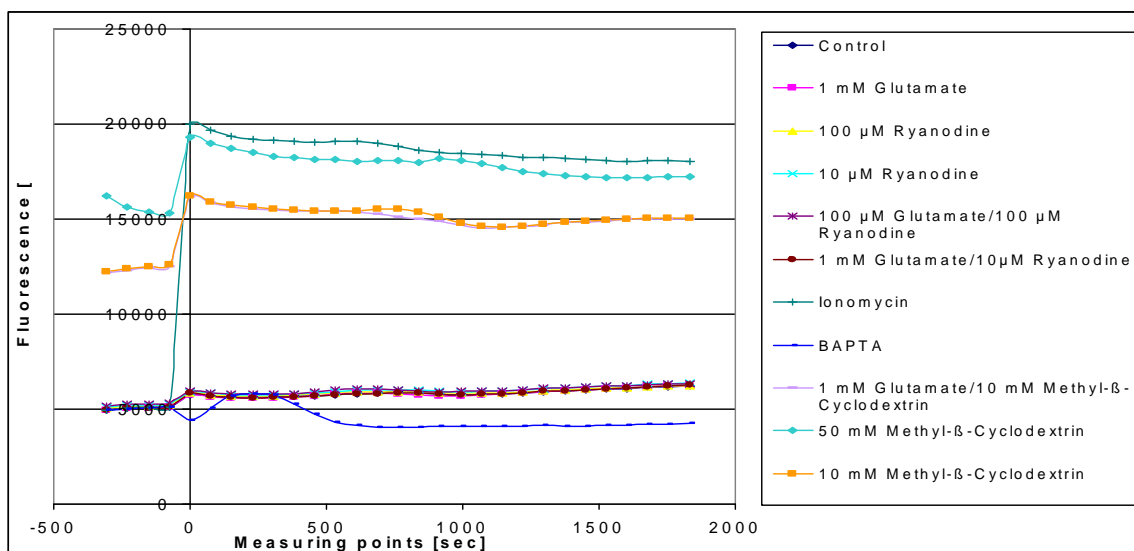


Fig. 4.2.16b: Absolute values of the experiment already seen in figure 4.2.16a, whereas the influence of the preincubation with methyl-β-cyclodextrin could not be seen there. ECV304 cells were used at passage 190. Values are expressed as means \pm SEM (n=8).

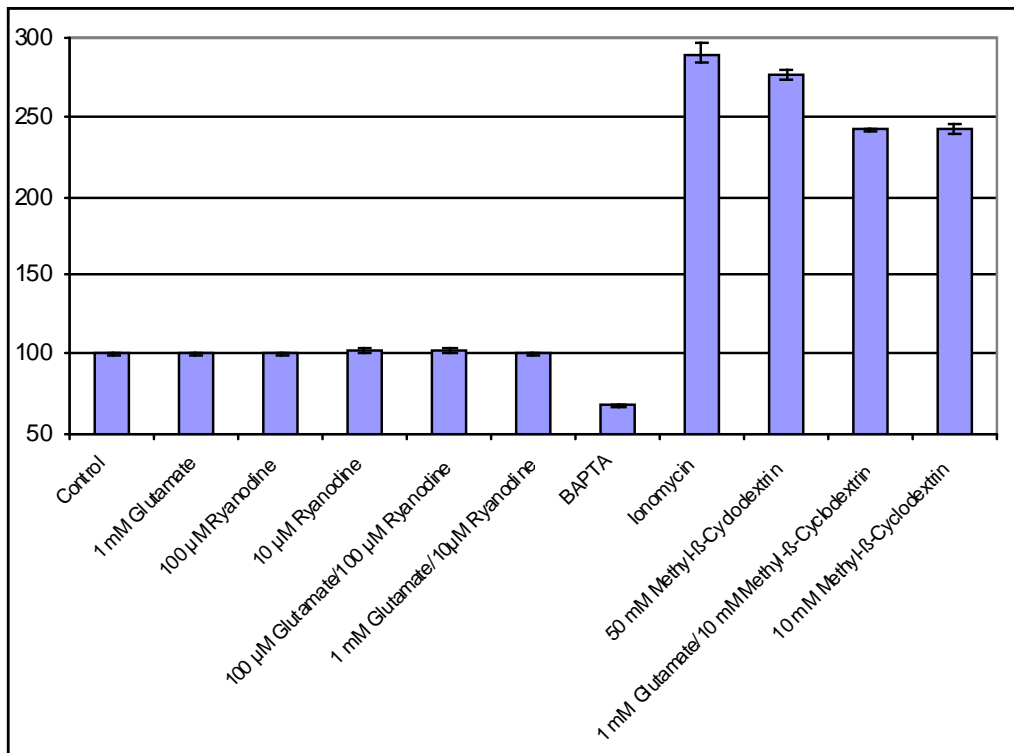


Fig. 4.2.16c: Difference between varying endpoint-concentrations of the absolute values of 1 mM glutamate with/without different concentrations of Ryanodine or Methyl-β-cyclodextrin compared to the control after 33 minutes. Control values were set to 100 %. Values are expressed as means +/- SEM (n=8).

4.3 Recheck for presence of the NMDA receptor in the cell membrane by immunofluorescence microscopy in cell line ECV304

4.3.1 Immunofluorescence images of non-permeabilized ECV304 cells

Although western blotting and immunofluorescence microscopy already suggested presence of NMDAR subunits in cell line ECV304, the lack of an increased intracellular calcium by agonists as glutamate or NMDA indicated probably a receptor, which is not functionally active. Therefore immunofluorescence microscopy was performed again in order to ensure the presence and to investigate the localisation of NMDA receptor subunits

in our cell line. Since many antibodies target protein domains which are located in the cytoplasm, a permeabilization of the cell's membrane is necessary to enable the contact to the antibody's target. However, next to the Abcam antibody for the NR-1 subunit (ab52177), we also purchased antibodies from Santa Cruz Biotechnology binding fragments of the NMDAR subunits which are located extracellularly. For these antibodies no permeabilization is needed in the first place. The recheck for the presence of the NMDA receptor should provide a better understanding if the NMDAR subunits are expressed on the surface of ECV304 cells. The used protocol is described in materials and methods, whereby the permeabilization step was not carried out. Intensity of the fluorescence signals were detected for Propidiumiodide at level 2 with an exposure time of 4 seconds and for the NR-subunits at level 3 with an exposure time of 6 seconds. The increased exposure time for Propidiumiodide was necessary for non-permeabilized cell layers, because this substance is generally excluded from viable cells, but can easily penetrate into dead (or permeabilized) cells.

Figures 4.3.1-4.3.6 show the immunofluorescence images for NMDA subunits NR-1, NR-2A – 2C of non permeabilised ECV304 cells. For NR-1 stainings the Abcam antibody was compared to the one obtained from Santa Cruz. Also according blank images with only the secondary antibody were shown in the figures in order to facilitate the comparison and to point out to significant stainings for NMDA-subunits. Cells were seeded at a density of 80,000cells/cm² and cultured for 10 days under optimal growth conditions with medium exchange every second day. Used protocol for the preparation was already described in 3.5.6.2.

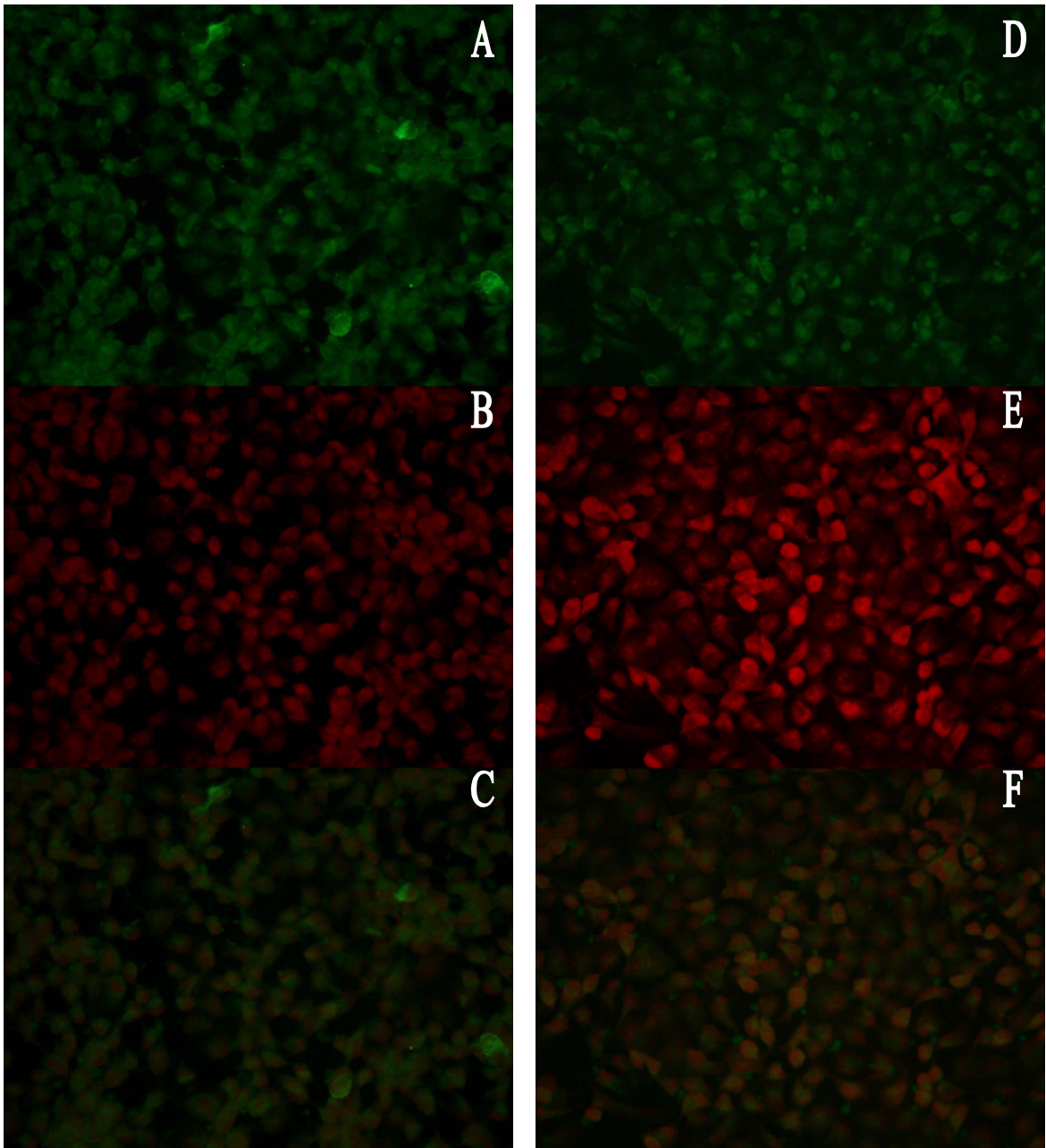


Figure 4.3.1: Immunofluorescence images of NR1 subunits of ECV304 cells using primary Abcam antibody [A], with the appropriate cell nuclei stain (propidium iodide) as control [B] and the merge of A and B [C]. This could be compared to control images, where only the secondary antibody was used (green fluorescence [D], cell nuclei [E], merge of D and E [F]).

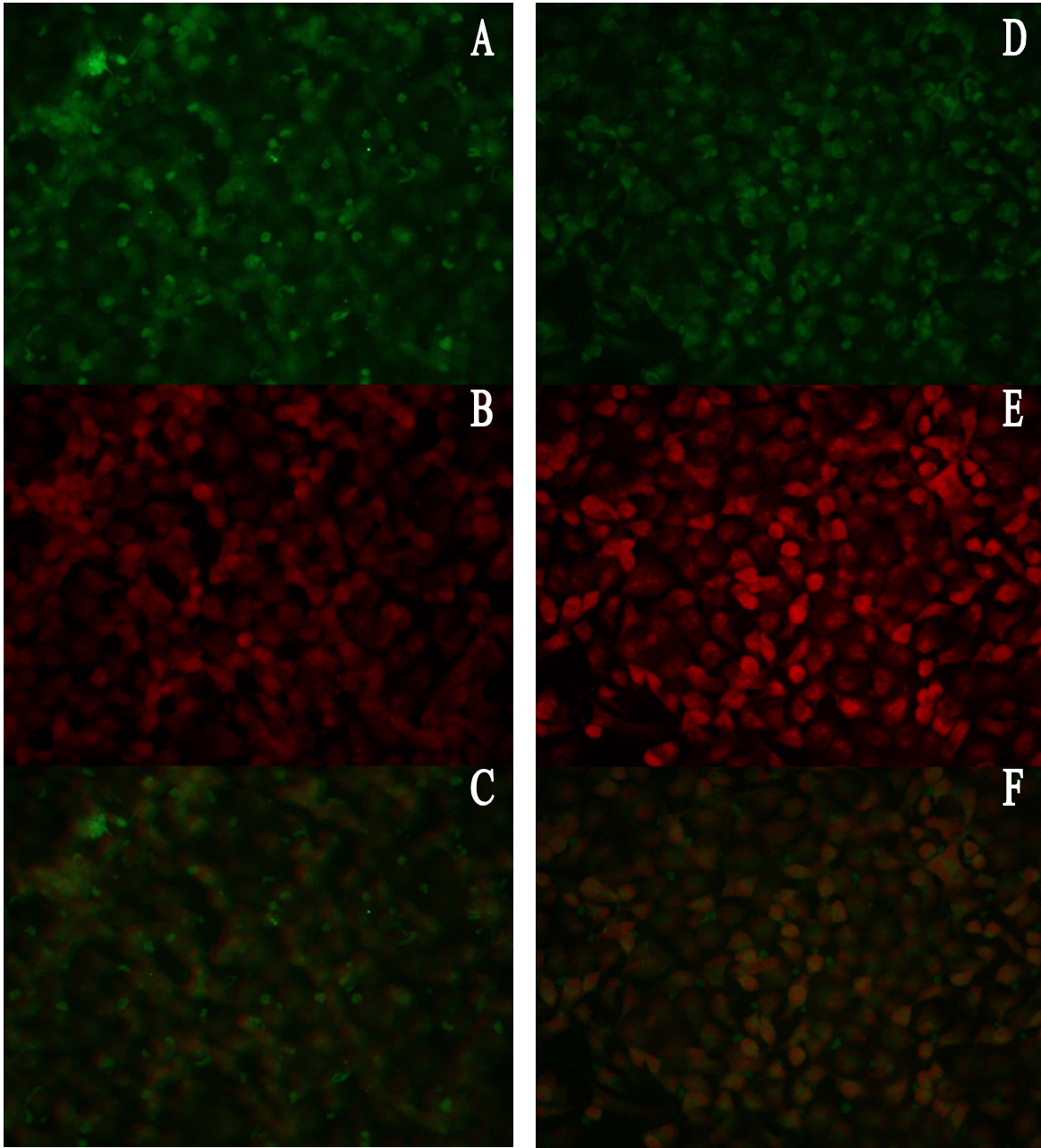


Figure 4.3.2: Immunofluorescence images of NR1 subunits of ECV304 cells using primary Santa Cruz Biotechnology antibody [A], with the appropriate cell nuclei stain (propidium iodide) as control [B] and the merge of A and B [C]. This could be compared to control images, where only the secondary antibody was used (green fluorescence [D], cell nuclei [E], merge of D and E [F]).

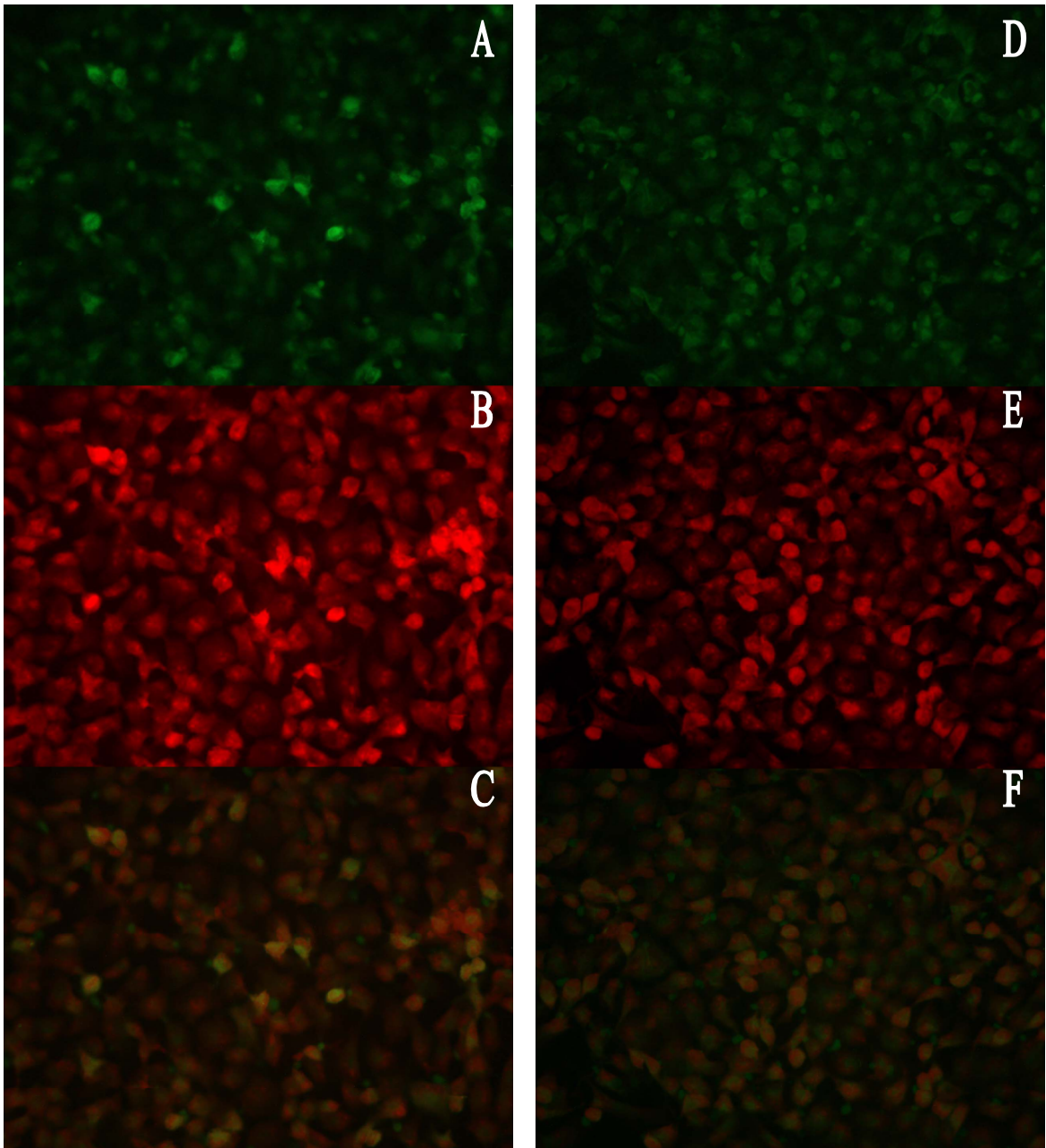


Figure 4.3.3: Immunofluorescence images of NR-2A subunits of ECV304 cells using primary Santa Cruz Biotechnology antibody [A], with the appropriate cell nuclei stain (propidium iodide) as control [B] and the merge of A and B [C]. This could be compared to control images, where only the secondary antibody alone was used (green fluorescence [D], cell nuclei [E], merge of D and E [F]).

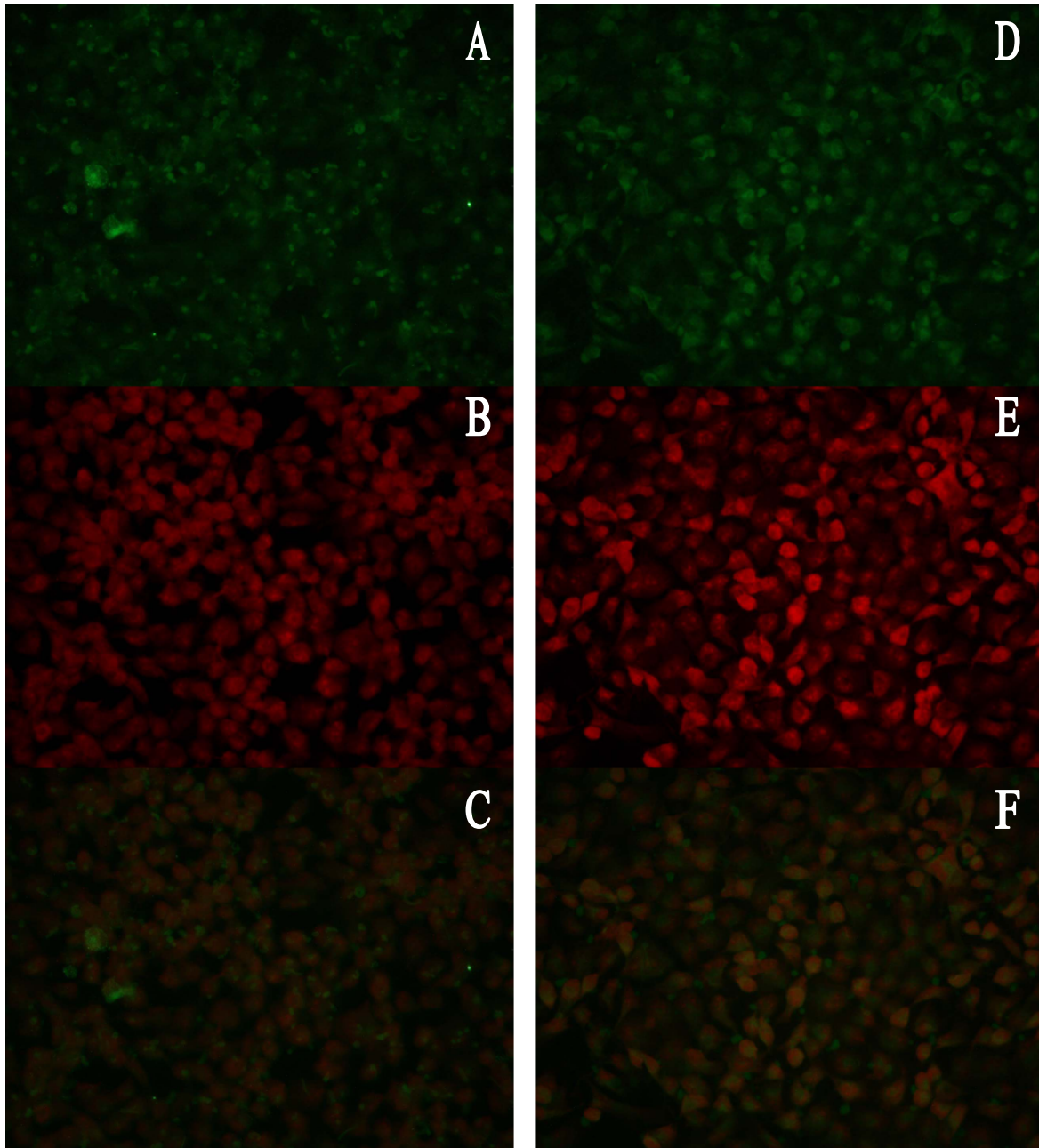


Figure 4.3.4: Immunofluorescence images of NR-2B subunits of ECV304 cells using primary Santa Cruz Biotechnology antibody [A], with the appropriate cell nuclei stain (propidium iodide) as control [B] and the merge of A and B [C]. This could be compared to control images, where only the secondary antibody alone was used (green fluorescence [D], cell nuclei [E], merge of D and E [F]).

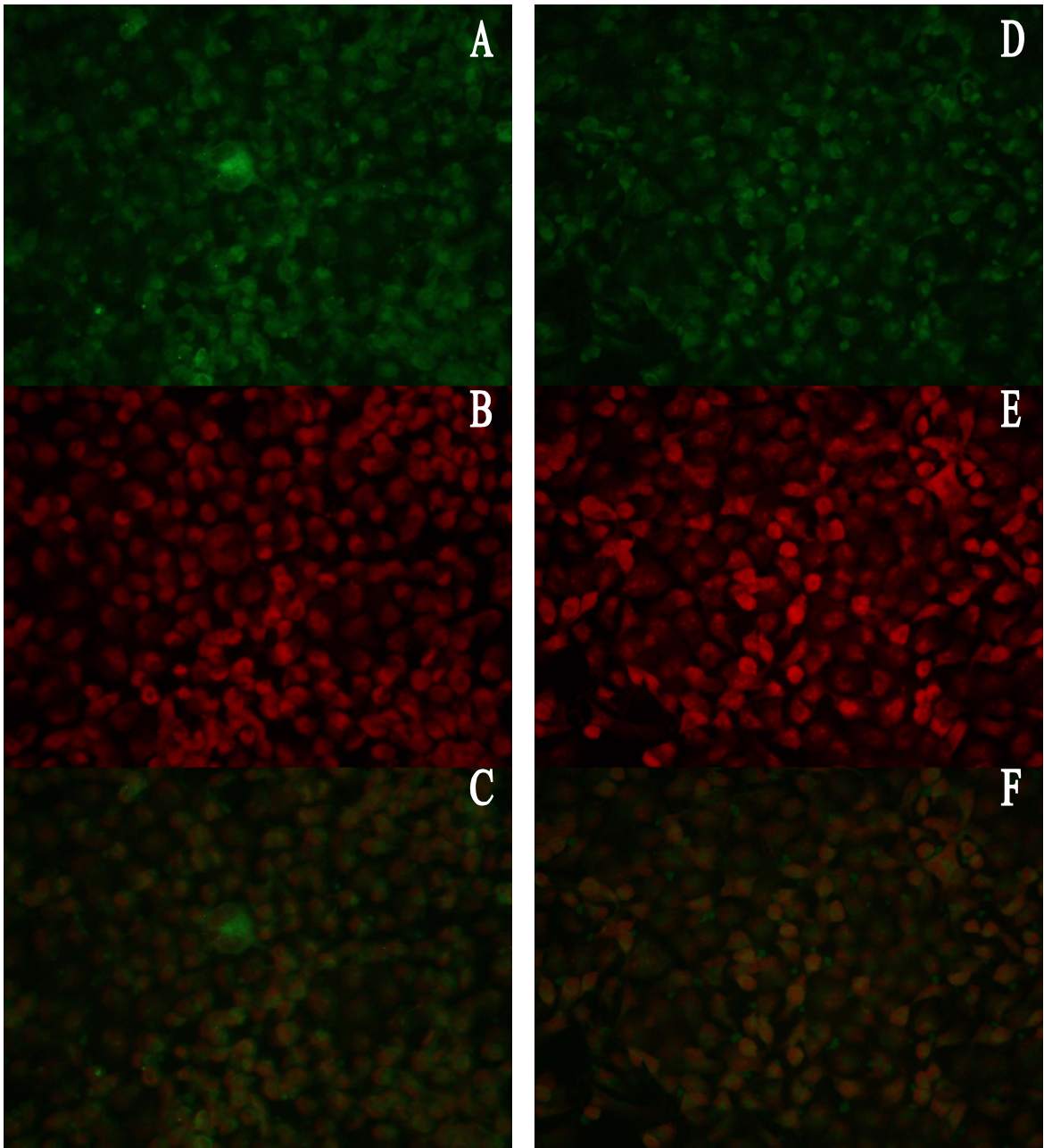


Figure 4.3.5: Immunofluorescence images of NR-2C subunits of ECV304 cells using primary Santa Cruz Biotechnology antibody [A], with the appropriate cell nuclei stain (propidium iodide) as control [B] and the merge of A and B [C]. This could be compared to control images, where only the secondary antibody alone was used (green fluorescence [D], cell nuclei [E], merge of D and E [F]).

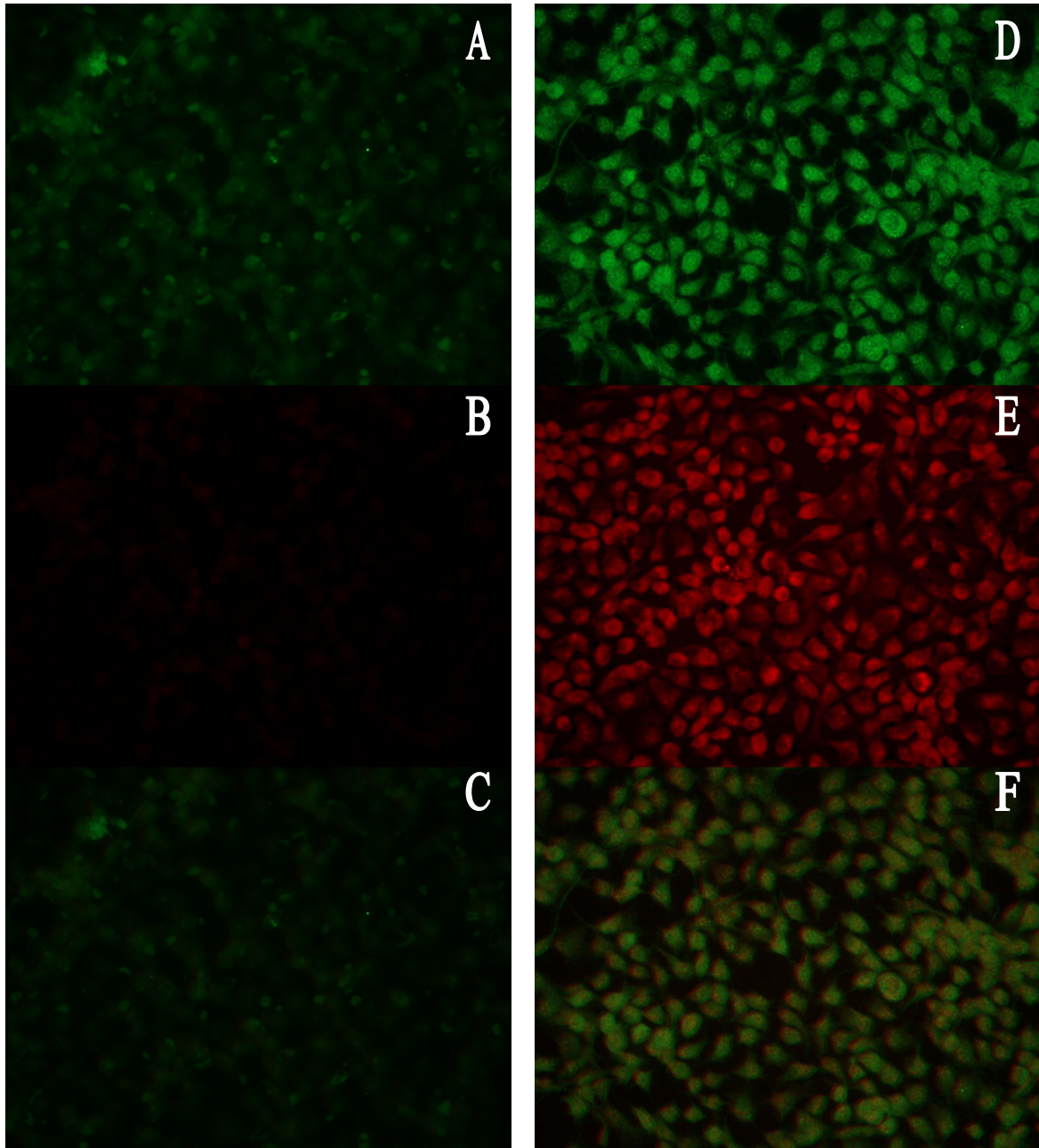


Figure 4.3.6: Immunofluorescence images of non permeabilized NR-1 subunits of ECV304 cells using primary Santa Cruz Biotechnology antibody [A], with the appropriate cell nuclei stain (propidium iodide) as control [B] and the merge of A and B [C]. This was compared with images of permeabilized ECV304 cells with the same antibody (green fluorescence [D], cell nuclei [E], merge of D and E [F]).

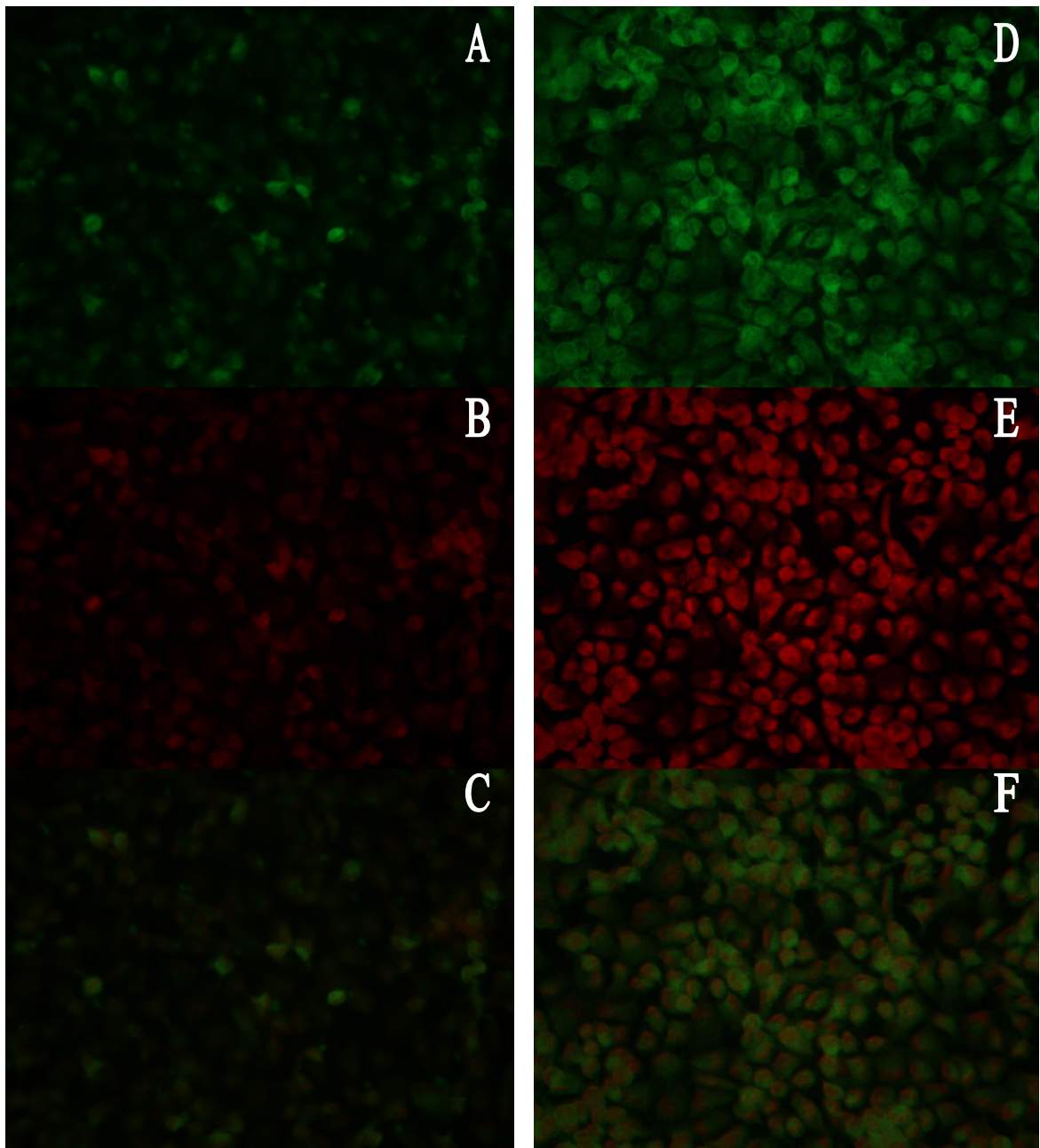


Figure 4.3.7: Immunofluorescence images of non permeabilized NR-2A subunits of ECV304 cells using primary Santa Cruz Biotechnology antibody [A], with the appropriate cell nuclei stain (propidium iodide) as control [B] and the merge of A and B [C]. This was compared with images of permeabilized ECV304 cells with the same antibody (green fluorescence [D], cell nuclei [E], merge of D and E [F]).

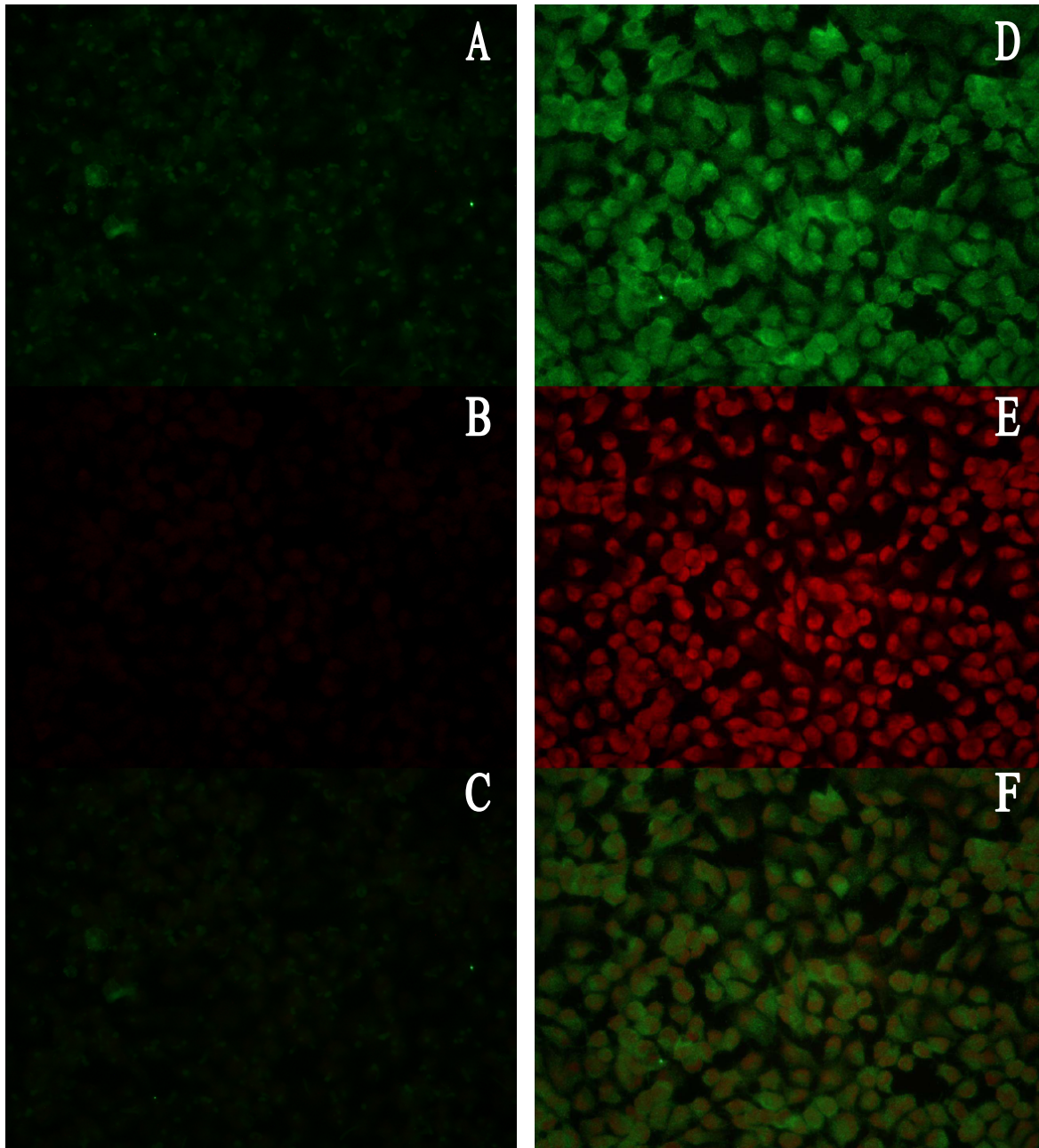


Figure 4.3.8: Immunofluorescence images of non permeabilized NR-2B subunits of ECV304 cells using primary Santa Cruz Biotechnology antibody [A], with the appropriate cell nuclei stain (propidium iodide) as control [B] and the merge of A and B [C]. This was compared with images of permeabilized ECV304 cells with the same antibody (green fluorescence [D], cell nuclei [E], merge of D and E [F]).

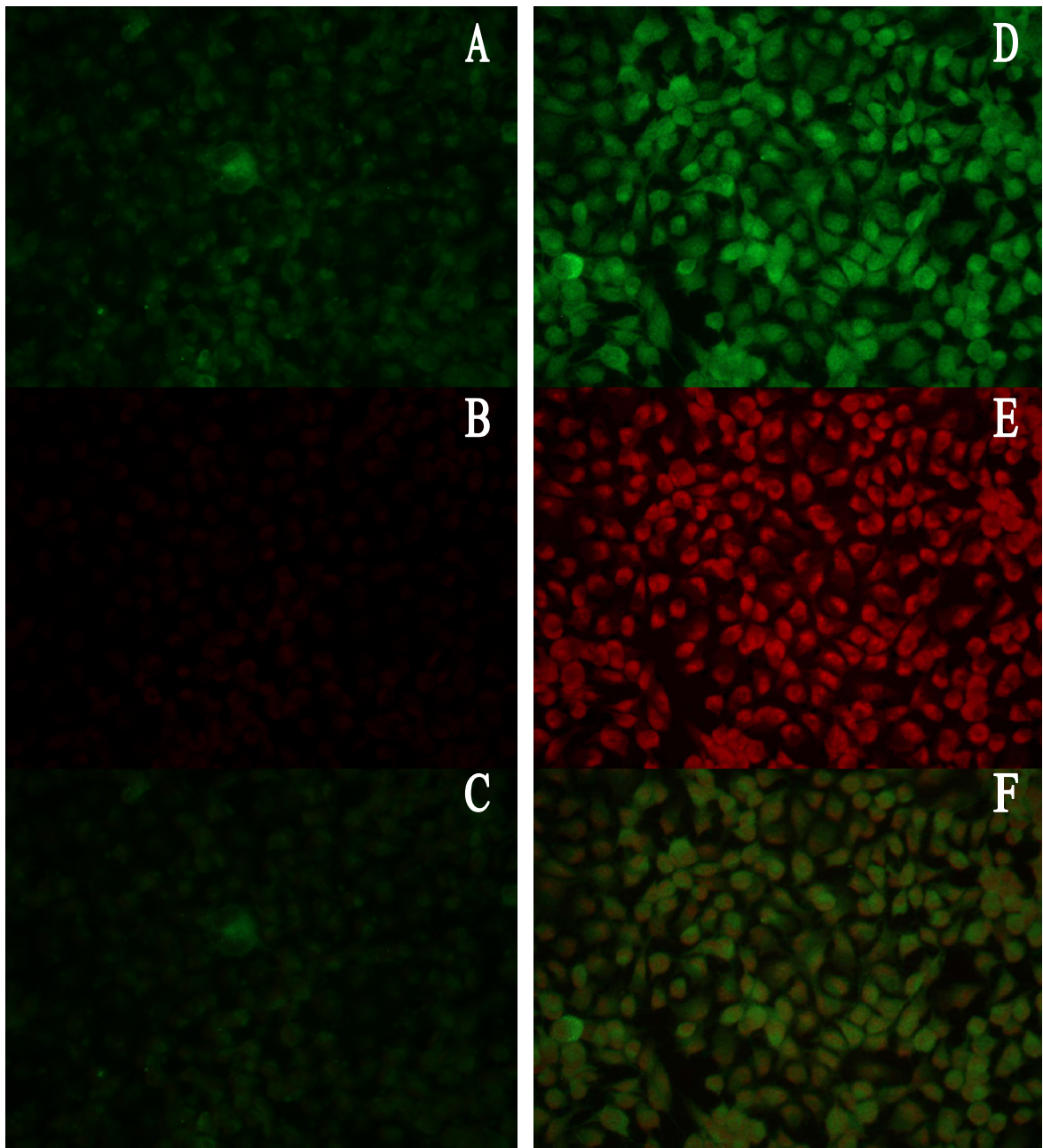


Figure 4.3.9: Immunofluorescence images of non permeabilized NR-2C subunits of ECV304 cells using primary Santa Cruz Biotechnology antibody [A], with the appropriate cell nuclei stain (propidium iodide) as control [B] and the merge of A and B [C]. This was compared with images of permeabilized ECV304 cells with the same antibody (green fluorescence [D], cell nuclei [E], merge of D and E [F]). Although a smaller fluorescence

4.3.2 Attempt to induce NMDA receptor expression on the surface of ECV304 cells by a pre-stimulation with 1 mM glutamate

Since previous experiments suggested that the NMDA receptor is mostly located in the cytoplasm of the cells, ECV304 cells were pre-incubated on cover slips with 1 mM glutamate for 30 minutes. The idea was that the stimulation should increase the presence of the intracellular found fragments on the surface of the cell. This was then investigated by immunofluorescence microscopy. This pre-incubation was made, since stimulation may lead to an increased shuttling of the receptor to the surface in order to interact with the agonist.

Intensity of the fluorescence signals of non-permeabilized cell layers was detected for Propidiumiodide at level 3 with an exposure time of 2 seconds and for the NR-subunits at level 3 with an exposure time of 4 seconds. The increased exposure time and the higher fluorescence intensity level of Propidiumiodide avowed itself by the fact that this substance is generally excluded from viable cells, but can easily penetrate into dead cells.

Figures 4.3.10 and 4.3.11 show the immunofluorescence images of non permeabilized ECV304 cells. Thereby a normal prepared image of the NR-1 subunit (Fig. 4.4.1) is compared to an image (4.4.2) where the cover slips were pre-incubated with 1 mM glutamate for 30 minutes. Also according blank images with only the secondary antibody were shown in the figures in order to facilitate the comparison and to show the significant stainings for NMDA-subunits. Cells were seeded at a density of 80,000cells/cm² and cultured for 10 days under optimal growth conditions with medium exchange every second day. Used protocol for the preparation was already described in 3.5.6.2.

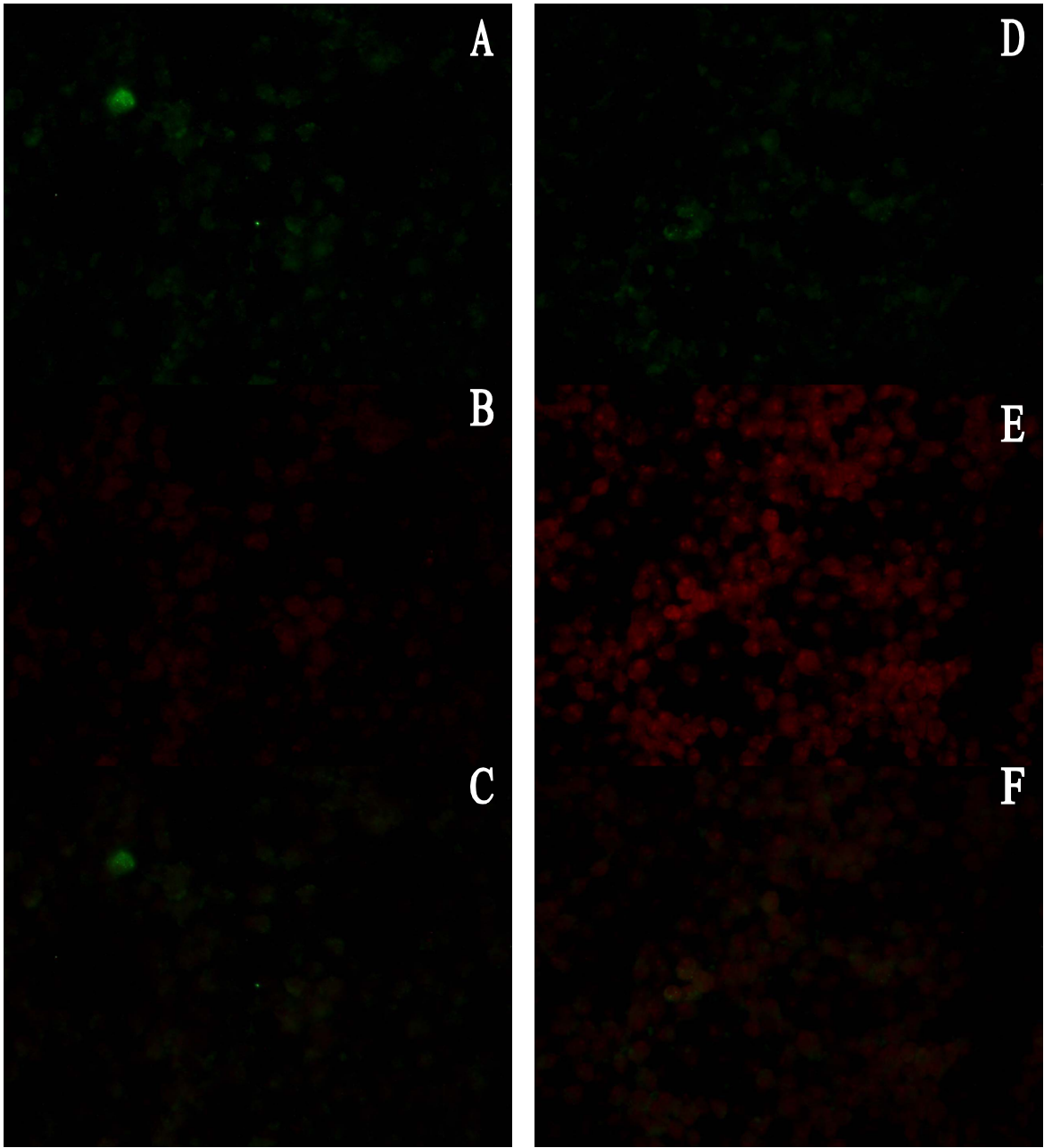


Figure 4.3.10: Immunofluorescence images of NR-1 subunits of ECV304 cells which were not stimulated für with 1 mM glutamate for 30 minutes. Used primary Santa Cruz Biotechnology antibody [A], with the appropriate cell nuclei stain (propidium iodide) as control [B] and the merge of A and B [C]. This could be compared to control images, where only the secondary antibody alone was used (green fluorescence [D], cell nuclei [E], merge of D and E [F]).

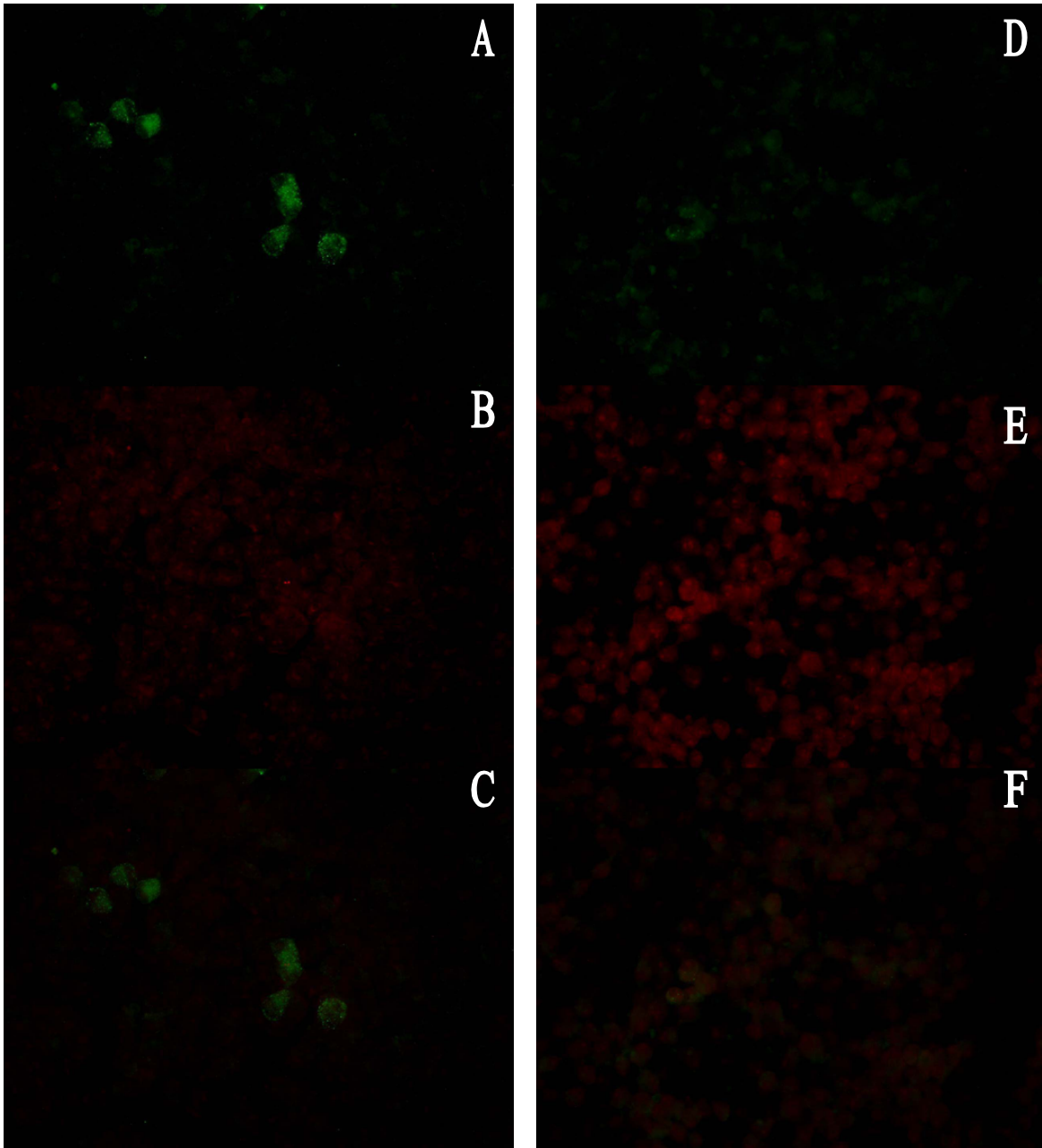


Figure 4.3.11: Immunofluorescence images of NR-1 subunits of cells which were pre-incubated with 1 mM glutamate for 30 minutes. Used primary Santa Cruz Biotechnology antibody [A], with the appropriate cell nuclei stain (propidium iodide) as control [B] and the merge of A and B [C]. This could be compared to control images, where only the secondary antibody alone was used (green fluorescence [D], cell nuclei [E], merge of D and E [F]).

It was assumed that these slight differences in fluorescence could also be due to unspecific binding extracellularly. Moreover, the fluorescence intensity of images with permeabilized ECV304 cells from chapter 4.1.2 were even stronger compared to the non-permeabilized ones (see figures 4.3.6 – 4.3.9). For a better comparison those images were also presented with the same fluorescence intensity (propidium iodide at level 2, NR-subunits at level 3) and the same exposure time (propidium iodide for 2/3 seconds, NR-subunits for 4 seconds). This indicates that NMDA receptor subunits are mostly expressed and located in the cytoplasm in our ECV304 cell line.

Therefore an experiment was performed to induce NMDAR-subunit expression on the surface of ECV304 cells by a pre-incubation step with 1 mM glutamate. These images showed that some cells were sensitive to 1 mM glutamate and induced NR-1 subunit expression on the surface of ECV304 cells. However, if this induced binding of the primary antibody could also be related to an increased NMDAR functionality is still unclear.

4.4 Influence of 1 mM glutamate with or without 10 μ M MK801 on the transendothelial electrical resistance (TEER)

Several groups have recently shown that increased glutamate is able to decrease the barrier integrity of BBB in vitro models [18,20]. It was suggested that the decrease of TEER was mediated by the NMDAR, since NMDAR antagonist MK801 was able to block these effects. Since no significant increase of the intracellular calcium level as well as no expression of the NMDA receptor on the surface were found, no decrease of TEER could have been expected based on these data. In order to assess the influence of glutamate on the integrity of the BBB model, cells were seeded on collagen-coated 6 well Transwell inserts and were cultured for 14 days. Figure 4.4.1 shows the effects of 1 mM glutamate with or without 10 μ M MK801 and the appropriate controls. Interestingly, these experiments confirmed previously published data from other research groups. 1 mM glutamate decreased the TEER in a time-dependent manner in serum and heparin free medium. This negative effect was slightly prevented by 10 μ M of the NMDAR-antagonist MK801 during the exposure time of 3 hours. After the 3 hour exposure, the medium was changed to normal serum and heparin free growth medium for another 21 hours. After 24

hours TEER was still decreased after the glutamate treatment, whereas addition of MK801 to the glutamate during prior treatment was able to restabilize the BBB within this time-frame. Interestingly, these effects were only detected in serum and heparin free medium, but not in basic growth medium containing serum and heparin. This could be a hint for serum and/or heparin BBB stabilising effects during glutamate treatment.

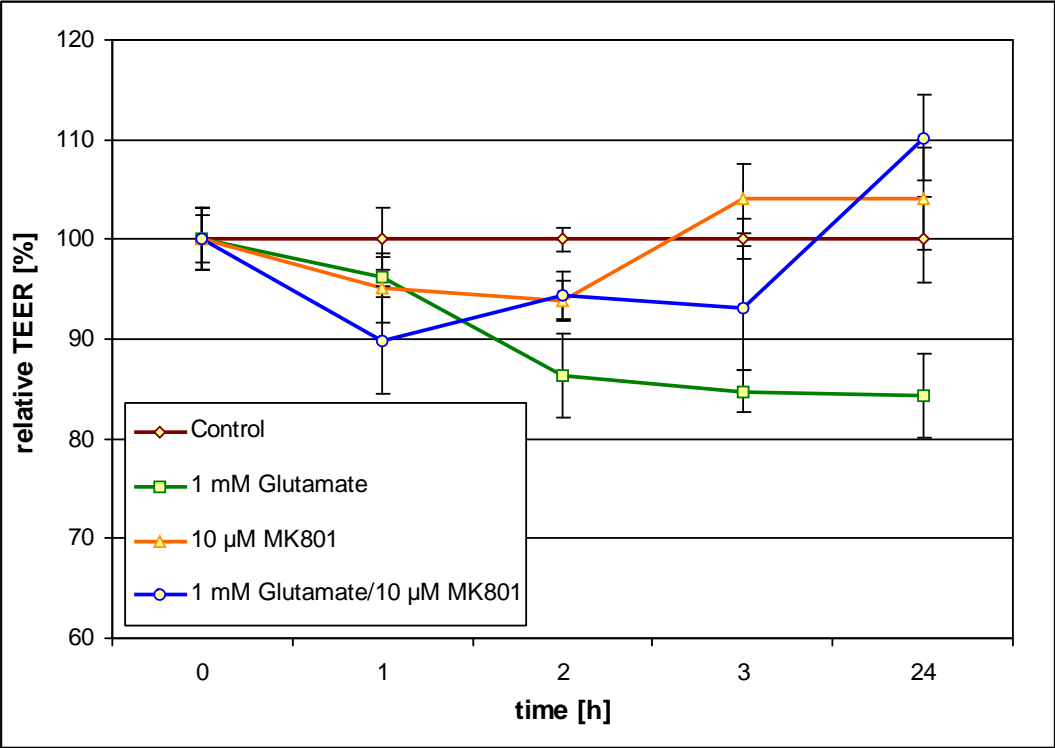


Fig. 4.4.1: Loss of TEER by 1 mM glutamate exposure over a period of time. Addition of 10 μM MK801 was able to reduce this effect. Values are expressed as means +/- SEM (n=3).

4.5 Influence of 1 mM glutamate with/without 10 μ M MK801 on specific protein-expressions

As described in materials and methods (3.5.4-3.5.5), cells grown on Transwell inserts were treated with 1 mM glutamate with/without 10 μ M MK801 for 3 hours, then the experimental medium was removed, refilled with serum- and heparin- free C6-medium and incubated for another 21 hours. These treatments led partly to decreased TEER values. In order to investigate the effects onto the expression levels of several proteins, western blots were carried out. Prior to subsequent western blot analysis, cells were lysed and protein concentrations were determined by a Bradford protein assay.

Tight junction proteins (Occludin, ZO-1):

Figure 4.5.1 shows the influence of 1 mM glutamate with/without 10 μ M MK801 on the protein expression of occludin and ZO-1 compared to the control. Thereby 1 mM glutamate was able to reduce the amount of total occludin level compared to the control. Even addition of 10 μ M MK801 was not able to reduce this glutamate-induced down-regulation.

The tight junction protein ZO-1 showed other effects compared to occludin. Here, 1 mM glutamate seemed to induce a small increase in the total ZO-1 protein level. However, on the other hand 1 mM glutamate with 10 μ M MK801 induced ZO-1 expression in ECV304 cells, by what partially protection of the BBB could be assumed.

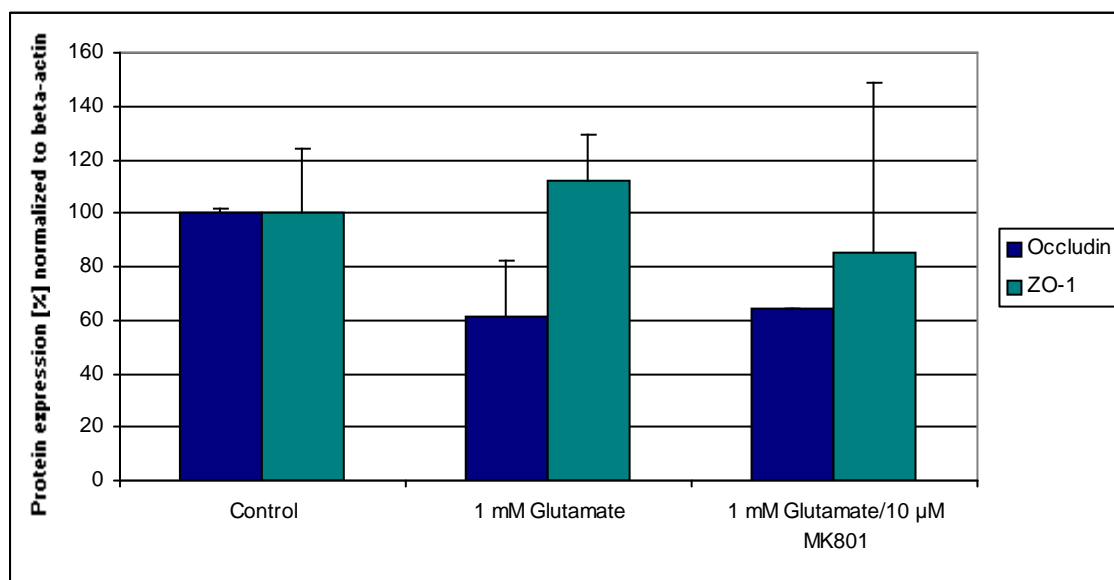
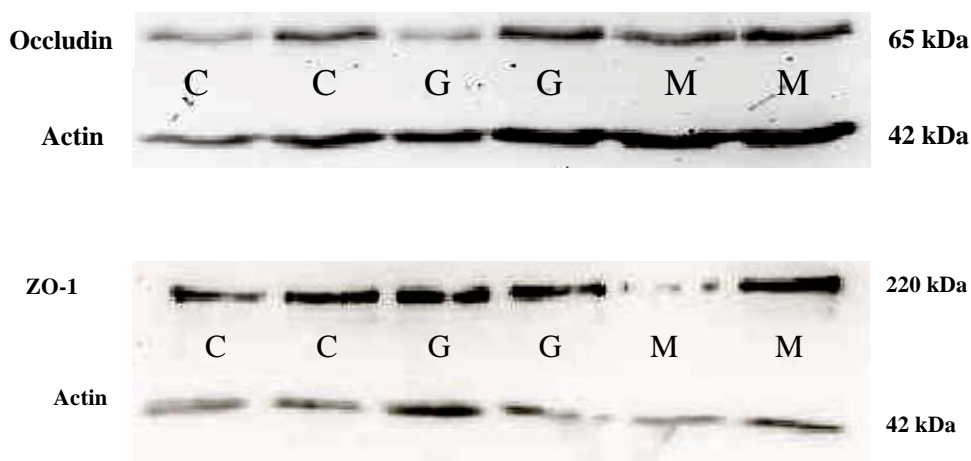


Fig. 4.5.1: Influence of 1 mM glutamate with/without 10 μ M MK801 on the total protein level of Occludin and ZO-1. C = Control, G = 1 mM glutamate, M = 1 mM glutamate/10 μ M MK801. Values are expressed as means \pm SEM (n=2).

Efflux transporter proteins (P-gP, MRP-1):

In figure 4.5.2 the influence of 1 mM glutamate with/without 10 μ M MK801 on the protein level of P-gP and MRP-1 were illustrated. Due to a bigger standard deviation it is hard to say, if 1 mM glutamate really could decrease the expression of P-gP significantly. However, 1 mM glutamate with 10 μ M MK801 probably had a tendency to decrease the total P-gP level.

The expression of the efflux pump MRP-1 seemed to be almost not, or just slightly influenced by 1 mM glutamate with/without 10 μ M MK801 compared to the control. However, a small decreasing tendency was visible.

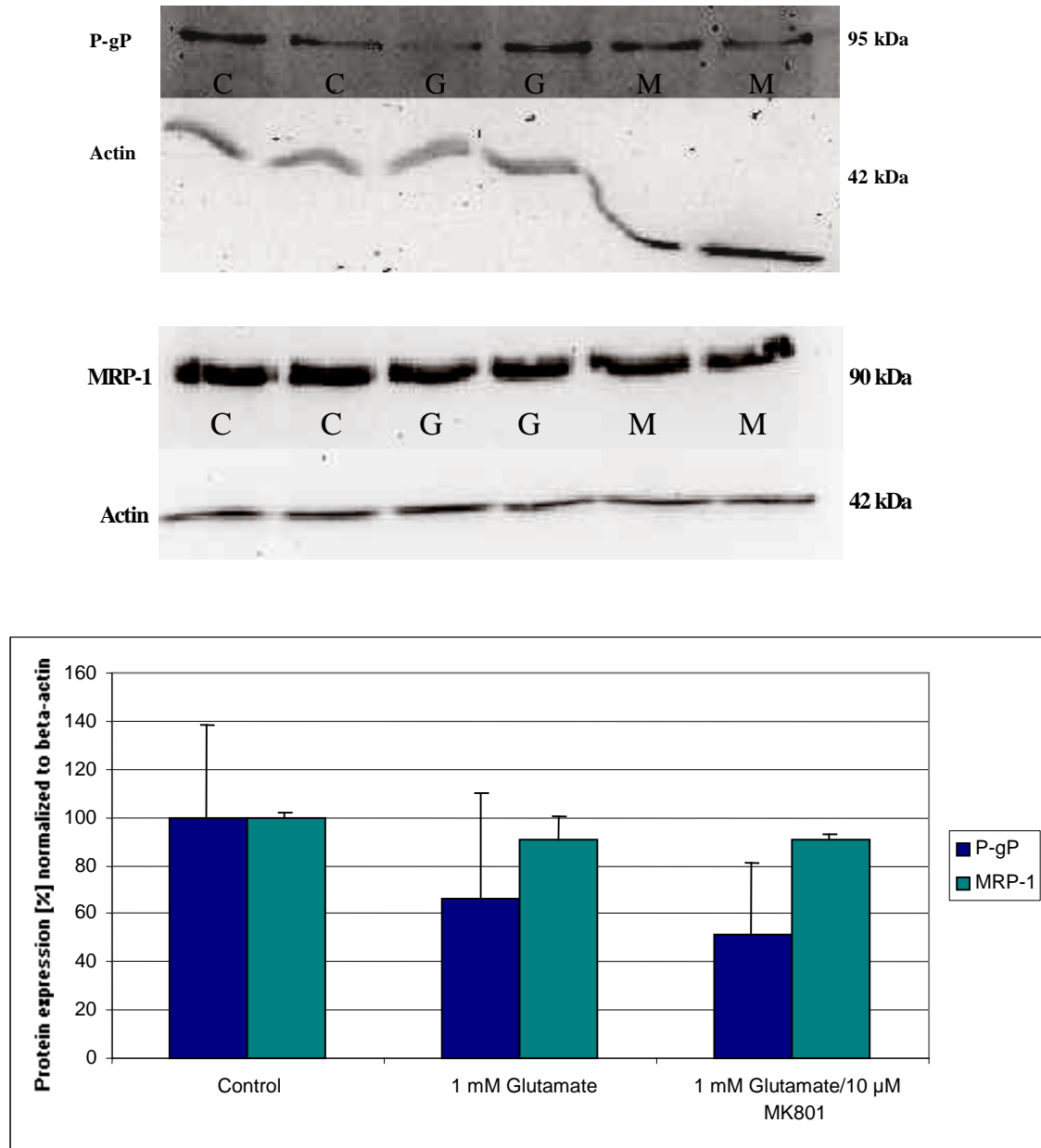


Fig. 4.5.2: Influence of 1 mM glutamate with/without 10 μ M MK801 on the total protein level of P-gP and MRP-1. C = Control, G = 1 mM glutamate, M = 1 mM glutamate/10 μ M MK801. Values are expressed as means \pm SEM (n=2).

Cell-adhesion molecules (ICAM-1, E-Selectin):

Figure 4.5.3 shows the influence of 1 mM glutamate with/without 10 μ M MK801 on the total protein level of ICAM-1 and E-selectin. Thereby, it appeared that 1 mM glutamate did not influence the protein level of ICAM-1, but in combination with 10 μ M MK801 the protein level has doubled compared to the control values.

No E-selectin was found at all. This indicates that the cells were not induced to an inflammatory status. For a better demonstration samples positive for E-selectin were additionally shown.

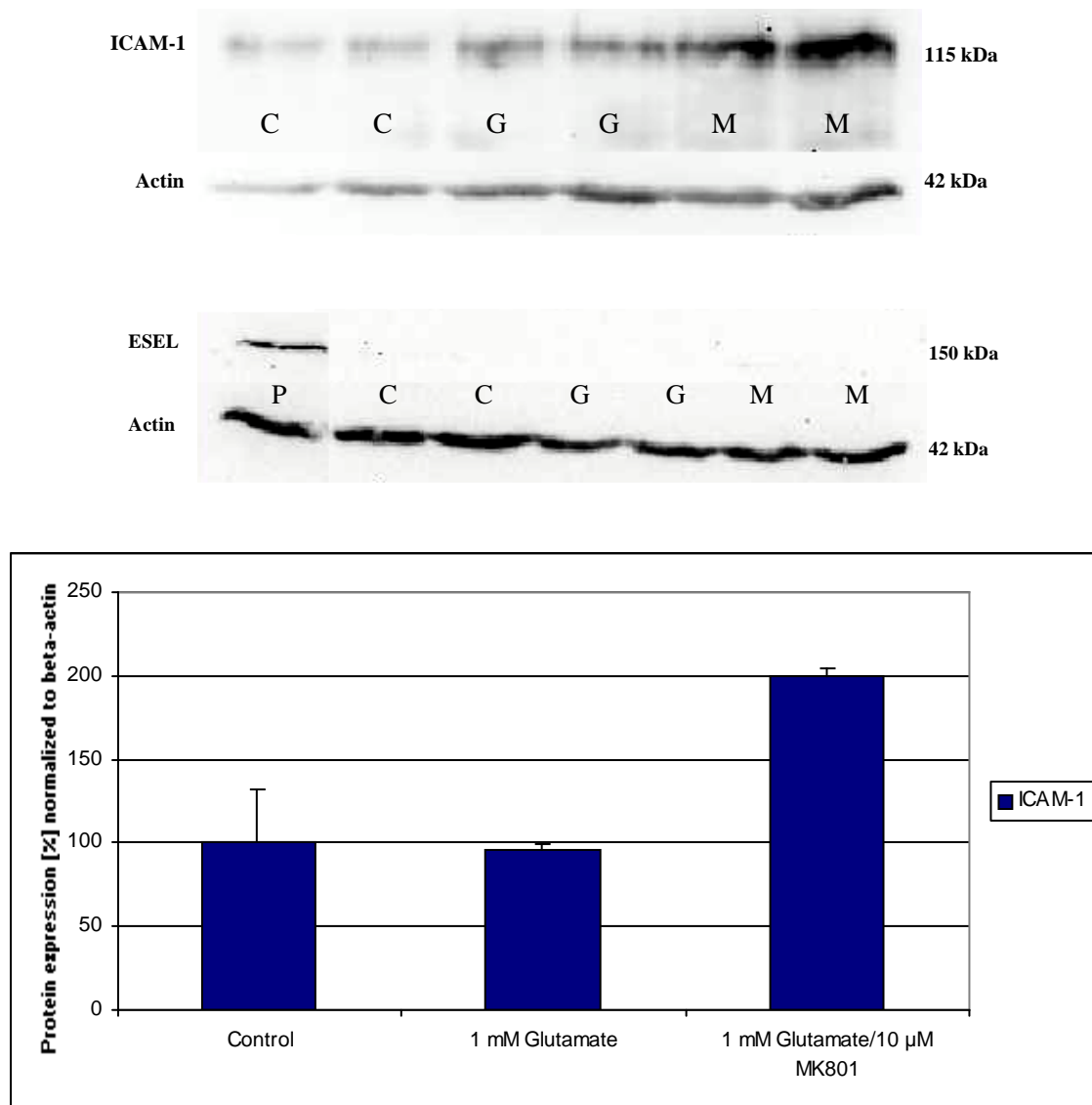


Fig. 4.5.3: Influence of 1 mM glutamate with/without 10 μ M MK801 on the expression of ICAM-1 and E-selectin. C = Control, G = 1 mM glutamate, M = 1 mM glutamate/10 μ M MK801, P = Positive match for E-selectin. Values are expressed as means \pm SEM (n=2).

Cyclooxygenases (COX-1, COX-2):

The influence of 1 mM glutamate with/without 10 μ M MK801 on cyclooxygenases were also tested and shown below in figure 4.5.4. 1 mM glutamate seemed to decrease COX-1 expression slightly, whereas it decreased COX-2 expression distinctly. Moreover, it was quite interesting that 10 μ M MK801 seemed to influence protein expression significantly, both COX-1 as well as COX-2 expression was drastically decreased by this channel blocker.

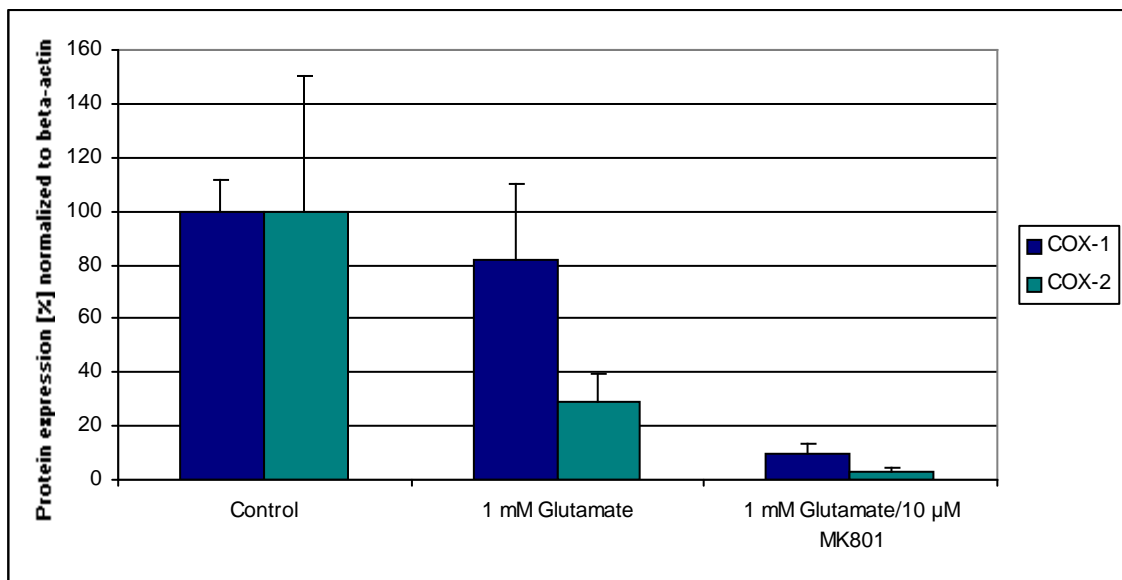
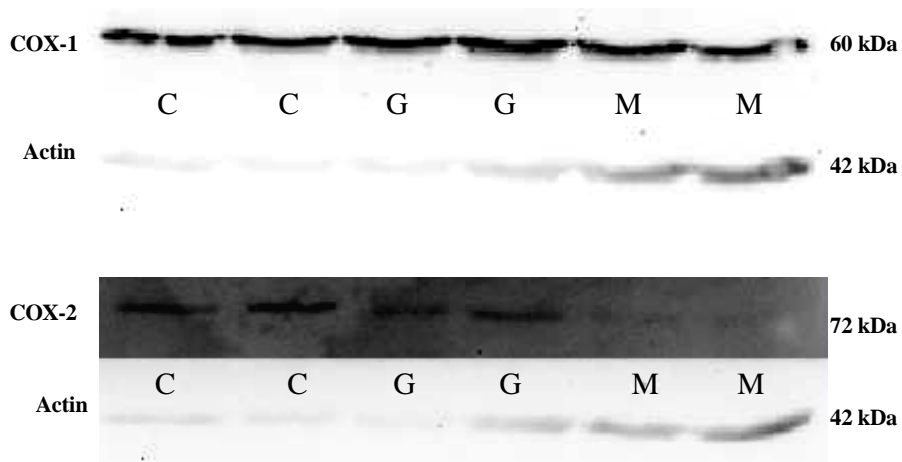


Fig. 4.5.4: Influence of 1 mM glutamate with/without 10 μ M MK801 on the total protein level of COX-1 and COX-2. C = Control, G = 1 mM glutamate, M = 1 mM glutamate/10 μ M MK801. Values are expressed as means \pm SEM (n=2).

5 Discussion

Although diseases such as Alzheimer's disease, schizophrenia, epilepsy or stroke are caused by different mechanism they share one common target, the NMDA-receptor [16]. The presence and participation of this glutamate-gated ion channel in major regulatory mechanisms had also been reported more and more often at the BBB [18, 20, 21]. Therefore it is not astonishing that such pathological conditions must be seen as a critical event causing a failure of protective and regulative functions at the blood-brain barrier. At this, not only an increased BBB permeability [18, 20] and a decreased expression of tight junctions [21] resulting in a BBB disruption. Studies also already showed that overstimulation of the NMDA-receptor is a possible pathway that lead to an up-regulation of the ABC-transporter P-gP [25,26] what is a major problem in the therapy of many brain disorders and the cause of resistance in several kinds of treatment [22, 23].

One main goal of the thesis was to establish a 96-well plate fluorescence method, which should be used to measure changes in the intracellular calcium level by an activation of the NMDA receptor in ECV304 cells. Based on data of Kuhlmann et al. [20] who published already the presence of the NR-1 subunit in cell line ECV304 by immunofluorescence microscopy and influence of glutamate onto barriers integrity and formation of reactive oxygen species (ROS), the idea was to measure the influence of NMDAR modulators on the intracellular calcium level and to link these effects to BBB properties.

In spite of everything, the presence of the NMDA-receptor in cell line ECV304 had to be verified first, since this was the basic prerequisite for successful subsequent studies, although Kuhlmann et al. [20] has already shown the presence of NR-1 subunit in cell line ECV304. However, a recheck was conducted in order to confirm his finding and amend it with the detection of NR-2A, -2B and -2C subunits also by immunofluorescence microscopy. To compare our results with the work of Kuhlmann et al. [20], a similar protocol was used, using methanol to fix and permeabilize the cells. In addition, cells were alternatively fixed with paraformaldehyde and permeabilized with Triton-X 100. Due to similar results the images of the methanol protocol were not presented in this thesis. In order to confirm immunofluorescence images and presence of the NMDAR subunits western blot analysis for the NMDA-receptor subunits were performed additionally to check their presence with a second method on the protein level. Interestingly the bands

which were obtained did not match to the predicted molecular weight of the respective subunit, but since bands at the same height were always found in the positive controls, either some sort of decomposition during the assay or unspecific binding of the primary antibody were assumed. Nearly all subunits showed at least one strong band at an appropriate molecular weight, which could be compared with the positive control. Only those samples of NR-2C subunits showed just a slightly visible band what could be compared with a strong band of the positive control. Somehow this outcome of a low visible NR-2C band did not match to the intense fluorescence images of the immunofluorescence microscopy, unlike it was possible for the other subunits. However, although polyclonal antibodies were purchased, the strong bands which were seen in the western blot analysis were assumed to be related to NMDA-sequence-binding.

Since the presence of the NMDA-receptor was more or less shown, it was focused onto the main goal of this thesis to establish a 96-well plate fluorescence method for measuring the change of the intracellular calcium level. Already the first few experiments showed interesting results, since choosing of an adequate multiplate reader was of high importance. Hardly any differences could be seen or conclusions made from the results obtained with the Polarstar galaxy microplate reader except a concentration-dependent effect of the fluorescent dye with the positive control Ionomycin and that an uptake of the fluorescence-dye Fluo3-AM into the cells proceeds. Compared to both other used multiplate readers, the Polastar galaxy can not keep up with, probably because of its technical equipment. On the other hand, measurements with the two different Tecan multiplate readers revealed better and also more useful data. Even kinetic-like experiments were tried to perform, to obtain information from the change of intracellular calcium level in the early phases. However, although all measured pairs of rows were treated the same, the factor „time“, what was needed between two pairs of rows, seems to have an important influence which adulterate the values and the intracellular calcium level. Due to this experience kinetic-like experiments were stopped, since those results were quite questionable.

Steady-state measuring showed stable and more interesting results after a capable protocol was set up by checking out and changing different parameters (NBS vs. Albumin, HBSS with/without Mg^{2+} , loading time of fluorescence-dye-solution, use of Probenecid, Fluo3-AM vs. Calcium-Green-AM,...). An increasing intracellular calcium level was always assumed after activating the NMDA receptor with either different concentrations of glutamate or NMDA, but somehow our established 96-well fluorescence measuring method was not able to show such effects. A few similar methods with other cell lines exist

[44, 45, 46] that presented results where the intracellular calcium level increases after glutamate or NMDA stimulation, and even Kuhlmann et al. [20] showed that this should be possible with ECV304 cells after glutamate addition. However, somehow it seems that influxes into the cells by other channels and/or maybe a release from intracellular stores were seen everytime, whereby the increased intracellular calcium level of the control could be taken as best example for this effect. Since those values were not stimulated by any substance the measured increased intracellular calcium level were quite interesting. In contrast to this effect, concentration-dependent changes in intracellular calcium level of NMDA and also once with glutamate were obtained. Though here the calcium level after NMDA application did not increase, it rather decreased. This maybe could be related to some sort of counter-regulations by efflux-pumps like the $\text{Na}^+/\text{Ca}^{2+}$ -exchanger or the ubiquitous PMCA, or an induced uptake into the internal stores [56].

Although the effect of a decreased intracellular calcium level caused by NMDA is quite strange, the NMDA-receptor blocker MK801 was able to show an effect that was assumed prior to our experiments. By the binding of MK801 at the PCP binding site, inside of the NMDA receptor channel influx of calcium through the channel is prevented. This effect of a decreased intracellular calcium level was seen in a concentration-dependent manner, whereby a significant effect was seen with 100 μM MK801. Interestingly, this effect was only seen in Mg^{2+} -free solution. In this regard, in a recent publication where the influence of different NMDAR-subunit compositions onto the calcium influx was investigated used also only Mg^{2+} -free solution to assess their effects [57]. Maybe Mg^{2+} -free solutions are necessary to detect the effects in a more significant manner since present Mg^{2+} possible would lead after opening the channel to a subsequent closing. Furthermore, it could be possible that no sufficient depolarization was reached to alleviate the Mg^{2+} -block in a voltage-dependent manner in normal HBSS (8264), by what good effects were only seen in Mg^{2+} -free solutions. Therefore calcium measurements over the NMDA-receptor were normally carried out in Mg^{2+} -free solutions to reach a maximal calcium response [47] and moreover studies already revealed that the depolarization can vary depending on the formation of the NMDA-receptor subunits [48]. If in retrospect the NMDA-receptor turns still out to be not functional, another alternative could be a block of a different Ca^{2+} -increasing mechanism by MK801. Diverse dissociative anaesthetics like phencyclidine or ketamine already revealed that NMDA receptors and nicotinic acetylcholine receptors, although they are not structurally related, share certain pharmacological properties [49]. Referring to this, MK801 could also inhibit both receptors by binding to different domains

than that for each specific neurotransmitter and moreover it is suggested that this inhibition may not simply be the result of a steric blockade of open-channel acetylcholine receptors [50]. Therefore, to test a possible contribution of acetylcholine-receptors the influence of ACh on the intracellular calcium level in ECV304 cells was tested. The outcome of these experiments in solutions with/without Mg^{2+} revealed that different concentrations of ACh had no effect on the intracellular calcium level in our model, moreover the decreased intracellular calcium level of MK801 was only seen in Mg^{2+} -free medium. However, ACh is a very unstable substance, thus other ACh-receptor agonists as well as antagonists should be tested in order to check the hypothesis that ACh-receptors may play an important role in ECV304 cells for the calcium level.

Since the controls had always one of the highest intracellular calcium levels, the influence of a different possible activated calcium channel was tested. Evidence of beneficial effects in reducing the rate of stroke in hypertensive patients by calcium channel antagonists were reported [51]. As a commonly used L-type-calcium channel blocker acting in the periphery and not in the CNS Verapamil was tested. A pre-test already showed that Verapamil is able to keep the intracellular calcium level lower compared to the control. Thus, the influence of this L-type calcium channel agonist with/without the antagonist was tested in solutions with/without Mg^{2+} . Verapamil was able to keep the intracellular calcium level lower in solutions with as well as without Mg^{2+} compared to the control or the also tested L-type channel agonist (S)-(-)-BayK8664. Thus, this partial inhibition of an increasing calcium seems not to be as Mg^{2+} -dependent as it was in the MK801 experiments and could be another hint for the cause of the increased control-values due to an maybe always activated voltage-gated calcium channel. Moreover, concentration-dependent effects of the L-type calcium channel activator (S)-(-)-BayK 8664 were found. Curve progressions similar to the NMDA-experiments were recorded for BayK 8664. This substance was also able to influence the intracellular calcium level, whereby a concentration of 100 μ M had nearly no effect. If we abstract away the fact that calcium channel activators normally increase the level of intracellular calcium, it was quite interesting to see that 100 μ M BayK 8664 seems to be able to completely nullify the effects that were normally seen by the control. Although an enantiomere pure (S)-(-)-BayK 8664 was obtained, what is said to be an L-type-channel activator [52], the outcome fits more to the results of an antagonist. Only considering the data, it could be speculated that maybe (R)-(+)-BayK 8664, a L-type-calcium channel blocker was instead used. However, since similar effects were already

seen in the NMDA-experiments, again some sort of counter-regulation should not be excluded during the course of the experiments [56].

Due to those outcomes we also tested for possible counter-regulations or a possible release of internal stores after Ca^{2+} -channel stimulation. Since some studies assume that the efflux of calcium is mainly caused by PMCA in ECV304 cells [53], it was decided to focus on PMCA and not on $\text{Na}^+/\text{Ca}^{2+}$ -exchanger. Ryanodine, a SERCA-inactivator and methyl- β -cyclodextrine, a dextrine that removes the PMCA out of the plasma membrane, were tested in order to see their influence on the intracellular calcium level. Based on the obtained results, tendencies of a lowered intracellular calcium level were seen in the ryanodine treated cells. Addition of ryanodine maybe resulted in a higher intracellular calcium level, whereon PMCAs were probably activated and subsequently calcium in the cells was reduced. Methyl- β -cyclodextrine had a big impact on the basic fluorescence. After PMCA were removed from the surface of the membrane, probably the calcium equilibrium was disturbed and just less calcium could be transported outside of the cells. The basic fluorescence increased ~2-3 times in comparison to observed basic fluorescence in all other experiments. This effect maybe indicated the importance and activity of the PMCA in ECV304 cells and it moreover explains, why lower intracellular calcium concentrations were observed after stimulation with NMDA or BayK 8664, since this stimulation maybe induced a higher activation of the efflux-transporter. However, it has to be mentioned that the treatment with methyl- β -cyclodextrine can also lead to a loss of cholesterol in the membrane and thus maybe result in a generally disintegrated membrane and an imbalance in the intracellular calcium level. In order to investigate this in more detail, more specific peptides blocking PMCA should be tried out in following experiments. Despite of this, the methyl- β -cyclodextrine experiment confirmed the suitability of the Calcium-assay since the enormous increase of intracellular calcium was able to be detected.

Due to the questionable outcomes, the high concentrations that were needed to see effects and the differing effects of NMDA compared with glutamate, a re-check for the NMDA-receptor presence was made, where cells for immunofluorescence microscopic images were not permeabilized. In general many studies where a participation of the NMDA receptor was assumed, the channel was either detected by western blot analysis [18, 21], or immunofluorescence confocal microscopy [20]. However, most reports did not show the molecular weight of the NMDA receptor bands in their western blots, furthermore NMDAR subunits could probably be detected, but if the target is really expressed on the surface could not be analysed by western blots. Results of immunofluorescence images are

also somehow questionable, when cells had to be permeabilized so the primary antibody can bind to a sequence that is located in the cytoplasm. As seen in our results, the permeabilized images suggested also a high expression of the subunits in our cell line, but as seen in non-permeabilized ECV304 cells, nearly no binding of the primary antibody could be seen. Thus, although the primary antibodies target extracellular domains of the NMDA-receptor nearly no or just a small amounts of NMDA-receptors could be found on the surface. In general, the presence of the NMDA-receptor on the BBB is a very controversially discussed topic. Some reseachers showed the presence of this target [18] on the BBB and others, who hypothesize no expression [54]. Another possibility why hardly any NMDA-receptor subunits were found on the surface of ECV304 cells could be due to an incomplete formation of a functional receptor. Studies already revealed that the LIVBP-domain of the NMDA receptor must interact with other regions of the receptor to form a stable subunit association [17].

Since the functionality of the NMDA-receptor on ECV304 cells became from experiment to experiment more unclear, it was decided to test the influence of 1 mM glutamate with/without 10 μ M MK801 on another parameter, namely the transendothelial electrical resistance (TEER). This is a commonly used method to check the integrity of BBB layers. Previous publications showed a decrease of electrical resistance after application on glutamate which was blocked by addition of MK801. Thus these effects were mostly attributed to an activation of NMDA receptors [18, 20]. Generally glutamate (probably to stimulate “normal” pathological conditions) was used for most NMDA receptor experiments [20, 21, 26, 55], instead of the more specific NMDA [18, 25]. Effects of other pathways like metabotropic glutamate receptors that could be activated by glutamate were mostly not considered there. However, since the functionality of the NMDA-receptor is more or less disputable in our ECV304 cell line, the loss in the BBB integrity caused by glutamate maybe approved that also other pathways could play an important role in those effects, but would confirm data of already published reports.

The cells of those TEER-experiments were lysed and western blot analysis were performed in order to investigate changes in protein expressions additionally. Although, as mentioned before, ECV304 cells seems not to express the NMDA-receptor highly on the surface of the cells, the influence of the TEER-experiments were quite interesting and even the outcome fits to studies who assumed NMDA-receptor presence and function on their cell line [18, 20]. Since effects also on the protein expression level were supposed to be mediated by the NMDA-receptor, the influence of glutamate with/without MK801 on the

expression on specific proteins, which was also already shown in other studies [21, 25], was additionally investigated. Our goal was to test for some of those published results and compare them with our results.

Treatment with 1 mM glutamate resulted in a decrease in the total protein level of Occludin what even could not be prevented by the NMDA-receptor antagonist MK801. Such an effect was already shown before. In this regard, it was assumed that changes in Occludin-phosphorylations were responsible for the protective effect of MK801 and not a reduced decrease of the protein level [21]. Although it was said that the effects of glutamate on tight junctions proteins have the earliest and most dramatic effects on Occludin [21], the influence on ZO-1 was also observed. The outcomes showed that glutamate really had no big effect on the protein level of ZO-1, it moreover seemed to increase it slightly. However, somehow glutamate in combination with MK801 seemed to induce ZO-1 expression. This could maybe interpreted as a counter-regulation due to the loss of the total protein level of Occludin, perhaps to bind to or tighten the remaining Occludin proteins to the actin cytoskeleton.

Stimulation with glutamate is said to increase the P-gP expression over an NMDA-receptor mechanism what could be attenuated by MK801 [25, 26]. Interestingly, exactly an opposite effect was observed in our experiments, where the expression due to glutamate with/without MK801 stimulation seems to decrease P-gP expression. Because of the bigger standard deviation it is possible that those values just changed slightly or nearly not at all it was observed by the bars only. This fits to the hypothesis, where the expression of P-gP is regulated by a NMDA-mechanism, if our ECV304 cells really had no functional NMDA-receptor. However, in this context it has also to be mentioned that the analysed P-gP band in the western blotting was at 95 kDa, whereas the expected band should be at app. 170 kDa. Thus, these results should only be considered as preliminary. The influence of glutamate with/without MK801 on another efflux pump MRP-1 was also tested. As a result of the outcomes we could say that MRP-1 was probably not affected in our model.

Also the influence of 1 mM glutamate with/without 100 μ M MK801 on the expression of adhesion molecules was tested. Compared to the control, 1 mM glutamate had no influence on the expression of ICAM-1. However, 1 mM glutamate with 100 μ M MK801 drastically increased the expression what is normally seen from cytokine stimulation. This observation could link recently published results that the NMDAR subunit NR1 should play an important role in the transmigration of monocytes across the BBB during conditions of multiple sclerosis [58] However, E-selectine expression was not induced by glutamate

plus/minus MK801, therefore inflammation caused by cytokines could be excluded in this case, since E-selectin is only expressed in endothelial cells which were activated by cytokines. This was also confirmed for ECV304 cells in our lab previously.

Since there were also studies which assumed an induction of P-gP by a glutamate/NMDA-receptor/COX-2 signalling pathway [25], the influence of glutamate with/without MK801 on the protein expression of cyclooxygenases were tested. Interestingly, we could not observe any induction of cyclooxygenases, rather the protein level of COX-1 was slightly and of COX-2 more drastically decreased by 1 mM glutamate. However, 1 mM glutamate with 100 μ M MK801 drastically decreased the protein expression, by what a conversion of arachidonic acid to prostaglandin H₂ is probably suppressed. In contrast to this, Bauer et al. proposed no regulation of COX enzymes on the expression level, but changes on the functional level [25].

6 Conclusions

- The presence of NR-1, -2A, -2B and -2C subunits could be shown in ECV304 cells by methods as western blot analysis and immunofluorescence microscopy. An expression of those targets was mostly found in the cytoplasm and not on the cell surface whereby the functionality is still disputable.
- The major goal of this thesis was to develop a fluorescence method for measuring the changes in the intracellular calcium level. Therefore, a solid working protocol was successfully established within this diploma thesis and was then used for investigations with regard to the NMDAR. Applications of NMDAR modulators (NMDA, glutamate, MK801, D-APV) as well as other calcium modulators as e.g. BayK8664 and Verapamil provided interesting insights in the regulation of the intracellular calcium level of ECV304 cells, which partly confirmed known literature, but would also need further investigations to clarify observed effects in detail.
- The influence of glutamate on the transendothelial electrical resistance, a parameter for BBBs integrity, was moreover assessed. In concordance to literature, it was able to show that 1 mM glutamate decreased the integrity of the blood-brain barrier model, which was blocked by NMDAR antagonist 10 μ M MK801, indicating a possible role of the NMDAR during this process. Furthermore, changes of the expression of several proteins as tight junctional proteins Occludin, ZO-1 and Claudin-5, as well as ICAM-1 and P-gP were observed.
- However, since the NMDA-receptor seemed to be expressed in the cytoplasm mainly, these effects as well as changes of the intracellular calcium level by MK801 could probably be caused by other signalling pathways than primarily assumed. Thus, in conclusion the presented data showed effects of NMDAR-modulators on the blood-brain barrier *in vitro* model based on ECV304 cells, but did not confirm a direct link to a typically functional NMDA-receptor.

7 References

- [1] J. Abbott, Astrocyte-endothelial interactions and blood-brain barrier permeability, *J. Anat.*200, 2002, 629-638
- [2] Britta Engelhardt, Development of the blood-brain barrier, *Cell Tissue Res*, 2003, 119-129
- [3] Yuri Persidsky et al., Blood-brain barrier: Structural components and function under physiologic and pathologic conditions, *J. Neuroimmune Pharmacol*, 2006, 223-236
- [4] Jacek Bernacki et al., Physiology and pharmacological role of the BBB; *Pharmacological Reports*60, 2008, 600-622
- [5] J. Abbott et al., Astrocyte-endothelial interactions at the blood-brain barrier; *Nature Reviews Neuroscience*7, 2006, 41-53
- [6] W. Neuhaus et al., Validation of in vitro cell culture models of the BBB: Tightness Characterization of two promising cell lines, *J. Pharmaceutical Sciences*, 2008, 1-18
- [7] B.T. Hawkins and T.P. Davis, The BBB/neurovascular unit in health and disease, *Pharmacol. Reviews*, 2005, 173-185
- [8] Jacek Bernacki et al., Physiology and pharmacological role of the BBB; *Pharmacological Reports*60, 2008, 600-622
- [9] M. D. Bootman et al., Calcium signalling – an overview; *Seminars in Cell & Developmental Biology*, 2001, 3-10
- [10] G. Popescu, Mechanism-based targeting of NMDA receptor functions; *Cell. Mol. Life Sciences*62, 2005, 2100-2111
- [11] Y. Gasche, The role of metalloproteinases on blood-brain-barrier breakdown after ischemic stroke; *Inflammation and Stroke* ©2001 Birkhäuserverlag Basel/Swz
- [12] P. Ballabh et al., The blood-brain barrier: an overview. Structure, regulation, and clinical implications, *Neurobiology of disease*16, 2004, 1-13
- [13] C. Rachel et al., Calcium modulation of adherens and tight junction function, *Stroke*33, 2002, 1706-1711
- [14] EMD Biosciences, Signal transduction resource-Calcium signaling/calcium metabolism, http://www.emdchemicals.com/life-science-research/signal-transduction-resource-calcium-signaling-calcium-metabolism/c_bb6b.s1Ok5EAAAEix4I5hDcj

- [15] G.E. Hardingham, H. Bading, The Yin and Yang of NMDA receptor signalling, *TRENDS in Neurosciences* 26, 2003, 81-89
- [16] B.C. Albensi, The NMDA receptor/ion channel complex: a drug target for modulating synaptic plasticity and excitotoxicity, *current pharmaceutical design* 13, 2007, No.00
- [17] R.A.J. McIlhinney et al., Assembly of N-methyl-D-aspartate (NMDA) receptors, *Biochemical Society Transactions* 31, 2003, Part 4
- [18] C.D. Sharp et al., Glutamate causes a loss in human cerebral endothelial barrier integrity through activation of NMDA receptor, *10.1152/ajpheart.0052.2003*
- [19] I.A. Krizbai et al., Expression of glutamate receptors on cultured cerebral endothelial cells, *J Neurosci Res* 54, 1998, 814-819
- [20] C.R.W. Kuhlmann et al., Fluvastatin prevents glutamate-induced blood-brain barrier disruption in vivo, *Life Sciences* 82, 2008, 1281-1287
- [21] I.E. András et al., The NMDA and AMPA/KA receptors are involved in glutamate-induced alterations of occludin expression and phosphorylation in brain endothelial cells, *JCBFM*, 2007, 27, 1431-1443
- [22] W. Löscher, H. Potschka, Drug resistance in brain diseases and the role of drug efflux transporters, *Nature Reviews Neuroscience* 6, 2005, 591-602
- [23] D.S. Miller et al., Modulation of P-glycoprotein at the blood-brain barrier: opportunities to improve central nervous system pharmacotherapy, *Pharmacological Reviews* 00, 2008, No.0
- [24] A. Lazarowski et al., ABC transporters during epilepsy and mechanisms underlying multidrug resistance in refractory epilepsy, *epilepsia* 48, 2007, 140-149
- [25] B. Bauer et al., Seizure-induced up-regulation of P-glycoprotein at the blood-brain barrier through glutamate and cyclooxygenase-2 signaling, *Mol Pharmacol*, 2008, 73: 1444-1453
- [26] H.J. Zhu, G.Q. Liu; Glutamate up-regulates P-glycoprotein expression in rat brain microvessel endothelial cells by an NMDA receptor-mediated mechanism; *life sciences* 75 (2004) 1313-1322, doi:10.1016/j.lfs.2004.02.027
- [27] D. McNamara, R. Dingledine, Dual effect of glycine on NMDA-induced neurotoxicity in rat cortical cultures, *J. Neuroscience* 10, 1990, 3970-3976
- [28] D.R. Giovannucci, E.L. Stuenkel, An NMDA receptor on isolated secretory nerve endings, *Brain Research* 792, 1995, 246-250
- [29] C. Allgaier et al., NMDA receptor characterization and subunit expression in rat cultured mesencephalic neurons, *British J. Pharmacology* 126, 1999, 121-130

- [30] C.G. Parsons et al., Comparative patch-clamp studies with freshly dissociated rat hippocampal and striatal neurons on the NMDA receptor antagonistic effects of Amantadine and Memantine, *Eur. J. Neuroscience*8, 1996, 446-454
- [31] P.Görtz et al., Neuronal network properties of human teratocarcinoma cell line-derived neurons, *Brain Research*1018, 2004, 18-25
- [32] R. Zwart et al., Differential modulation of $\alpha3\beta2$ and $\alpha3\beta4$ neuronal nicotinic receptors expressed in *Xenopus Oocytes* by flufenamic acid and niflumic acid, *J. Neuroscience*15, 1995, 2168-2178
- [33] S.L. Hamilton et al., A comparison between the binding and electrophysiological effects of dihydropyridines on cardiac membranes, *Mol. Pharmacology*31, 1986, 221-231
- [34] S.B. Freedman et al., Identification and characterization of voltage-sensitive calcium channels in neuronal clonal cell lines, *J. Neuroscience*4, 1984, 1453-1467
- [35] J.L. Sutko et al., The pharmacology of Ryanodine and related compounds, *Pharmacological Reviews*49, 1997, 53-98
- [36] K. Takahashi, et al., Spontaneous transformation and immortalization of human endothelial cells, *In Vitro Cell. Dev. Biol.* 25, 1990, 265-274
- [37] H. Shen et al., The protective effects of *Achyranthes bidentata* polypeptides against NMDA-induced cell apoptosis in cultured hippocampal neurons through differential modulation of NR2A- and NR2B-containing NMDA receptors, *Brain Research Bulletin* 77, 2008, 274-281
- [38] V. Saraswathi et al., Linoleic acid-induced endothelial activation: role of calcium and peroxynitrite signaling, *Journal of Lipid Research*, Vol. 45, 2004, 794-804
- [39] R.C. Brown et al., Protection against hypoxia-induced blood-brain barrier disruption: changes in intracellular calcium, *Am J Physiol Cell Physiol* 286, 2004, C045-C1052
- [40] E.R.Kokoska et al., Role of calcium in adaptive cytoprotection and cell injury induced by deoxycholate in human gastric cells, *Am J Physiol Gastrointest Liver Physiol* 175, 1998, 322-330
- [41] Molecular Probes™, Invitrogen Detection Technologies, Product Information Fluo Calcium Indicators
- [42] Molecular Probes™, Invitrogen Detection Technologies, Product Information Long-Wavelength Calcium Indicators
- [43] H.R.Arias et al., Characterization of the dizocilpine binding site on the nicotinic acetylcholine receptor, *Mol Pharmacol*, 2001, 59:1051-1060

- [44] D. Reigada et al., Glutamate acts at NMDA receptors on fresh bovine and on cultured human retinal pigment epithelial cells to trigger release of ATP, *J.Physiol*, 575.3, 2006, pp707-720
- [45] C. Rachel et al., Protection against hypoxia-induced blood-brain barrier disruption: changes in intracellular calcium, *Am J Physiol Cell Physiol*, 286: C1045-C1052, 2004
- [46] FcεRI Signaling of Mast Cells Activates Intracellular Production of Hydrogen Peroxide: Role in the Regulation of Calcium Signals, Y. Suzuki et al.,
- [47] E. Avignone et al., Differential responses to NMDA receptor activation in rat hippocampal interneurons and pyramidal cells may underlie enhanced pyramidal cell vulnerability, *Eur J Neurosci*, 2005, 22(12):3077-90
- [48] S. Cull-Candy et al., NMDA receptor subunits: diversity, development and disease, *Current opinion in Neurobiology*, 2001, 11:327-335
- [49] M.D. Krasowski and N.L. Harrison, General anaesthetic actions on ligand-gated ion channels, *Cell Mol Life Sci*. 1999, 55(10):1278-303
- [50] R. Hugo et al., Characterization of the Cizocilpine Binding Site on the Nicotinic Acetylcholine Receptor, *Mol Pharmacol*, 59:1051-1060, 2001
- [51] R.C. Brown, T.P. Davis, Calcium Modulation of Adherens and Tight Junction Function, A Potential Mechanism for Blood-Brain Barrier Disruption After Stroke, *Stroke*, DOI:10.1161/01.STR.0000016405.06729.83
- [52] Tocris Bioscience, (S)-(-)-BayK 8664 Product Information (Cat.Nr.: 1546)
- [53] J. Zhang et al., Phosphatidylserine externalization in caveolae inhibits Ca²⁺ efflux through plasma membrane Ca²⁺-ATPase in ECV304, *Cell Calcium*45, 2009, 177-184
- [54] P.Morley et al., Evidence that functional glutamate receptors are not expressed on rat or human cerebromicrovascular endothelial cells, *J Cereb Blood Flow Metab*, 18:396-406, 1998
- [55] C.D. Sharp et al., N-Methyl-D-aspartate receptor activation in human cerebral endothelium promotes intracellular oxidant stress, *Am J Physiol Heart Circ Physiol* 288: H1893-H1899, 2005; doi:10.1152/ajpheart.01110.2003
- [56] E. Besancon et al., Beyond NMDA and AMPA glutamate receptors: emerging mechanisms for ionic imbalance and cell death in stroke, *Trends in Pharmacological Sciences*29, 2008, 268-275
- [57] D. Feuerbach et al., Comparative pharmacology of the human NMDA-receptor subtypes R1-2A, R1-2B, R1-2C and R1-2D using an inducible expression system, *European Journal of Pharmacology*637, 2010, 46-54

[58] A. Reijkerk et al., The NR1 subunit of NMDA receptor regulates monocyte transmigration through the brain endothelial cell barrier, *Journal of Neurochemistry*, 2010, 447-453, doi:10.1111/j.1471-4159.2010.06598x

8 Abbreviations

ABC-transporter	ATP-binding cassette transporter
AC	Astrocytes
ACh	Acetylcholine
ACM	Astrocyte conditioned medium
AJ	Adherens junctions
AP	Alkaline phosphatase
APS	Ammonium persulfate
AQP4	Aquaporine 4
BBB	Blood brain barrier
BMEC	Brain microvascular endothelial cells
BSA	Bovine standard albumin
CIF	Calcium-influx factor
CNS	Central nervous system
COX	Cycooxygenase
D-APV	2-amino-5-phosphonopentanoic acid
DMSO	Dimethylsulfoxid
DTT	Dithiothreitol
EC	Endothelial cells
ER	Endoplasmatic reticulum
EtOH	Ethanol
FITC	Fluorescin isothiocyanate
GGTP	γ -glutamyl-transpeptidase
Ham's F12	Ham reg. Nutrients mixture F12

HBSS	Hank's balanced salt solution
Hepes	4-(2-hydroxyethyl)piperazine-1-ethanesulfonic acid
HRP	Horseradish peroxidase
ICAM	Intracellular adhesion molecule
IMDM	Iscove's modified Dulbecco's medium
InsP ₃	Inositol 1, 4, 5, triphosphate
JAM	Junctional adhesion molecule
LAF	Laminar air flow
MAGUK	Membrane associated guanylate kinase
MDR	Multidrug-resistance
MeOH	Methanol
MK801	Dizocilpine
MRP	Multidrug resistance associated protein
NCS	Newborn calf serum
NMDA	N-methyl-D-aspartic acid
NMDAR	NMDA-receptor
OAT	Organic anion transporter
PBMEC	Porcine brain microvascular endothelial cells
PC	Pericycte
P-FA	Paraformaldehyde
P-gP	P-glycoproteine
PMCA	Plasma membrane Ca ²⁺ -ATPase
PVDF	Polyvinylidene fluoride
ROC	Receptor operated channels
RT	Room temperature
RZR	Ryanodine receptor

SDS	Sodium dodecyl sulfate
SDS-Page	Sodiumdodecylsulfate polyacrylamid gel electrophoresis
SERCA	Sarco/endoplasmatic reticulum Ca ²⁺ -ATPase
SOC	Store operated channels
SR	Sarcoplasmatic reticulum
TBS	Tween buffered saline
TEER	Transendothelial electrical resistance
TEMED	N, N, N', N'-tetramethylethylene diamine
TJ	Tight junction
TRIS	Tris(hydroxymethyl)-aminomethane
VE-cadherin	Vascular endothelial cadherin
VOC	Voltage operated channels
Vs.	versus
ZO	Zonula occludens

9 Curriculum Vitae

Personal data

Name: Michael FREIDL
Date of birth: 15.06.1984
Place of birth: Baden, NÖ
Nationality: Austria

Education

09/1990 – 06/1994 Elementary-school Pfarrplatz, Baden
09/1994 – 06/1998 BG/BRG Biondegasse, Baden
09/1998-06/2002 BORG Wr. Neustadt
10/2003 Inscription at the University of Vienna
Diploma study in pharmacy

Professional experience and further activities

01/2003-09/2003 Basic military service “Martinek-Kaserne Baden”
with an apprenticeship as emergency medical
technician
07/2004, 08/2005, 08/2006 Landschaftsapotheke Baden
04/2004 – 03/2008 Landeskrankenhaus Thermenregion Baden, Apotheke
(uncontinuously)
08/2008 Landeskrankenhaus Wr. Neustadt, Anstaltsapotheke
09/2008 – 06/2009 Diploma thesis at the “Blood-brain barrier” group,
Department of medicinal chemistry, University of
Vienna
04/2009 Poster-presentation and participation at the 21. ÖPHG-
symposium
10/2009 – 6/2010 Tutor for practical “Arzneimittelanalytik &
Wirkstoffentwicklung”, Module “Biotechnologie &
Bioanalytik”